

**VCAM-directed Immunoliposomes Loaded with Vascular–
Disrupting Agents for Selective Targeting and Occlusion of the
Tumor Vasculature - As a Novel Therapeutic Strategy**

Dissertation

zur
Erlangung des Doktorgrades (Dr. rer. nat.)
der
Mathematisch-Naturwissenschaftlichen Fakultät
der
Rheinischen Friedrich-Wilhelms-Universität Bonn

vorgelegt von
Sara Gosk
aus Lisabon, Portugal

Bonn, Januar 2007

Angefertigt mit Genehmigung der Mathematisch-Naturwissenschaftlichen Fakultät der Rheinischen Friedrich-Wilhelms-Universität Bonn

Gutachter:

1. Prof. Dr. Gerd Bendas
2. Prof. Dr. Ulrich Jaehde

Tag der mündlichen Prüfung: 3. Juni 2008-05-30

Diese Dissertation ist auf dem Hochschulschriftenserver der ULB Bonn elektronisch publiziert (http://hss.ulb.uni-bonn.de/diss_online). Erscheinungsjahr 2008.

Zusammenfassung

Die gezielte Beeinflussung des Blutgefäßsystems eines soliden Tumors hat ein herausragendes Potential für verschiedene therapeutische Anti-Tumor-Strategien. So erscheint beispielsweise die Targetierung von Tumorgefäßen mittels Arzneistoffcarriern, die Wirkstoffe für eine Intervention der Endothel- bzw. Gefäßfunktion enthalten, als innovatives und neuartiges therapeutisches Prinzip. Für diese Targeting-Strategien müssen geeignete Carrier entwickelt werden. Als Zielstrukturen bieten sich solche endotheliale Epitope an, die spezifisch nur oder verstärkt von Gefäßsystem des Tumors exprimiert werden. Hierbei eignet sich besonders das vascular cell adhesion molecule 1 (VCAM-1).

In der vorliegenden Arbeit wurden Immunliposomen (Antikörper-gekoppelte Liposomen), die gegen VCAM-1 gerichtet sind, hergestellt und hinsichtlich ihrer endothelialen Targetierung unter *in vitro*- und *in vivo*-Bedingungen untersucht. Als vaskulär aktive Wirkstoffe wurden Tumor Nekrose Faktor-alpha (TNF- α) und der TNF- α -induzierende Wirkstoff DMXAA in den Liposomen eingeschlossen. Diese Wirkstoffe sollten die Exprimierung von Tissue Faktor an den Endothelzellen und damit einen prokoagulativen Zustand in den Tumorgefäßen induzieren, der letztendlich mit der Kollabierung der Gefäßfunktion seine Anti-Tumor-Wirksamkeit entfaltet. Für die Untersuchungen des liposomalen Targetings wurden die Liposomen unter Verwendung verschiedener Ankerlipide mit anti-VCAM-Antikörpern gekoppelt und umfassend charakterisiert. Das Bindungsverhalten an zwei verschiedene Endothelzelllinien wurde unter *in vitro*-Bedingungen mittels unterschiedlicher Techniken quantifiziert und erwies sich gegenüber Kontrollliposomen als positiv.

Das Targeting der Immunliposomen unter *in vivo*-Bedingungen wurde in Colo 677-Tumorxenograft-Mäusen untersucht. Dabei zeigten die Organverteilungs-Studien mittels Tritium-gelabelter Liposomen, 30 Minuten bzw. 24 Stunden nach i.v. Injektion keine deutlichen Vorteile der VCAM-Immunliposomen hinsichtlich der Akkumulierung im Tumor. Fluoreszenzmikroskopische und immunhistochemische Untersuchungen der Tumoren zeigten aber, dass die Lokalisierung der Liposomen innerhalb der Tumoren sehr differierte. Während nicht-gerichtete Liposomen unspezifisch vom Tumorgewebe aufgenommen und dort akkumuliert wurden, binden die VCAM-gerichteten Immunliposomen hochspezifisch am Gefäßsystem. So konnte erstmals die Funktion von Immunliposomen als spezifischer vaskulärer Carrier verdeutlicht werden.

Die Wirkung von TNF- α und DMXAA hinsichtlich einer verstärkten Tissue Faktor-Exprimierung auf Endothelzellen wurde zuerst in Endothelzell-Kulturen verifiziert. Für den Einbau beider Wirkstoffe in Liposomen in ausreichendem Maße wurden die Herstellungsbedingungen optimiert, letztendlich resultierten Liposomen mit einer prozentualen Einschlussquote von 33% für TNF- α und 18 % für DMXAA. Deren Wirkung wurde wiederum in den Colo 677-Mäusen hinsichtlich einer Wachstumsverzögerung der Tumoren analysiert. Es zeigte sich eindeutig, dass der Wachstums-verzögernde Effekt beider Wirkstoffe nur in Kombination mit dem VCAM-Targeting der Liposomen zum Tragen kommt. Zur Aufklärung der molekularen Mechanismen der Anti-Tumor-Wirkung wurden verschiedene immunhistochemische Untersuchungen der behandelten Tumore angeschlossen. Die Anwendung eines TNF- α -ELISA, eines Tissue Faktor-Stainings sowie die Verwendung des TUNEL-Assays zur Überprüfung der apoptotischen Aktivität konnten nicht eindeutig die Wirkung über die Tissue Faktor Exprimierung und damit Koagulation beweisen.

Orientierende erste therapeutische Experimente mit TNF- α -Liposomen zeigten aber nach 24 und 72 Stunden erhöhte Tissue Faktor Werte im Tumor und stellen somit dieses postulierte Prinzip der Anti-Tumor-Wirkung als sehr aussichtsreich dar.

Abstract

Targeting the tumor vasculature and selectively modifying endothelial functions with agents that exert their action on the tumor endothelial cells instead of the tumor cells themselves, is an attractive anti-tumor strategy. Polyethylenglycol modified immunoliposomes (IL) directed against vascular cell adhesion molecule 1 (VCAM), a surface receptor over-expressed on tumor vessels, were prepared and investigated the liposomal targetability *in vitro* and *in vivo*. The vascular destructing agents, tumor necrosis factor alpha (TNF- α) and the TNF- α inducing drug, DMXAA, are known to selectively target the tumor endothelium and induce a pro-coagulative state, which leads to a collapse of the tumor vasculature. The hypothesis that TNF- α and DMXAA modulate the coagulative state of the endothelium through the up-regulation of tissue factor (TF) was investigated *in vitro*. VCAM-targeted and non-targeted liposomes loaded with either TNF- α or DMXAA were formulated and upon administration tumor growth delay was investigated *in vivo*.

In vitro, VCAM antibodies conjugated to PEGylated liposomes through the cyanur anchor displayed specific binding to activated endothelial cells under static conditions, as well as under simulated blood flow conditions. The *in vivo* targeting of IL was analyzed in mice bearing human Colo 677 tumor xenografts 30 min and 24 h post i.v. injection. Whereas biodistribution studies using [³H]-labeled liposomes displayed only marginal higher tumor accumulation of VCAM targeted vs. unspecific ILs; fluorescence microscopy evaluation revealed that their localization within tumors differed strongly. VCAM targeted ILs accumulated in tumor vessels with increasing intensities from 30 min to 24 h, while control ILs accumulated in the tumor tissue by passive diffusion.

TNF- α and DMXAA displayed a direct cytotoxic effect on the murine endothelial cells, and induced an 3-fold up-regulation of TF expression and activity after 6 and 12 hours *in vitro*. TNF- α and DMXAA were encapsulated into PEGylated liposomes with reasonable encapsulation efficiencies of 33 % and 18 %, respectively. Treatment of mice bearing human Colo 677 xenografts with VCAM-targeted liposomes loaded with TNF- α or DMXAA delayed the tumor growth compared to mice treated with non-targeted TNF- α liposomes and non-treated mice. The mechanism behind the tumor growth delay was investigated using TNF- α ELISA, TUNEL assay and TF immunohistochemistry, but did not add to the understanding of the mechanism behind the tumor growth delay. However, in a pilot experiment, tumors from mice treated with VCAM-targeted TNF- α liposomes displayed an increased TF expression after 24 and 72 hours, indicating that the mechanism behind the targeted TNF- α liposomes might be the induction of TF.

This is the first morphological evidence for selective *in vivo* targeting of tumor vessels using ILs and the first study to show that VCAM-targeted TNF- α loaded liposomes have an antitumor effect in a human xenograft model.

Abbreviations

IFP	Interstitial fluid pressure
DT	Diphtheria toxin
HER-2	Human epidermal growth factor receptor 2
RES	Reticuloendothelial system
PEG	Polyethylene glycol
VEGF	Vascular endothelial growth factor
bFGF	basic Fibroblast growth factor
TGF- β	Transforming growth factor β
VCAM	Vascular endothelial adhesion molecule 1
IL	Immunoliposome
ScFv	Single chain fragment variable
EPR	Enhanced permeability and retention
VLA-4	Very late antigen 4
TNF- α	Tumor necrosis factor α
IL	Interleukin
HUVEC	Human umbilical vein-derived endothelial cells
VDA	Vascular disrupting agents
ATP	Adenosin triphosphate
TF	Tissue factor
LPS	Lipopolysaccharide
PS	Phosphatidylserine
TNFR60	TNF- α receptor of 60 kDa
TNFR80	TNF- α receptor of 80 kDa
NF- $\kappa\beta$	Nuclear factor $\kappa\beta$
EGR-1	Early growth response 1
DD	Death domain
SODD	Silencer of death domain
TRADD	TNFR-associated death domain
RIP	Receptor interacting protein
TRAF-2	TNFR-associated factor 2
FADD	Fas-associated death domain

ROS	Reactive oxygen species
FAA	Flavone acetic acid
DMXAA	5,6-dimethylxanthenone-4-acetic acid
IFN- γ	Interferon γ
SPC	Soy phosphatidylcholine
PEG-PE	PEG phosphatidylethanolamine
NgPE	N-glutaryl-PE
Chol	Cholesterol
DiO	3,3'- Dioctadecyloxacarbocyanine perchlorate
EDC	1-ethyl-3-(3-dimethylaminopropyl)carbodiimid
TUNEL	Terminal deoxynucleotidyl tranferase dUTP nick end labeling
TMB	3, 3', 5, 5'-tetramethyl benzidine
ELISA	Enzyme-linked immunosorbent assay
FCS	Foetal calf serum
TLC	Thin layer chromatography
FITC	Fluorescein isothiocyanate
mAb	Monoclonal antibody
pAb	Polyclonal antibody
BSA	Bovine serum albumin
PI	Propidium iodide
MTT	3-(4,5-dimethylthiazol-2-yl)-2,5-diphenyl tetrasodiumbromide
DAB	Diaminobenzidine
NL	NgPE-liposome
CL	Cyanur-liposome
ICAM	Intracellular adhesion molecule
α VCAM	Anti-VCAM
hIgG	Human fractionated IgG
rIgG	Rat IgG ₁
Alb	Albumin

Contents

1. Introduction	5
1.1 Targeting solid tumors	5
1.1.1 Disadvantages of targeting the tumor cells in solid tumors.....	5
1.1.2 Advantages of targeting the tumor vasculature.....	9
1.2 Immunoliposomes as a drug delivery system.....	11
1.2.1 Liposome distribution in vivo	12
1.2.2 Vascular-targeted liposomes.....	14
1.2.3 VCAM as a target on the tumor endothelium	16
1.3 Vascular targeting drugs.....	18
1.3.1 Ligand-directed VDAs.....	20
1.3.2 Coagulation inducing VDAs.....	22
1.3.3 TNF- α ; as a VDA.....	27
1.3.4 DMXAA as a TNF- α inducing small molecule VDA	31
1.4 Aim of study.....	34
2. Material and Methods.....	37
2.1. Reagents.....	37
2.2. Cell lines.....	38
2.3 Synthesis of the cyanur-PEG-PE anchor.....	38
2.4. Liposome preparation	39
2.4.1 Preparation of empty liposomes	39
2.4.2 Preparation of TNF- α and DMXAA liposomes.....	40
2.4.3 Coupling proteins to the liposomes	41
2.5 Liposome characterization	42
2.5.1 Particle sizing.....	42

2.5.2 Phospholipid concentration determination	43
2.5.3 Protein concentration determination according to Peterson-Lowry	43
2.6 VCAM expression and liposome targeting to bEnd3 cells <i>in vitro</i>	44
2.6.1 VCAM expression and liposome binding using flow cytometry (FACS) analysis	44
2.6.2 Fluorescence- based cell assay	45
2.6.3 Dynamic flow assay	46
2.7 α -VCAM IL targeting and biodistribution <i>in vivo</i>	47
2.7.1 Xenograft mouse model and biodistribution studies.....	47
2.7.2 Fluorescence microscopy of tissue sections	48
2.8 Cytotoxicity studies.....	48
2.8.1 Propidium iodide (PI) assay.....	49
2.8.2 3-(4,5-dimethylthiazol-2-yl)-2,5-diphenyl tetrasodium bromide (MTT) assay	49
2.9 TNF- α induced TF expression and activity <i>in vitro</i>	50
2.9.1 TF cell-based enzyme-linked Immunosorbent Assay (ELISA)	50
2.9.2 TNF- α induced TF expression analyzed with flow cytometry	50
2.9.3 Western Blot.....	51
2.9.4 TF induced coagulation	52
2.10 Treatment of colo 677 tumors with DMXAA and TNF- α liposomes <i>in vivo</i>	53
2.10.1 Treatment with TNF-alpha and DMXAA liposomes.....	53
2.10.2 TNF- α ELISA	54
2.10.3 Immunohistochemistry and histology.....	55
2.11 Statistical analysis	56
3. Results and Discussion	57
3.1 <i>In vitro</i> targeting of VCAM-1	57

3.1.1 VCAM-1 expression in two different endothelial cells	57
3.1.2 Targeting VCAM on activated endothelium in vitro with α -VCAM liposomes.....	58
3.1.3 The targeting of activated endothelium in a dynamic flow assay	66
3.2 <i>In vivo</i> targeting of VCAM-1 expressed on tumor endothelium.....	69
3.2.1 VCAM expression on the vasculature of the human Colo 677 xenograft model.....	69
3.2.2 Tumor distribution of ^3H -labelled targeted and non-targeted liposomes	69
3.2.3 The localization of liposomes in organs.....	73
3.3 TNF- α and DMXAA induced cytotoxicity and TF expression and activation <i>in vitro</i>	77
3.3.1 TNF- α and DMXAA induced cytotoxicity on endothelial cells	78
3.3.2 TNF- α induced TF expression and activity	83
3.4 Combing VCAM-targeted liposomes and induction of TF activity	89
3.4.1 Encapsulation of TNF-alpha and DMXAA into ILs.....	89
3.4.2 Treatment of tumor xenografts with TNF- α and DMXAA loaded VCAM-targeted liposomes.....	91
4. Conclusions	101
5. References.....	103
Acknowledgements.....	139
Erklärung	141
Curriculum Vitae	143

1. Introduction

1.1 Targeting solid tumors

Solid tumors account for at least 85 % of cancerous deaths [Jain, 2005]. Therefore it is essential to develop treatments which kill tumor cells efficiently without damaging healthy cells. While traditional therapeutics, such as chemotoxic drugs or ionizing radiation, are very successful at killing tumor cells, they often fail to adequately discriminate between normal and malignant tissues. Thus, the severe side effects of these treatments often limit dosages to suboptimal levels or the duration of patient's treatment, resulting in poor outcomes for the management of disease, quality of life, and overall survival. Also, tumor cell resistance in itself restricts the use and effect of cytostatic treatment in therapy and calls for targeted therapy forms. However, targeting tumor cells with monoclonal antibodies or immuno-conjugates is hampered by an uneven spatial distribution of the drugs in the tumor and inadequate accumulation of the injected antibodies at the target site [Christiansen and Rajasekaran, 2004].

1.1.1 Disadvantages of targeting the tumor cells in solid tumors

Solid tumors are composed of two distinct compartments: the malignant cells (parenchyma) and the supporting stroma. All solid tumors, regardless of their cellular origin require stroma and cannot grow beyond the minimal size of 1 - 2 mm without it [Dvorak *et al*, 1979; Folkman, 1986]. The stroma provides the vasculature needed for the supply of nutrients and oxygen. It also sets up a barrier that limits the influx of inflammatory cells. Therefore, the stroma acts as both a lifeline for tumor cells and a barrier that can regulate the interchange of cells and molecules with the host [Nagy *et al*, 1988]. There are at least three different physiological barriers that can inhibit therapeutics from reaching their target: the endothelial barrier, interstitial pressure, binding to stromal components and in some tumors the epithelial barrier [Christiansen and Rajasekaran, 2004].

The microenvironment of solid tumors is distinguished from normal tissue by exhibiting high interstitial fluid pressure (IFP), hypoxia and low extracellular pH [Tannock, 2001; Cairns *et al.*, 2006]. The mechanisms responsible for this microenvironment are shown in Fig.1. In normal tissues the vascular system is regulated

by a balance of anti-angiogenic and pro-angiogenic factors which ensure the formation and maintenance of a functional and orderly network of blood vessels. In addition, a network of lymphatics drains away waste, such as cellular by-products and fluids. However, in solid tumors the balance is shifted towards the pro-angiogenic, which leads to the formation of a disorganized vasculature with structural and functional abnormalities [Vauple, 2004]. The vasculature is often leaky due to an incomplete endothelial lining, to the lack of a layer of pericytes and to a leaky basal membrane [Vauple, 2004; Kumagai *et al.*, 2006].

The tumor vessels are generally long and the vessel organization is often chaotic and heterogeneous with vessel hotspots, blind ends, arteriolar-venous shunts and plasma channels devoid of red blood cells [Dewhirst *et al.*, 1996]. Solid tumors characteristically lack lymphatics, which leads to an increased accumulation of fluid and waste products in the tumor and further to an elevated IFP [Leu *et al.*, 2000; Cairns *et al.*, 2006] and a hydrostatic pressure gradient that causes fluid to move toward the periphery [Jain, 1987; Boucher *et al.*, 1990]. The net outward flow inhibits the extravasation of therapeutics, such as antibodies, immuno-conjugates or small drug molecules like doxorubicin [Lankelma *et al.*, 1999] by reducing their penetration depth into the tumor by convection [Jain and Baxter, 1988; Burrows and Thorpe, 1994]. Thus, molecules can only penetrate the tumor by diffusion which is a slow process [Jain and Baxter, 1988].

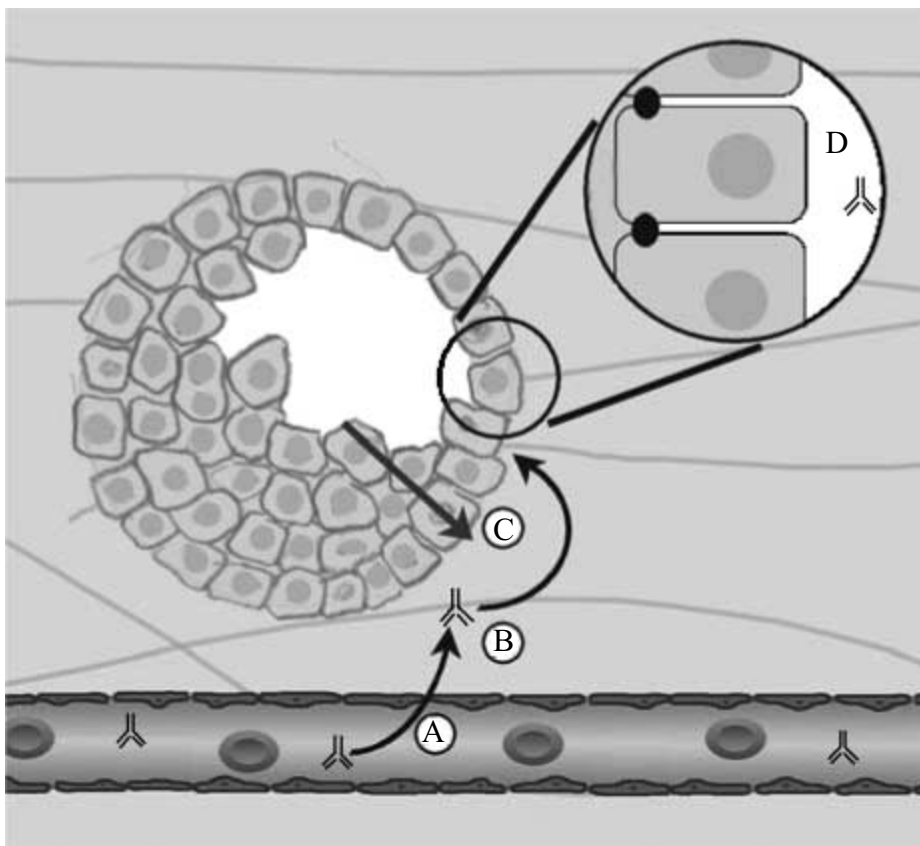


Figure 1. Schematic overview of biological barriers to effective treatment of solid tumors with monoclonal antibody-based immunotherapy. To reach a target antigen at the surface of a solid tumor, i.v. injected monoclonal antibody must first traverse the microvascular endothelium (A), and must subsequently contend with stromal barriers (B), and high interstitial fluid pressure characteristic of bulky tumor masses (C). Monoclonal antibodies may also confront epithelial barriers (D), including E-cadherin and tight junctional complexes that may have a profound impact on therapy [From Christiansen and Rajasekaran, 2004].

Another possible barrier against the homogenous distribution of antibodies/immuno-conjugates is the binding-site barrier [Burrows and Thorpe, 1994], in which monoclonal antibodies with high affinity for tumor antigens bind stably to the first encountered tumor antigen leading to a heterogeneous antibody delivery to the tumor cells [Adams *et al.*, 2001; Juweid *et al.*, 1992]. Sung *et al.*, compared the spatial distribution of the diphtheria toxin (DT) and non-binding DT linked to a transferrin antibody. They found that the spatial distribution of the toxin was remarkably even throughout the tumor compared to the anti-transferrin coupled toxin, which was localized primarily in the perivascular space [Sung *et al.*, 1993]. It was suggested that as the tumor cells in this study exhibited an extremely low number of DT receptors (< 3000/cell), DT was therefore not depleted rapidly by the perivascular tumor cells, whereas the tumor cells exhibited a high number of transferrin receptors (60,000 receptors/cell). Therefore, the immuno-toxin was quickly sequestered by the perivascular tumor cells [Sung *et al.*,

1993]. The difference in distribution could also have been due to the different sizes of the two tested molecules. Site-directed mutagenesis made it possible to compare the distribution of antibodies targeting the same epitope with different affinities. One study showed that single chain fragments (scFv) targeting the human epidermal growth factor receptor 2 (HER-2) with low affinity (3.2×10^{-7} M) were distributed homogeneously throughout the tumor, whereas the same scFv with a higher antigen affinity (1.5×10^{-11} M) only traversed 2-3 cell diameters [Adams *et al.*, 2001]. In summary, targeting the tumor cells with antibodies or immuno-conjugates is often hampered by a combination of an elevated IFP and sequestering of the antibody by various cellular barriers, such as the binding-site barrier.

Another problem with targeting tumor cells is the heterogeneous expression of antigens within a given tumor population and between various tumors [Burrows and Thorpe, 1994]. Epithelial cancer cells are known for their genetic instability generating a high degree of heterogeneity of the different tumor cell clones found in an individual tumor [Braun *et al.*, 1999]. This is thought to impose a major limitation on treatments aimed at targeting the tumor cells. Much work has been put into refining the selectivity of monoclonal antibodies to target a larger fraction of the tumor population and successful candidates have indeed been found [Christiansen and Rajasekaran, 2004]. The therapeutic antibody Herceptin[®] against HER-2, a member of class 1 receptor tyrosine kinases, is approved for treatment of metastatic breast cancer [Cobleigh *et al.*, 1999]. Also, an antibody against the epithelial cellular adhesion molecule Panorex[®] is being used in the treatment of colorectal cancer [Riethmuller *et al.*, 1994; Riethmuller *et al.*, 1998]. However, due to the heterogeneous expression of tumor antigens, different antibodies must be developed for different types of cancer. Extensive typing of the different cellular subtypes in the individual tumor needs to be carried out during treatment, making it difficult to develop a targeted therapy with a broad applicability [Burrows and Thorpe, 1994].

Targeting tumor cells in solid tumors has encountered several problems, such as heterogeneous distribution of antibodies and immuno-conjugates, and antigen heterogeneity within one tumor and between tumors. However, targeting the tumor vasculature instead of the tumor cells could prove to be an advantage because of several distinctive features, which will be described below.

1.1.2 Advantages of targeting the tumor vasculature

Historically, the vasculature has been known as the “Achilles heel” of solid tumor growth [Siemann *et al.*, 2005] and has been an indirect target in cancer therapy since the 1700s, where bacterial infections were used in the treatment of cancer [Starnes, 1992]. As previously mentioned, the tumor needs to form new blood vessels by the process of angiogenesis in order to grow beyond ~ 2 mm [Brem *et al.*, 1976; Folkman, 1986]. Angiogenesis occurs rarely in healthy adults, i.e. during the menstrual cycle, wound healing and embryonic development. The angiogenic tumor vasculature is therefore an interesting and selective target in solid tumors, present in both primary tumors and metastases [Bazan-Peregrino *et al.*, 2007]. Vascular-targeted drugs inhibit or kill tumors by starvation with agents that target and selectively damage tumor endothelium by either inhibiting angiogenesis or inducing a vascular collapse as opposed to exerting a direct effect on the rapidly growing tumor cells, [Huang *et al.*, 1997; Philipp *et al.*, 2003; Siemann *et al.*, 2005]. Vascular targeting looks promising for the delivery of drugs [Pastorino *et al.*, 2003], genes [Hood *et al.*, 2002] and radionuclide’s [Li *et al.*, 2004] to the tumor.

One advantage of vascular targeting is the easy accessibility of the tumor endothelial cells. Targeting tumor vasculature with antibodies or immuno-conjugates is attractive because receptors and other target structures are readily available for binding directly in the blood stream [Oh *et al.*, 2004; Simberg *et al.*, 2007]. The direct access to the target skips the extravasation step from the blood into the tumor parenchyma [Oh *et al.*, 2004]. In addition, accumulation of antibodies at the endothelium is fast compared to accumulation in the solid tumor parenchyma [Burrows *et al.*, 1992]. Kennel *et al.*, showed that the maximal level of IgG accumulation in solid tumors was reached after 7 days [Kennel, *et al.*, 1991], whereas a saturation of endothelial binding sites at the tumor endothelium could be seen after 1 hour [Burrows *et al.*, 1992; Kennel, *et al.*, 1991]. It might therefore be easier and quicker to achieve accumulation of antibodies or immuno-conjugates at the tumor vasculature as compared to tumor cells.

In normal tissues, there are usually 1 or 2 layers of cells surrounding an individual vessel; in muscle tissue several capillaries supply one muscle fiber. The vessel network is highly organized and responds well to extra demands during stress [Denekamp, 1999]. In contrast, in tumor tissues one vessel supplies many hundreds or even thousands of tumor cells (Fig. 2). Untreated tumors show viable cells lying in a cuff around open vessels

corresponding to the limit of oxygen diffusion ($\sim 100 \mu\text{m}$) [Vauple *et al.*, 1989]. These cuffs are however surrounded by foci of necrosis [Kerbel and Folkman, 2002]. The destruction of one vessel therefore results in massive tumor cell death [Burrows and Thorpe, 1994; Denekamp, 1999], thereby amplifying the initial response.

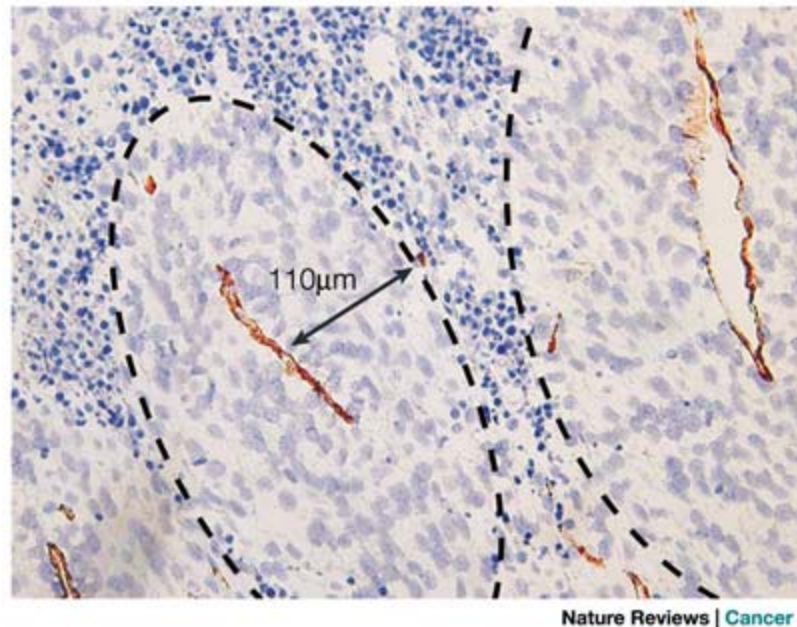


Figure 2. Tumor cells within $110 \mu\text{m}$ of a microvessel are viable (dashed line). Outside of this radius, tumor cells are dead [Kerbel and Folkman, 2002].

During the transformation from normal cell to neoplastic cells, tumor cells undergo multiple genetic changes [Hoffmann, 1990], which enables the tumors to quickly adapt to hostile environments by generating a new subpopulation. The plasticity of the tumor cell genome induces the development of resistance to therapies which are aimed directly at the tumor cell population [Kerbel, 1991]; in contrast, the tumor endothelial cells are genetically stable and therefore less likely to acquire mutations and develop drug resistance [Kerbel, 1991; Boehm *et al.*, 1997; Kerbel and Folkman, 2002].

Tumor endothelial cells have a relatively high proliferation due to the tumor cell production of pro-angiogenic cytokines, such as vascular endothelial growth factor (VEGF), basic fibroblast growth factor (bFGF), transforming growth factor β (TGF- β) and various interleukins [Kerbel and Folkman, 2002]. The pro-angiogenic state results in the expression of surface antigens that are not expressed by normal endothelium [Burrows and Thorpe, 1994]. The similarities in tumor vasculature and behavior between various tumors make it possible to target the same tumor endothelial antigen in a broad

variety of solid tumors [Denekamp, 1990; Lee *et al.*, 2007]. In contrast to when targeting tumor cells, a single antibody could have a broad applicability. Furthermore, tumor endothelial cells express several proteins, including adhesion molecules, such as vascular cell adhesion molecule 1 (VCAM), E-selectin and endoglin [Burrows and Thorpe, 1994], α -integrins [Arap *et al.*, 1998; Lee *et al.*, 2007] and receptors for certain angiogenic growth factors [Arap *et al.*, 1998; Bazan-Peregrino *et al.*, 2007], or stromal components [Simberg *et al.*, 2007], which are not expressed by normal endothelium and can therefore be used to specifically target tumor vasculature.

The development of a drug delivery system that specifically targets tumor endothelium has many advantages; one such delivery system could be liposomes.

1.2 Immunoliposomes as a drug delivery system

Liposomes are nanoscale biocompatible drug carriers which can accommodate large amounts of both hydrophilic and lipophilic drugs entrapped in the aqueous core or the lipid bilayer, respectively [New, 1990; Sharma and Sharma, 1997]. Liposomes have been used as delivery systems for a broad spectrum of drugs including chemotherapy, imaging agents, antigens, lipids and nucleic acids [Marty *et al.*, 2002].

Plain liposomes are made of phospholipids and sometimes cholesterol [Torchilin, 1994]. When these liposomes are introduced into circulation, they are rapidly sequestered by macrophages of the reticuloendothelial system (RES) mainly located in the liver and spleen [Papahadjopoulos *et al.*, 1991]. Thus, they display a short blood half-life (min) and have a limited use as drug delivery carriers for transporting drugs to other sites than the RES. This led to the development of long-circulating liposomes, where specific amphiphiles, such as polyethylene glycol (PEG)-coupled phospholipids [Lasic *et al.*, 1991], the ganglioside GM1 [Allen and Chonn, 1987; Gabizon and Papahadjopoulos, 1992] or hydrogenated phosphatidylinositol [Gabizon and Papahadjopoulos, 1992], were incorporated into the lipid membrane. This created a sterical stabilisation, which to increased liposome stability and blood half-lives required to ensure targeted delivery of the liposome to the right place of action [Allen *et al.*, 1995]. PEG turned out to be the most applicable to sterically stabilise liposomes and other nano-carriers, because it is easy to prepare, its molecular weight is easy to control, it links easily to lipids and increases circulation time most effectively [Maruyama *et al.*, 1995].

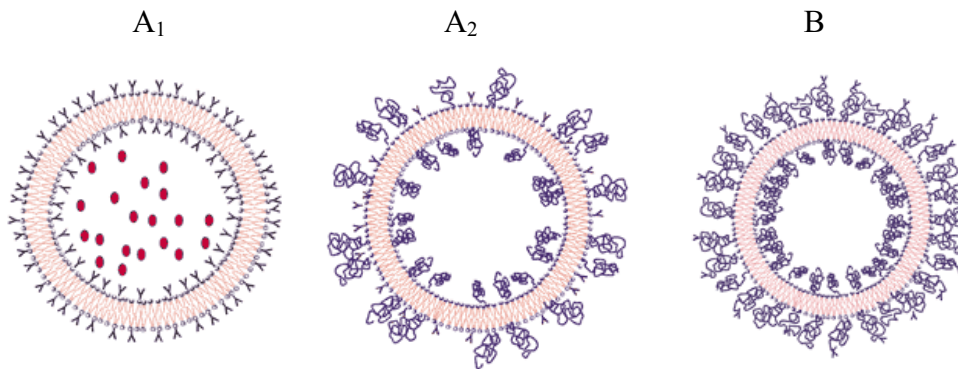


Figure 3. Immunoliposomes - (A₁) antibodies attached to the surface of conventional liposomes; (A₂) antibodies attached to the surface of sterically stabilized liposomes (B) antibodies attached to the distal ends of polyoxyethylene chains in sterically stabilized liposomes. [Modified from www.pjonline.com/.../education/parenteral.html]

The coupling of antibodies or antibody fragments to the surface of liposomes for site-specific targeting results in immunoliposomes (ILs) (Fig. 3) [Kontermann, 2006]. Three different types of ILs have been investigated. Type A₁ where the antibody is conjugated to the lipids of the lipid bilayer, type A₂ where the antibody is conjugated to the lipid bilayer on the surface of a PEG-liposome and type B where the antibody is conjugated to the distal end of the PEG chain [Maruyama *et al.*, 1995]. Type A₁ liposomes are, like conventional liposomes, cleared rapidly from circulation by RES, which reduces the targetability of the liposome [Torchilin, 1994; Hansen *et al.*, 1995]. Type A₂ liposomes attain longer circulation time because of the PEG, but encounter problems with binding to the target site. This is due to the steric barrier created by PEG [Klibanov *et al.*, 1991]. Type B ILs have the advantage over type A₁ and type A₂ in that they bind to their binding site efficiently, because the antibody is presented on the tip of the PEG [Blume *et al.*, 1993; Maruyama *et al.*, 1995]; and at the same time they retain a long circulation time [Maruyama *et al.*, 1995].

1.2.1 Liposome distribution in vivo

The process of targeted drug delivery can be divided into two phases after administration [Mastrobattista *et al.*, 1999]. The transport phase, where liposomes travel to the target cells, and the effector phase, where the liposomes are taken up by cells or deliver the drug at the target site. During the transport phase the liposomes encounter various problems that are discussed below.

The biodistribution of systemically administered liposomes has been studied extensively, and unspecific localization of liposomes, especially to the liver and spleen, has been observed [Proffitt *et al.*, 1983; Dams *et al.*, 2000; Bendas *et al.*, 2003]. Elimination of liposomes through the RES [Gabizon and Papahadjopoulos, 1988] presents a problem, since it reduces the effective bioavailability of administered drugs.

The removal of foreign particles in RES is part of a host defense mechanism, where macrophages in various tissues, such as the liver and spleen, remove foreign particles from the circulation [Oku and Namba, 1994]. Plasma proteins and components play an important role in RES-mediated clearance as it has been shown that liposomes in media without blood components are not taken up by the liver [Semple *et al.*, 1998]. Liposome uptake is believed to involve opsonic and scavenger receptors. Opsonins bind to the surface of liposomes and tag them so that they are recognized and engulfed by macrophages of the RES [Semple *et al.*, 1998; Ishida *et al.*, 2002]. The rate of clearance and opsonization is dependent on lipid composition, particle size and surface hydrophilicity [Allen and Chonn, 1987; Gabizon and Papahadjopoulos, 1992]. Thus small liposomes with a rigid membrane and incorporated PEG are removed slower from circulation by opsonization and RES [Gabizon and Papahadjopoulos, 1988].

There are other clearance problems specific for immunoliposomes. The clearance of immunoliposomes is enhanced when the target moiety is a whole antibody with a Fc-domain. This makes the immunoliposome susceptible to Fc-mediated phagocytosis by Fc-receptor expressing cells from RES [Aragnol and Leserman, 1986; Mastrobattista *et al.*, 1999]. Instead of using whole antibodies, several investigators have suggested the use of Fab' [Maruyama *et al.*, 1997], scFv [Xu *et al.*, 2002; Völkel *et al.*, 2004; Mamot *et al.*, 2005] or peptides [Kondo *et al.*, 2004; Simberg *et al.*, 2007], which could reduce the interaction with the RES and thereby prolong circulation time [Shahinian and Silvius, 1995].

Another factor that influences immunoliposomal clearance is the amount of antibody coupled to the liposome. Allen *et al.* showed that a high antibody density (140 $\mu\text{g}/\mu\text{mol}$ lipid) increased the plasma clearance of IL as compared to moderate antibody densities (20-80 $\mu\text{g}/\mu\text{mol}$ lipid) [Allen *et al.*, 1995].

Antibodies on the liposomal surface have been shown to induce an immune response [Phillips *et al.*, 1994; Harding *et al.*, 1997; Bendas *et al.*, 2003] and that repeated administration of ILs results in drastically decreased circulation times. Antibody titers

against ILs were elevated in individuals compared to those injected repeatedly with free antibody or PEG-liposomes and antibody separately [Harding *et al.*, 1997]. Thus, it seems that it is the administration of the whole immunoliposomal complex that induces the immune response [Phillips *et al.*, 1995]. Bendas *et al.* investigated the influence of the grafted position of the antibody (i.e. type A₂ vs. type B) on the immunogenicity and found that ILs with antibodies on the tips of the PEG chains exhibited sufficient circulation time, also after repeated injections [Bendas *et al.*, 2003]. It was suggested that the coupling method has an important impact on the immunogenicity and should therefore be determined for individual liposome preparations.

The binding of antibodies to the surface of liposomes and the macrophages of the RES are factors that reduce the circulation time thereby preventing the liposome from reaching its target in the tumor. However, there are also forces that enhance the accumulation of liposomes in solid tumors. These forces are the result of the enhanced vascular permeability of the endothelial barrier and the lack of lymphatics in tumors, and are termed “the enhanced permeability and retention (EPR) effect” [Matsumura and Maeda, 1986; Maeda *et al.*, 2004]. As previously mentioned, it has been shown that macromolecules, such as albumin, poly-(styrene-co-maleic acid half-*n*-butylate), conjugated neocarzinostatin [Matsumura and Maeda, 1986], proteins and liposomes [Kirpotin *et al.*, 2006], exhibit an enhanced accumulation in solid tumors [Noguchi *et al.*, 1998]. EPR is responsible for the passive accumulation of non-targeted sterically stabilized liposomes in the tumor, and the reason why non-targeted and targeted liposomes targeting the tumor endothelium or cells accumulate in the tumor to the same degree [Kirpotin *et al.*, 2006]. Therefore, it is essential to determine the exact localization of the targeted liposomes when evaluating whether the ILs target successfully.

1.2.2 Vascular-targeted liposomes

The advantages of targeting the tumor endothelium and using ILs instead of immuno-conjugates as a drug delivery system have been combined in the development of vascular targeted liposomes. Several *in vitro* studies report on targeting endothelial cells with ILs in an effort to ultimately place liposomes at sites of inflammation or tumor vasculature. The targeted receptors in those studies include endoglin [Volkel *et al.*, 2004], vascular endothelial growth factor receptor 2 [Benzinger *et al.*, 2000], galectin-1

[Brandwijk *et al.*, 2007] intercellular adhesion molecule 1 [Bloemen *et al.*, 1995] E-selectin [Spragg *et al.*, 1997; Kessner *et al.*, 2001], P-selectin [Scott *et al.*, 2006] and VCAM [Chiu *et al.*, 2003; Voinea *et al.*, 2005, Gosk *et al.*, 2005]. *In vivo*, ILs can be made to target inflamed vasculature [Everts *et al.*, 2003] or vessels in areas of myocardial infarction [Nallamotheu *et al.*, 2006; Scott *et al.*, 2006]. Several *in vivo* studies have investigated the tumor vascular targetability of liposomes decorated with peptides. These peptides include RGD motifs binding to $\alpha_v\beta_3$ integrins [reviewed in Temming *et al.*, 2005; Nallamotheu *et al.*, 2006; Lee *et al.*, 2007], NGR motifs binding to aminopeptidase N [Pastorino *et al.*, 2006], CREKA binding to fibrinogen or fibrin [Simberg *et al.*, 2007], GPLPLR binding to membrane type-1 matrix metalloproteinase [Kondo *et al.*, 2004], peptides binding to unknown receptors such as APRPG [Maeda *et al.*, 2004], and the synthetic angiostatic peptide aniginex binding to galectin-1 [Brandwijk *et al.*, 2007], which is a carbohydrate-binding protein with affinity for β -galactosidase [Camby *et al.*, 2006].

Much research is being carried out with liposomes coupled to peptides. Peptides, instead of antibodies, have the advantage of a lesser clearance from the circulation by escaping the Fc-receptor containing cells [Maruyama *et al.*, 1997] and properly also reducing the immunogenic response. Conceptually, peptides should also be superior to antibodies when aiming at targeting a compartment. Their small size and generally lower affinity potentially facilitates penetration into the tumor tissue. Furthermore, the generally lower binding affinity of peptides compared to antibodies can be of advantage when targeting the *tumor cell* compartment [Maeda *et al.*, 2004], by escaping the binding site barrier. In contrast, high affinity binding would be preferable for robust *tumor vascular* targeting, since ligands that bind to the luminal side of blood vessels are exposed to the dynamic flow environment of the blood stream. It is generally believed that most antibodies possess higher affinity binding properties than peptides. For example, to block the VCAM mediated leukocyte-endothelium interaction, a VCAM-binding peptide was applied at a 650-fold higher molar concentration than a VCAM-binding antibody to obtain similar degrees of inhibition [Kelly *et al.*, 2005].

1.2.3 VCAM as a target on the tumor endothelium

As mentioned earlier the tumor vasculature expresses molecules that are not present on normal endothelium. In the development of a vascular targeting drug delivery system it is important to choose a target, which ensures specificity and is widely applicable. VCAM was chosen for the work described here.

VCAM is an immunoglobulin-like transmembrane glycoprotein of 110 KDa (Fig. 4) expressed on activated endothelial cells during inflammation and cancer [Osborn *et al.*, 1989].

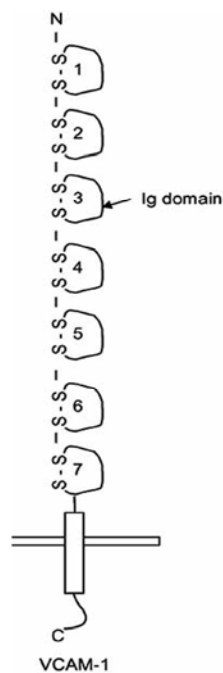


Figure 4. Protein structure of VCAM. VCAM-1 has 6-7 immunoglobulin-like domains [Kobayashi *et al.*, 2007].

VCAM, also known as CD106, is a molecule with a well-characterized role in the immune system where it promotes firm cell-cell adhesion between migrating leukocytes and activated endothelial cells (Fig. 5). The mechanism of leukocyte migration to sites of inflammation is well characterized. Briefly, the cells interact in a sequential manner, where different types of adhesion molecules play different roles. First, the circulating leukocytes bind to selectins on the activated endothelium; this induces the leukocytes to roll along the endothelium. Following the rolling movement, other cell adhesion molecules of the integrin family that interact with members of the Ig-superfamily, such as VCAM or ICAM-1, mediate firm adhesion of leukocytes to the activated endothelium.

Subsequently, this leads to the transendothelial migration of the leukocytes [Kobayashi *et al.*, 2007].

VCAM is an endothelial ligand for both integrins, very late antigen 4 (VLA-4) and $\alpha_4\beta_7$ [Wu *et al.*, 2007], where VLA-4 is the most common receptor [Charpin *et al.*, 1998]. VLA-4 is expressed on inflammatory leukocytes, on some tumor cells and also on tumor endothelial cells. Besides their role in promoting cell-cell contacts between leukocytes and inflamed endothelium [Rice *et al.*, 1990], the VCAM-VLA-4 interactions mediate binding of VCAM-positive pericytes and tumor endothelium [Garmy-Susini *et al.*, 2005], pro-angiogenic macrophages and tumor endothelium [Jin *et al.*, 2006], or metastatic tumor cells and tumor vasculature [Klemke *et al.*, 2007]. Therefore, VCAM plays an important role in tumor angiogenesis and metastasis.

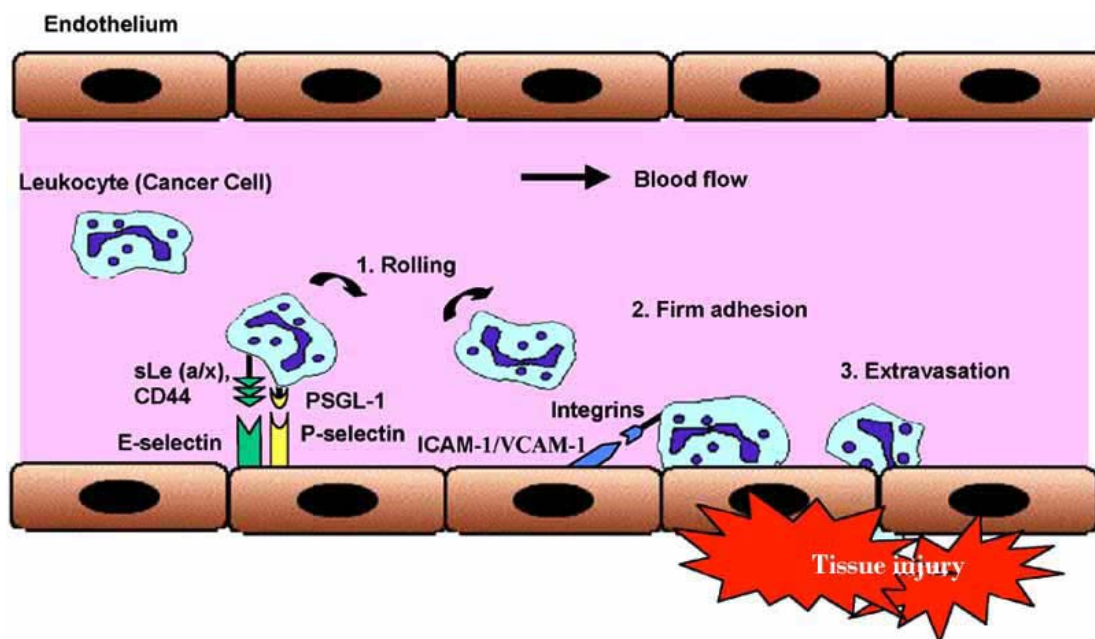


Figure 5. Leukocytes or cancer cells interact in a sequential fashion with adhesion molecules on vascular endothelium; 1) Rolling along the endothelial surface; 2) Firm adhesion to endothelium; 3) Extravasation of leukocytes or cancer cells to targeted tissue [Kobayashi *et al.*, 2007].

If VCAM is to be considered a potential target structure in the tumor vasculature, VCAM expression needs to exhibit some degree of tumor vasculature specificity. VCAM expression is inducible and virtually absent in normal human vasculature [Kuzu *et al.*, 1993]. Its expression is induced by pro-inflammatory cytokines such as tumor necrosis factor α (TNF- α), interleukin 1 β (IL-1 β) [Wuthrich, 1994], IL-4 and interferon- γ (INF- γ) [Wu *et al.*, 2007]. Non-vascular cells with VCAM expression include bone marrow cells,

follicular dendritic cells, fibroblasts, and epithelial cells in the kidney [Ryan *et al.*, 1991; Seron *et al.*, 1991]. However, the expression of VCAM outside the vasculature does not pose a major problem when targeting VCAM on tumor vascular, as the targeted liposomes will not come into contact with the other cells.

Several diseases are associated with VCAM expression on the vascular endothelium, such as atherosclerosis, inflammatory diseases and autoimmune diseases [Dedrick *et al.*, 2003]. In cancer, robust vascular VCAM expression has been observed in leukemias and lymphomas, such as Hodgkin's disease and B-cell chronic lymphatic leukemia, and to varying degree in a variety of solid tumors such as lung cancer, breast cancer, melanoma, renal cell carcinoma, gastric cancer and neuroblastoma [reviewed in Dienst *et al.*, 2005]. The expression of VCAM on various solid tumors makes VCAM an ideal target on the tumor endothelium.

The fate of VCAM upon binding to its ligand is controversial. One study showed that after ligand binding, VCAM was internalized via a clathrin-dependent pathway with a half-life of 15 minutes in human umbilical vein-derived endothelial cells (HUVEC) [Ricard *et al.*, 1998]. Another study found that VCAM remained mostly on the surface of the activated HUVEC [Kuijpers *et al.*, 1994], whereas other studies suggest that parts of VCAM are shedded from the endothelial surface. The fate of VCAM after ligand binding needs still to be investigated.

An alternative to creating an immunoliposomal system that targets the tumor cells would be the development of a liposomal drug delivery system that targets the VCAM at the tumor endothelium. The development of vascular acting anti-tumor drugs is being studied extensively. They could be used alone or in concert with conventional chemotherapy.

1.3 Vascular targeting drugs

As described above, targeting tumor vasculature has many advantages. The use of conventional chemotherapy to kill tumor endothelium has been investigated. Two approaches have been tried; changing the treatment schedule [Hanahan *et al.*, 2000; Miller *et al.*, 2001] and targeting conventional cytotoxic anticancer drugs to the tumor endothelium using i.e. liposomes [Maeda *et al.*, 2004; Pastorino *et al.*, 2003; 2006; Lee *et al.*, 2007]. Conventional anticancer drugs are known to have an anti-angiogenic effect *in*

vitro and *in vivo* [Miller *et al.*, 2001]. The administration of low doses of conventional chemotherapy at constant intervals without resting periods can kill the tumor vasculature and at the same time exhibit low host toxicity [Browder *et al.*, 2000; Hanahan *et al.*, 2000].

Apart from conventional therapy, two novel classes of drugs have emerged. They primarily target the tumor endothelial cells and exhibit an alternative molecular action. One approach targets key factors required for the formation of new vessels: anti-angiogenesis agents [Kerbel, 2001; Siemann *et al.*, 2005], who inhibit angiogenesis and are thought to normalize the vascular function by reestablishing the balance between the pro- and anti-angiogenesis factors [Jain, 2005]. Some angiogenesis inhibitors have been clinically approved. One example is Bevacizumab, a humanized monoclonal antibody targeting VEGF. Bevacizumab has shown clinical effects on colorectal cancer, breast cancer and non-small cell lung cancer in combination with cytotoxic chemotherapy [Hurwitz *et al.*, 2004; Ramaswamy *et al.*, 2006; Sandler *et al.*, 2006]. Furthermore, it is used as a single agent in the treatment of metastatic renal cell carcinoma [Hinnen and Eskens, 2007].

The second approach takes advantage of the differences between blood vessels in normal tissue and those of the tumor vasculature by targeting and destroying the existing tumor vasculature. These agents are called vascular disrupting agents (VDA) [Dienst *et al.*, 2005; Siemann *et al.*, 2004].

VDAs destroy the tumors by inducing occlusion of the tumor vasculature. Occlusion leads to tumor cell starvation due to the lack of oxygen and nutrients [Thorpe, 2004] which in turn leads to widespread necrosis in the tumor. VDAs are distinguished from anti-angiogenic drugs by targeting existing vessels which makes them well suited in the treatment of large bulky tumors (Fig. 6) [Siemann *et al.*, 2004; Thorpe, 2004].

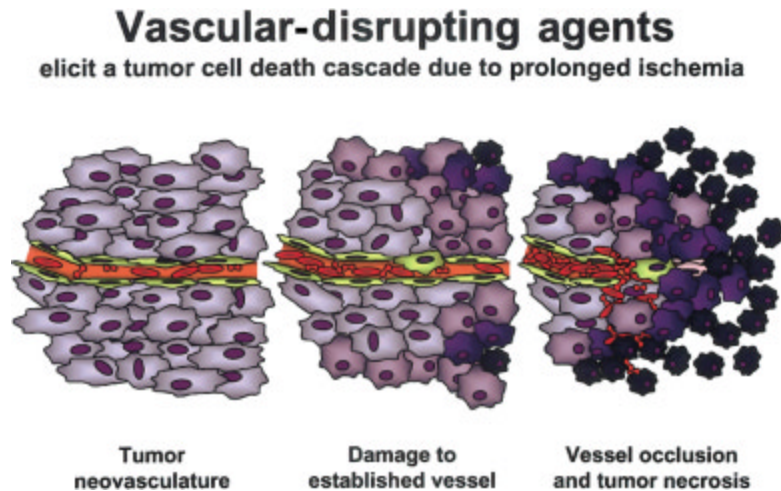


Figure 6. Proposed principle of action of vascular-disrupting agents. A single vessel provides nutritional support to large numbers of tumor cells. Treatment with a vascular-disrupting agent induces endothelial cell dysfunction, which leads to partial occlusion of the vessel. The resulting diminished blood flow causes tumor cells farthest from the vessel to become increasingly hypoxic. As damage to the endothelium progresses, coagulation events are initiated, and blockage of the vessel ultimately occurs. This loss of vessel patency results in widespread tumor cell necrosis. [From Siemann *et al.*, 2005]

VDAs can be divided into two types; the ligand-directed VDAs and the small molecule VDAs. The ligand-directed VDAs use targeting ligands that specifically bind to structures on tumor endothelium and thereafter induce occlusion of the tumor vessel [Huang *et al.*, 1997; Ran *et al.*, 1998; Chiu *et al.*, 2003; Dienst *et al.*, 2005]. The small molecule VDAs exploit the pathophysiological differences between tumor and normal vasculature, i.e. increased proliferation, permeability and a reduced reliance on the tubulin cytoskeleton to maintain cell shape [Denekamp, 1990; Thorpe, 2004].

However, treatment with VDAs does not lead to complete tumor regression, but leaves a ring of viable tumor cells in the tumor periphery [Pastorino *et al.*, 2003; Huang *et al.*, 1997]. These tumor cells obtain oxygen and nutrition from normal tissue vessels that are not targeted by the VDAs and therefore exhibit a good oxygen status resulting in tumor cells that are susceptible to conventional therapies, i.e. radiation or chemotherapies, which are most effective on well-oxygenated cells [Siemann *et al.*, 2004; Horsman and Siemann, 2006].

1.3.1 Ligand-directed VDAs

Several approaches based on linking antibodies or peptides that recognize tumor endothelium epitopes to effector molecules, that induce endothelial damage by selective

occlusion, have been investigated. The properties essential for the targeting moieties have been described above. The effector molecules exhibit a variety of activities including a direct or indirect induction of thrombosis. They redirect the host defense to attack the tumor, or change the morphology of the tumor endothelial cells to physically block the vessel [Thorpe, 2004]. The direct killing of endothelial cells by targeting toxins to the tumor was proven to be a successful approach. Several studies used chimeric fusion proteins with a toxin as the effector moiety targeted to the VEGF receptor. The effects of at least two different toxins, gelonin [Veenendaal *et al.*, 2002] and diphtheria toxin [Arora *et al.*, 1999], have been studied *in vitro* and *in vivo*. They induced thrombotic damage selectively at the tumor vessels and delayed tumor growth [Arora *et al.*, 1999; Veenendaal *et al.*, 2002]. Matsuno *et al.*, targeted deglycosylated ricin A to the proliferation-associated antigen, endoglin, in mice bearing MCF-7 human breast cancer xenografts. This resulted in complete tumor regression [Matsuno *et al.*, 1999].

An alternative approach is to activate the host defense system by targeting inflammatory cytokines to the tumor vasculature. Targeting the tumor vasculature by creating a fusion protein in which the targeting part is the angiogenesis-associated isoform of fibronectin, ED-B, and the effector part being either IL-2 [Carnemolla *et al.*, 2002] or IL-12 [Halin *et al.*, 2002] resulted in a significant, higher accumulation of tumor infiltrating T-lymphocytes, natural killer cells, macrophages and a delay in tumor growth time [Carnemolla *et al.*, 2002; Halin *et al.*, 2002]. However, the clinical application of cytokines is often hampered by severe systemic side effects.

To avoid cytokine-induced side effects, ILs have been proposed as a delivery system in the development of ligand-directed VDAs. Liposomes have the advantage over immuno-conjugates in that they can encapsulate many effector molecules and therefore display a much higher ratio of effector molecules per targeting moiety [Marty *et al.*, 2002]. In addition, liposomes change the biodistribution and pharmacokinetics of drugs, thereby protecting the drug from metabolization and protecting the organism against the cytotoxic effects of the drug. The majority of studies on liposomal targeting of tumor vasculature have used liposomes encapsulated with conventional chemotherapeutics, such as doxorubicin [Volkel *et al.*, 2004; Hölig *et al.*, 2004; Pastorino *et al.*, 2003, 2006; Lee *et al.*, 2007] or adriamycin [Maeda *et al.*, 2004]. However, a few studies encapsulated a different class of drugs in the liposomes. Encapsulation of combretastatin A4, a small molecule VDA that induces depolymerisation of microtubules and disorganization of

actin and tubulin, was successful *in vitro* [Nallamotheu *et al.*, 2006]. Cationic liposomes were developed carrying a mutated form of the *Raf* gene, *ATP^u-Raf*, which blocks endothelial signaling and angiogenesis as a response to multiple growth factors. Treatment with these nano-particles resulted in endothelial apoptosis and regression of both primary and metastatic tumors [Hood *et al.*, 2002]. In addition, vascular targeted liposomes with the stable isotope ¹⁰B were shown to reduce cell viability *in vitro* by neutron capture therapy [Koning *et al.*, 2004].

1.3.2 Coagulation inducing VDAs

1.3.2.1 Tissue factor as the effector in ligand-directed VDAs

Another strategy that has proven successful is enhancing the pro-coagulative state of the tumor vasculature by directing truncated tissue factor (TF) to the tumor endothelium. Expression of TF at the tumor endothelium initiates the coagulation cascade leading to occlusion of the vessel. Truncated TF, consisting of the extracellular domain of the protein, has been investigated for anticancer treatment. The ability of truncated TF to induce coagulation is greatly reduced compared to full length TF [Philipp *et al.*, 2003]. Free truncated TF in circulation does not induce clotting but becomes pro-coagulant when in contact with the endothelium [Thorpe, 2004]. One study describing the effect of truncated TF on tumor vasculature showed that free truncated TF alone did not have significant effects on tumor cell death. In contrast, when truncated TF was given in combination with low concentrations of bacterial lipopolysaccharide (LPS), which is an initiator of the immune system and coagulation system, a selective thrombosis of tumor vessels was found [Philipp *et al.*, 2003]. This indicates that an additional pro-coagulative activation was essential for the non-targeted truncated TF to become fully active. Therefore, to increase the activity and localize the truncated TF directly to the tumor endothelium, several research groups created fusion proteins linking a targeting moiety to truncated TF.

Tumor vessel markers such as MHC class II [Huang *et al.*, 1997], VCAM [Ran *et al.*, 1998; Dienst *et al.*, 2005], the ED-B domain of fibronectin [Nilsson *et al.*, 2001], and prostate-specific membrane antigen [Liu *et al.*, 2002] conjugated to truncated TF, induced intravascular thrombosis and tumor growth delay in various solid tumors *in vivo* [Thorpe, 2004]. The hypothesis that an increase in TF concentration and activity at the tumor

endothelium could lead to tumor regression due to vessel occlusion was proven successful. However, inducing an up-regulation of native TF on the tumor vessels with cytokines or drugs could be an alternative to the treatment with truncated TF.

1.3.2.2 TF and the coagulation cascade

TF is a membrane-bound 47 kDa glycoprotein which plays an essential role in the initiation of extrinsic coagulation cascade *in vivo* (Fig. 7). The primary function of TF (in adults) is to initiate coagulation. This occurs when TF is exposed to coagulation factors in the bloodstream due to vascular injury. The extracellular domain of TF then becomes essential by binding to and acting as a cofactor for factor VII/ VIIa. The TF:VIIa complex acts as a serine protease converting factor IX and X to factor IXa and Xa, respectively, via limited proteolysis [Rehemtulla *et al.*, 1991; Bogdanov *et al.*, 2006]. The activated factor Xa together with its co-factor factor Va catalyses the conversion of prothrombin to thrombin. Thrombin cleaves fibrinogen to fibrin which together with platelets forms a stable clot (Fig. 7).

The vast majority of factor VII is found as a zymogene in circulation and less than 1 % is found as the activated factor VIIa. The conversion of factor VII in circulation is mediated by coagulation proteases, presumably primarily by factor XIa [Wildgoose *et al.*, 1992], but other factors such as factor IXa, Xa, XIIa, thrombin and plasmin have been shown to convert factor VII to factor VIIa *in vitro* [Morrissey, 2001]. TF can bind both the zymogene and the activated factor VIIa. The majority of factor VII is rapidly converted to its active state after binding to TF [Nemerson and Repke, 1985; Rao and Rapaport, 1988], and the TF:VIIa complex can catalyze the activation of factor VII in an auto-activation reaction [Morrissey, 2001].

The activity of coagulation proteins is strongly enhanced by binding to negatively charged membrane phospholipids, such as phosphatidylserine (PS). Therefore, free coagulation factors in the circulation display a negligible activity towards their respective substrates [Zwaal *et al.*, 1998]. Under normal conditions PS is found in the inner leaflet of the membrane. However, upon cell injury or platelet activation it is translocated to the outer leaflet, thereby controlling the coagulation cascade under normal conditions.

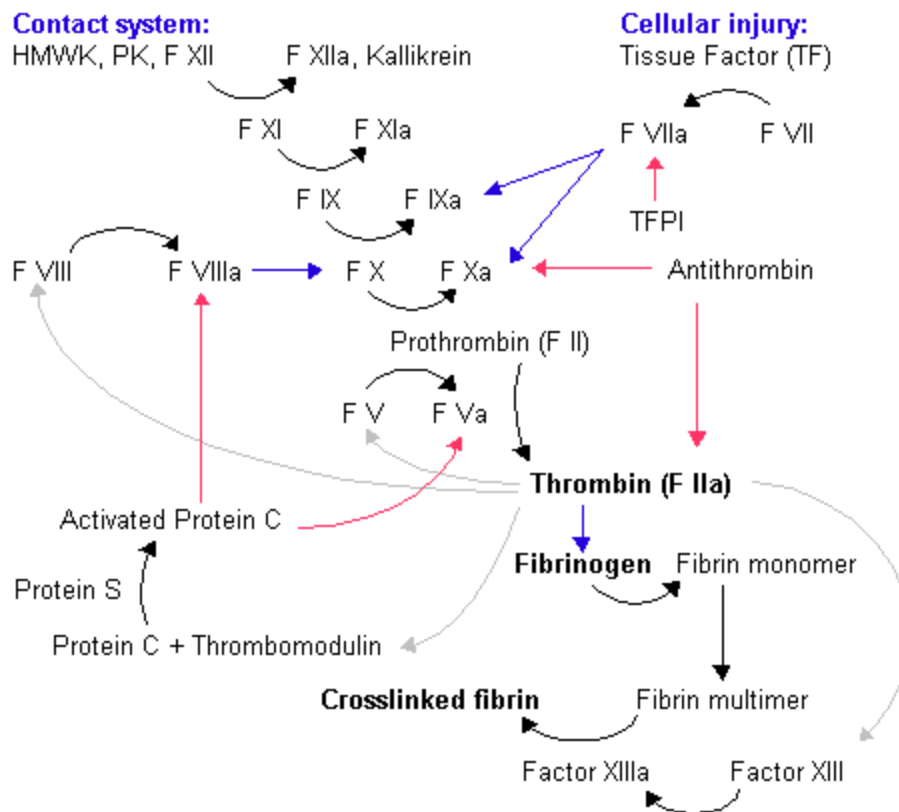


Figure 7. Schematic illustration of the intrinsic (contact system) and extrinsic (cell injury) coagulation cascade. Tissue factor pathway: the main role of the tissue factor pathway is to generate a "thrombin burst". TF forms a complex with FVIIa (TF-FVIIa) which activates FIX and FX. FVII itself is activated by thrombin, FXIa, plasmin, FXII and FXa. The activation of FXa by TF-FVIIa is almost immediately inhibited by tissue factor pathway inhibitor (TFPI). FXa and its co-factor FVa form the prothrombinase complex, which activates prothrombin to thrombin. Thrombin then activates other components of the coagulation cascade, including FV and FVII (which activates FXI which in turn activates FIX), and activates and releases FVIII from being bound to vWF. FVIIIa is the co-factor of FXIa and together they form the "tenase" complex which activates FX and so the cycle continues. The contact activation pathway: formation of the primary complex on collagen by high molecular weight kininogen (HMWK), prekallikrein and FXII (Hageman factor), prekallikrein is converted to kallikrein and FXII becomes FXIIa. FXIIa converts FXI into FXIa. FXI is also activated by FVIIa. Factor IX is in turn activated by FXIa which with its co-factor FVIIIa form the tenase complex which activates FX to FXa. Thrombin primary role is the conversion of fibrinogen to fibrin, the building block of a haemostatic plug. In addition, it activates Factors VIII and V and their inhibitor protein C (in the presence of thrombomodulin), and it activates Factor XIII, which forms covalent bonds that crosslink the fibrin polymers that form from activated monomers. http://www.biocrawler.com/encyclopedia/Image:Coagulation_cascade.png

The coagulation proteins that participate in the lipid-associated complexes can be divided into three categories. The first category includes factors VII, IX, X and protein C that have 9 to 12 γ -carboxyglutamic acid residues in the N-terminal, which are involved in the Ca^{2+} dependent binding to negative phospholipids. These residues are created by postribosomal vitamin K-dependent carboxylation [Zwaal *et al.*, 1998]. Secondly, non-enzymatic co-factors, such as factor V and VIII, are Ca^{2+} dependent, and need proteolytic

activation to facilitate the enzyme-substrate reaction [Davie *et al.*, 1991]. The last group contains TF, a member of the class 2 cytokine receptor super family and a type I integral protein. TF does not need proteolytic activation, but must be anchored to a membrane to fully support the proteolytic activity of factor VIIa [Morrissey, 2001].

1.3.2.3 Regulation of TF expression on endothelial cells

The level of TF expression varies in the different organs. Brain, lung, heart, kidney, uterus, testis, skin and placenta express high levels, whereas organs such as the liver, spleen and skeletal muscle express only low levels of TF [Fleck *et al.*, 1990]. Under normal conditions TF is not expressed on the surface of the endothelial cells, but by cells surrounding the vasculature that act as a protective haemostatic barrier upon disruption of the blood vessels. However, inflammatory mediators such as TNF- α , IL-1 β and LPS [Bevilacqua *et al.*, 1986], and angiogenetic stimuli such as VEGF and TGF- β , have been shown to induce TF expression on endothelial cells, monocytes and fibroblasts [Osterud and Bjorklid, 2001; O'Reilly *et al.*, 2003]. As a consequence, an inappropriate expression of TF is seen under various pathological conditions i.e. endotoxemia [Sharma *et al.*, 2004], atherosclerosis [Westrick *et al.*, 2001] and in the development and progression of cancer [Yu *et al.*, 2004].

VEGF is an important mediator of angiogenesis that activates endothelial cell survival, proliferation, migration and tube formation. VEGF also functions as a cytokine inducing the expression of different adhesion molecules (VCAM and integrins) and increasing endothelial permeability [Carmeliet, 2000]. Several studies have investigated the induction of TF on endothelial cells by VEGF alone or in synergy with TNF- α . The biological effects of VEGF are mediated by its binding to the two tyrosine kinase receptors Flt-1 and KDR, where the latter has been shown to be the main receptor associated with endothelial cell proliferation, migration, vascular permeability, cell survival and angiogenesis [Shinaruk *et al.*, 2003]. It has been suggested that KDR receptor signaling governs the VEGF-induced TF expression [Shen *et al.*, 2000] through activation of the early growth response-1 (EGR-1) transcription factor [Mechtcheriakova *et al.*, 2001].

TF expression is only slightly up-regulated by VEGF alone, but it is significantly enhanced when induced in synergy with TNF- α [Clauss *et al.*, 1996; Shen *et al.*, 2001].

TNF- α is a potent pro-inflammatory cytokine, which originally was described as a mediator of hemorrhagic necrosis in murine tumors. Furthermore, TNF- α affects the haemostatic properties of endothelial cells [Conway *et al.*, 1989] through stimulation of two receptors in the cell membrane, the 60 kDa TNF- α receptor (TNFR60) and the 80 kDa TNFR (TNFR80). The principle receptor involved in the TNF- α induced up-regulation of TF is TNFR60 [Clauss *et al.*, 1996].

TF is classified as an immediate-early response gene, because its transcription is directly induced before *de novo* synthesis of other proteins [Mackmann, 1995]. TNF- α induced *de novo* synthesis of the TF protein in human microvascular dermal endothelial cells. Experiments blocking either the nuclear factor- κ B (NF- κ B) or p38 mitogen-activated protein kinase partly blocked the expression of TF [O'Reilly *et al.*, 2003], indicating that these two signaling pathways are involved in the TNF- α induced TF expression in human microvascular dermal endothelial cells. In contrast, the expression of TF in porcine aortic endothelial cells after LPS treatment was the result of a concerted action mediated by transcription factor AP-1, NF- κ B and Sp-1-like factors, which lead to transcription from the TF promoter [Moll *et al.*, 1995]. It appears that different signaling pathways are involved in the induction of the TF protein, and the process might be both species and cell type specific.

In addition to the transcriptional control of TF activity, i.e. increasing its expression on the vasculature, it has been suggested that TF exists in an encrypted state on the surface of non-perturbed cells, and that encryption of TF may contribute to controlling its activity in coagulation. Previous studies have shown that some quiescent endothelial cells express TF on their surface, but exhibit limited TF activity. However, when detached with trypsin the TF activity was increased [Maynard *et al.*, 1975]. This suggests the existence of a mechanism that maintains TF in a protected or encrypted state, and that stress or stimulation can induce decryption of TF. The mechanisms behind decrypting TF are now being investigated. One study found that an increase in cytosolic Ca²⁺ concentrations increased TF activity [Bach and Rifkin, 1990]. Other studies found that the presence of the anionic lipid, PS, increased TF activity, and that PS therefore might participate in the activation of TF [Bach and Rifkin, 1990; Pendurthi *et al.*, 2007].

The TNF- α induced expression and activation of TF is well documented. Therefore the use of TNF- α to induce TF expression and clotting in the tumor vessels is an attractive strategy. In addition, solid tumors secrete VEGF due to their angiogenic

state. Thus tumor-derived VEGF, together with targeted TNF- α , can synergistically increase the TF expression on tumor endothelium. TNF- α has previously been used in the treatment of solid tumors and being a pleiotropic cytokine, it has multiple effects on the endothelium. The sum of these effects can induce vascular collapse.

1.3.3 TNF- α ; as a VDA

TNF- α is a multifunctional cytokine that plays an important role in inflammation and immunity, as well as in the control of cell proliferation, differentiation and apoptosis. TNF- α was isolated in 1975 from serum of mice treated with LPS as the active component of Coley's toxin. It got its name from its ability to induce necrotic hemorrhage in murine solid tumors [Carswell *et al.*, 1975; Wanatabe *et al.*, 1988]. Currently, TNF- α is used in anticancer treatment of soft tissue sarcoma, irresectable tumors of different histological origin and in-transit melanomas in the limbs by isolated limb perfusion [ten Hagen and Eggermont, 2004]. The antitumor effect induces vascular occlusion leading to tumor cell necrosis [Stoelcker *et al.*, 2000; Friedl *et al.*, 2002].

TNF- α is a 17 kDa protein that forms a homotrimer in solution. It is mainly produced by activated macrophages, T lymphocytes and natural killer cells, but other cell types such as fibroblasts, smooth muscle cells and tumor cells also produce low levels of TNF- α [van Horssen *et al.*, 2006]. TNF- α is synthesized as the membrane bound pro-TNF- α , which is cleaved by the TNF- α converting enzyme and released into the circulation [Bemelmans *et al.*, 1996]. As mentioned above, TNF- α exerts its action through two receptors. TNF- α has highest affinity for TNFR80 but seems to exert most of its biological function through the TNFR60 (also called TNFR1), which is expressed on all cell types. TNFR80 is mainly expressed on cells of the immune system [Aggarwal *et al.*, 2003]. The two receptor have been shown to cooperate; at low TNF- α concentrations TNFR80 seems to be involved in catching and passing the ligand on to the TNFR60 [Clauss *et al.*, 1996].

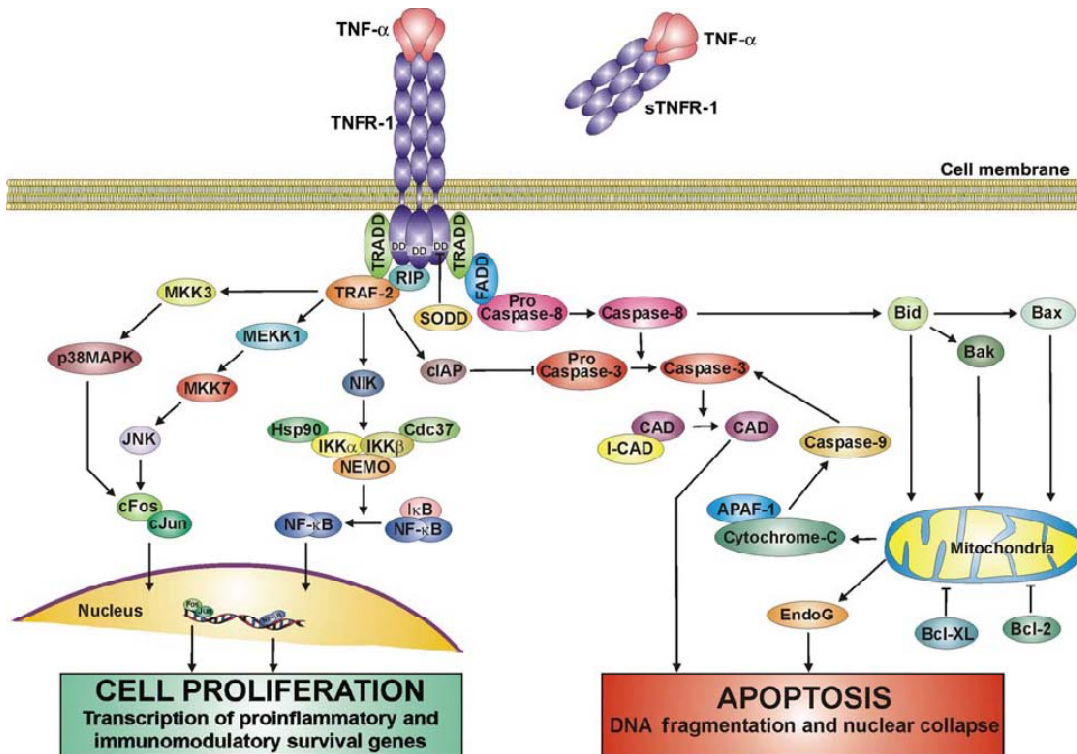


Figure 8. Schematic overview of the signaling pathways initiated upon binding of TNF- α and TNFR60 trimerization. The signaling pathways are reviewed in van Horssen *et al* (2006) [from van Horssen *et al.*, 2006]

The main difference between the two receptors is the presence of the death domain (DD) on the TNFR60, but not on TNFR80. The DD therefore makes TNFR60 a member of the family of death receptors, which are apoptosis-inducing receptors [van Horssen *et al.*, 2006]. Besides signaling apoptosis, the TNFR60 also signals cell survival and activation by inducing the expression of inflammatory proteins [Kuldo *et al.*, 2005].

When TNF- α homotrimer binds to the TNFR60, the receptor trimerizes, causing the protein silencer of death domain (SODD) to be released. Thereafter the protein TNFR-associated death domain (TRADD) binds to the DD, which in turn recruits the adaptor proteins receptor interacting protein (RIP), TNFR associated factor 2 (TRAF-2) and Fas-associated death domain (FADD) [Aggarwal, 2003; van Horssen *et al.*, 2006]. Here, the two signaling pathways split up depending on the outcome of the signaling. TNFR60 signals apoptosis when it recruits FADD which thereafter initiates the caspase cascade (Fig. 8). However, when it signals survival TRAF-2 is recruited to the complex. The binding of TRAF-2 inhibits apoptosis and induces phosphorylation and activation of more signaling pathways. This process results in the activation of the transcription factors cFos/cJun and NF- κ B, where NF- κ B constitutes the major signaling pathway [Devin *et*

al., 2000]. The effect that TNF- α exerts is concentration-dependent. High concentrations induce the vascular-toxic pathway, whereas lower concentrations promote DNA and protein synthesis [van der Veen *et al.*, 2000].

As mentioned above, TNF- α exerts many effects on endothelium. It can induce coagulation through up-regulation and activation of TF and it can permeabilize the endothelial barrier and induce vascular obstruction due to endothelial apoptosis.

The apoptotic effect of TNF- α on endothelial cells has been investigated in HUVECs [Ramana *et al.*, 2004; Carroll *et al.*, 2004] and bovine pulmonary arterial endothelial cells [Polunovsky *et al.*, 1994]. The inhibition of protein synthesis by treating the cells with either actinomycin D or cycloheximide attenuates the TNF- α induced apoptosis [Polunovsky *et al.*, 1994]. This could be due to the dual signaling of TNF- α where the cell upon TNFR60 activation up-regulates the pro-survival genes and renders the cells less sensitive to TNF- α mediated apoptosis [Jimenez *et al.*, 2003]. It has also been suggested that the production of reactive oxygen species (ROS) plays a role in TNF- α mediated cell death. TNF- α increases the production of ROS, but the role of ROS in the apoptotic pathway is conflicting. When initiating the apoptotic pathway, TNF- α also activates the anti-apoptotic pathway, including the transcription factor NF- κ B [Ramana *et al.*, 2004]. NF- κ B regulates genes that promote cell survival and their activation and might therefore rescue the cell from death. However, activation of NF- κ B is redox-sensitive, and it has been shown that ROS, as a secondary effect, inhibits NF- κ B activation [Ramana *et al.*, 2004] thereby promoting apoptosis.

TNF- α provokes the biosynthesis and release of multiple endogenous mediators that directly or indirectly influences the endothelial barrier function. Neumann *et al.* showed that Evans blue labeled albumin was cleared from the pulmonary micro-vessel endothelial monolayer within 30 min of TNF- α treatment [Neumann *et al.*, 2006]. The increased permeability of the endothelial barrier is mediated through the activation of multiple protein tyrosine kinases [Angelini *et al.*, 2006], which results in the down-regulation of primary endothelial intracellular adhesion molecules, vascular endothelial-cadherin, and in the contraction of F-actin cytoskeletal elements [Friedl *et al.*, 2002].

TNF- α induces a pro-coagulative state, increased permeability and apoptosis in endothelial cells. Treatment with TNF- α induces thrombosis and necrosis in mice bearing human xenograft tumors [Watanabe *et al.*, 1988; Nawroth *et al.*, 1988]. However as TNF- α is a multi-functional cytokine, systemic treatment with even the minimal clinical doses

is often hampered by severe side effects [Kim *et al.*, 2002a], such as hypotension, fever, nausea, headache, and tachycardia. Therefore, TNF- α is not applied in systemic treatment, but is given through isolated limb perfusion, often together with melphalan [Grunhagen *et al.*, 2006; Verhoef *et al.*, 2007]. This technique allows for 10-fold higher doses of the systemic mean-tolerated dose of TNF- α , with negligible systemic toxicity [Hayes *et al.*, 2006].

Treatment with low doses of TNF- α is another way to circumvent the severe side effects. Low doses of TNF- α in combination with liposomal doxorubicin (Doxil[®]) produces a better tumor response in osteosarcoma-bearing rats [Hoving *et al.*, 2005] and in B16BL6 melanoma xenograft-bearing mice [Seynhaeve *et al.*, 2007] as compared to treatment with Doxil[®] alone. Another study employed low doses of TNF- α and liposomal cisplatin and found that the combination resulted in a prolonged anti-tumor activity in rats bearing soft-tissue sarcomas, but not in rats bearing osteosarcoma [Hoving *et al.*, 2005]. The effect of the combination treatments is thought to be due to an increased vascular permeability, increased tumor accumulation and a more homogenous drug distribution in the tumor [Seynhaeve *et al.*, 2007]. However, the outcome might depend on the type of tumor [Hoving *et al.*, 2005].

Apart from isolated limb perfusion and low levels of TNF- α , investigators have tried to target TNF- α specifically to the tumor. TNF- α conjugated to the tumor cell antigen, carcinoembryonic antigen [Larbouret *et al.*, 2007] and NGR-peptide [Corti and Ponzoni, 2004], exhibited anti-tumor activity and resulted in fewer side effects [Larbouret *et al.*, 2007]. Another approach was to encapsulate TNF- α in sterically stabilized liposomes [Kim *et al.*, 2002a,b; Debs *et al.*, 1990; ten Hagen *et al.*, 2002; Morishige *et al.*, 1993]. Incorporation of TNF- α into sterically stabilized liposomes has many advantages in systemic treatment. Liposomal TNF- α exhibits a prolonged circulation time, accumulation in the tumor and decreased cytotoxicity [Debs *et al.*, 1990; van der Veen *et al.*, 2000; Kim *et al.*, 2002a; ten Hagen *et al.*, 2002].

The immunomodulatory and toxic effects of TNF- α liposomes were initially investigated in rats. Liposomal TNF- α exhibited the same immunomodulatory effects as free TNF- α , but with fewer toxic side effects [Debs *et al.*, 1990]. The anti-tumor effect of TNF- α liposomes alone or in combination with other conventional anti-cancer treatments has also been studied. Treated mice bearing LS174T human colon cancer xenografts exhibited prolonged the recruitment and activation of leukocytes as compared to

treatment with free TNF- α [Kim *et al.*, 2002a]. When TNF- α liposomes were given in combination with radiation, the inhibition of tumor growth was enhanced synergistically without the dose-limiting toxicities [Kim *et al.*, 2001]. It was suggested that the reason for this was that TNF- α liposomes resulted in a prolonged activation of the immune system [Kim *et al.*, 2002a]. Moreover, the combination of liposomal TNF and liposomal doxorubicin (Doxil[®]) markedly augmented the antitumor activity, without increasing the toxic side effects seen in the combination of free TNF- α and Doxil[®] [ten Hagen *et al.*, 2002]. Since the encapsulation of TNF- α reduced the systemic side effects, TNF- α liposomes seems to be a promising alternative when using TNF- α in anti-tumor treatment. It might even enhance the effects of TNF- α on the tumor endothelium when targeting the liposomes directly to the tumor endothelium.

1.3.4 DMXAA as a TNF- α inducing small molecule VDA

In an attempt to limit the TNF- α induced side effects, a search for agents that stimulate the synthesis of TNF- α in tumors was initiated. This led to the finding of flavone acetic acid (FAA), which by inducing TNF- α synthesis, is a potent drug against solid tumors in mice. FAA showed regression of Colon 38 tumors in mice [Plowmann *et al.*, 1986], but phase II trials showed that FAA had no effect on human tumors [Kerr and Kaye, 1989]. Derivatives of FAA were therefore synthesized, the most potent being 5,6-dimethylxanthenone-4-acetic acid (DMXAA, Fig. 9) [Rewcastle *et al.*, 1991].

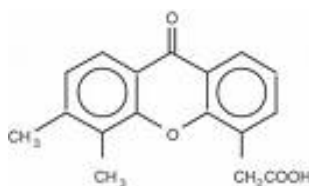


Figure 9. The chemical structure of DMXAA.

DMXAA's activities in mice include induction of TNF- α and INF- γ [Joseph *et al.*, 1999], serotonin release [Baguley *et al.*, 1997], increased vascular permeability [Chung *et al.*, 2007], tumor blood flow inhibition and induction of hemorrhagic necrosis and tumor regression (Fig. 10) [Zhao *et al.*, 2002]. In contrast to FAA, DMXAA was shown to induce TNF- α synthesis in both mouse and human cells *in vitro* [Philpott *et al.*, 1997].

DMXAA also induced a rapid vascular collapse in the tumors of mice transplanted with Colon 38 xenografts [Joseph *et al.*, 1999]. As mentioned above, apart from TNF- α , DMXAA also induces other cytokines, such as interferons. To investigate whether the antitumor effects of DMXAA were dependent on the synthesis of TNF- α and INF- γ , knock-out mice lacking their receptors were treated with DMXAA. Treatment of IFN- γ receptor knock-out mice bearing Colon 38 tumors with DMXAA resulted in 100% regression of the tumor, even though the required dose was higher and the reduction in tumor volume was slower. This suggested that IFN- γ was not crucial for the anti-tumor response [Pang *et al.*, 1998]. In order to evaluate the role of TNF- α in the DMXAA induced anti-tumor response, TNF- α receptor knock-out mice were compared to wild type mice with respect to the dose and curability. The TNF- α knock-out mice showed a considerably higher maximum-tolerated dose when compared to wild type mice (>100 mg/kg vs. 25mg/kg), and treatment with 50 mg/kg DMXAA resulted in a curative and comparable effect to wild type mice treated with 25 mg/kg DMXAA [Zhao *et al.*, 2002]. Although TNF- α plays an important role in the DMXAA-induced host toxicity and anti-tumor effect, it can be replaced with a TNF- α independent mechanism. Comparing the levels of TNF- α induced by DMXAA and LPS in the tumor it was shown that DMXAA induced a larger amount of TNF- α in tumors as compared to LPS [Joseph *et al.*, 1999], indicating that the activity of DMXAA is more specifically located to the tumor and that DMXAA is a potent inducer of TNF- α .

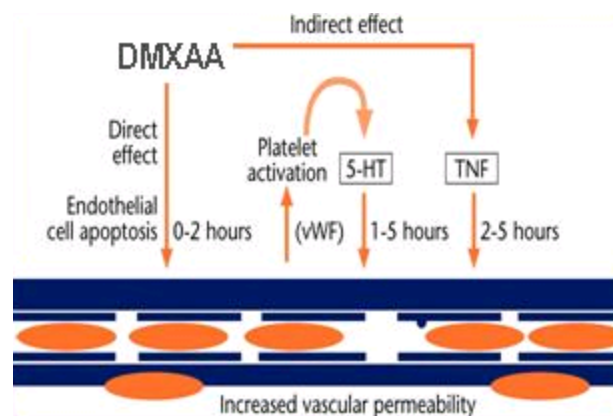


Figure 10. Schematic depiction of the direct and indirect activities of DMXAA. DMXAA exerts a direct effect on the endothelium where it induces apoptosis, but also indirect effects such as the synthesis of TNF- α and serotonin [Rosenthal and Pili, 2007].

Pre-clinically, DMXAA has been shown to target tumor vasculature and cause tumor regression, necrosis and a reduction in micro-vessel density in mice bearing head and neck squamous cell carcinomas [Seshadri *et al.*, 2006] and Colon 38 tumors [Zhao *et al.*, 2002] and in rats bearing chemically induced primary mammary tumors [Liu *et al.*, 2007a]. DMXAA exhibits anti-tumor activity and reduction in tumor blood flow at well tolerated doses in clinical phase I trials [Jameson *et al.*, 2003]. However, treatment with DMXAA alone, as with the other VDAs, does not lead to complete tumor regression. Currently, DMXAA is undergoing clinical phase II trials in combination with conventional anticancer drugs [McKeage, 2008]. One study is assessing the efficacy of a triple treatment with paclitaxel, carboplatin and DMXAA in patients with recurrent ovarian cancer. Preliminary data reveal that DMXAA does not add significantly to toxicity [Gabra, 2006]. No additional toxicity was found in patients with non-small cell lung cancer receiving the same triple treatment and initial data suggest that the combination has a beneficial effect compared to conventional treatment [McKeage, 2008]. The combination of docetaxel and DMXAA for patients with hormone-refractory metastatic prostate cancer did not add to the toxicities and showed promising activity [Rosenthal and Pili, 2007]. These phase II trials are encouraging and support further development of DMXAA as an anticancer drug.

One problem with DMXAA is that it exhibits a steep dose curve in mice, resulting in a narrow therapeutic window. Treatment with 15 mg/kg has no anti-tumor effect, while a treatment with 30 mg/kg kills the mice [Murate *et al.*, 2001]. Subsequently, employing a vascular targeted approach, with i.e. tumor endothelium targeted liposomes might broaden the therapeutic window by either making it possible to work with lower doses or by reducing the toxicity of higher doses.

1.4 Aim of study

The main goal of this project was to evaluate and develop a novel therapeutic principle for treating solid tumors by combining a non-cytostatic drug carrier targeted to the tumor vasculature and the occlusion and destruction of the tumor blood vessel system. Therefore, the project is divided into two parts; (i) a liposomal carrier system for specific targeting of the tumor vasculature had to be generated and evaluated under *in vitro* and *in vivo* conditions with respect to targetability, tumor specificity and the fate of the liposomes at the target site. (ii) The molecular mechanisms of TF expression by endothelial cells as a key for inducing blood coagulation had to be investigated. Potential inducers of TF expression were evaluated as possible agents for liposomal targeting and their anti-tumor activity was evaluated in a mouse tumor model.

VCAM appears to be the most attractive target molecule on the endothelium for a liposomal targeting strategy; VCAM is not expressed on normal endothelium but is up-regulated on tumor endothelial cells. Consequently, different VCAM-directed immunoliposomes were introduced and investigated. Special emphasis has been put on the vascular localization of these immunoliposomes vs. the unspecific uptake in the tumor tissue. As a novel approach, TNF- α and the TNF- α inducing, DMXAA was encapsulated into targeted liposomes. This will protect the organism against potential systemic effects of TNF- α , and simultaneously, ensure selective delivery to the tumor endothelial cells. This should lead to an induction of TF expression and activity with a subsequent initiation of the coagulation cascade and ultimately, to occlusion of the tumor vessels and starvation of the tumor cells (Fig. 11). Hence, the strategy is to starve tumor cells by injuring existing tumor-feeding blood vessels by inducing occlusion of the vessel and stopping the flow of nutrients and oxygen to the tumor cells. This will lead to killing the cancer cells in the core of the tumor, which will make the peripheral parts of the tumor particularly amenable for adjuvant therapy with radiation or cytostatic treatment (cf. Horsman and Siemann, 2006). The aim of the thesis is schematically summarized in Fig. 11.

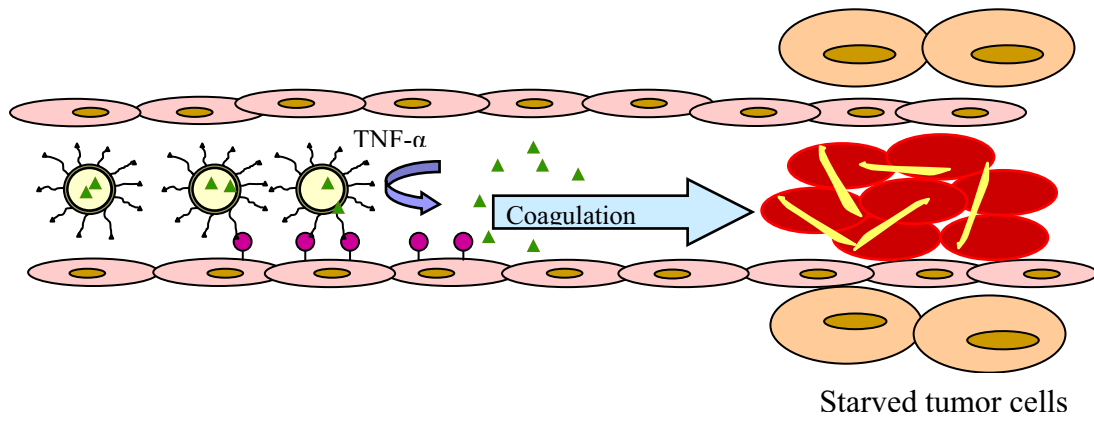
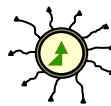


Figure 11. Illustration of intra-tumor blood coagulation induced by the release of TNF- α from vascular-targeted liposomes conjugated with anti-VCAM antibodies.

 = TNF-loaded liposomes coated with anti-VCAM antibodies target VCAM-expressing endothelial cells of the tumor.

2. Material and Methods

2.1. Reagents

Reagents were obtained from the following sources: soy phosphatidylcholine (SPC) was kindly donated by Lipoid AG Ludwigshafen (Germany), polyethyleneglycol (2000)-phosphatidylethanolamine (PEG-PE), Lissamine[®] Rhodamine-B-DPPE, N-glutaryl-PE (Ng-PE) were purchased from Avanti Polar Lipids (Alabaster, USA). Cyanuric chloride, cholesterol (Chol), 1-ethyl-3-(3-dimethylaminopropyl)carbodiimid (EDC), N,N diisopropylethylamin, 3,3'- Dioctadecyloxycarbocyanine perchlorate (DiO) and recombinant murine TNF- α were from Sigma-Aldrich (Deisenhofen, Germany). DMXAA was a kind gift from M. Horseman, (Århus University, Denmark).

The antibodies were as follows: rat anti-mouse VCAM (clone MK271, rat anti-mouse CD31 (clone 390) and rat anti-mouse Meca32 antigen (clone Meca32) were purified from hybridoma cell supernatant (see section 2.2) using rat anti-mouse-IgG-agarose affinity columns (resin from Sigma-Aldrich); isotype-matched rat control antibodies (IgG1) and anti-CD11b (clone OX 42) were obtained from BD Pharmingen (Heidelberg, Germany); fractionated human IgG with irrelevant specificity and FITC-conjugated goat anti-rat secondary antibody came from Sigma-Aldrich; anti-macrophage BM8 antibody, recognizing the F4/80 maturation antigen, came from Dianova (Hannover, Germany), Alexa Fluor[®] 568 conjugated goat anti-rat secondary antibody and goat anti-mouse came from Molecular Probes (Invitrogen, Karlsruhe, Germany). Rabbit anti-mouse tissue factor from immunized rabbit was a kind gift from C. Gottstein (Santa Barbara, USA). Goat anti-rabbit IgG conjugated to horseradish peroxidase was obtained from BD Pharmingen (Heidelberg, Germany) and FITC-conjugated goat anti-rabbit IgG was from Sigma-Aldrich (Deisenhofen, Germany).

Octyl- β -D glucopyranoside was obtained from Alexis (Grünberg, Germany). The salts used to prepare the buffers (PBS, TRIS, HEPES, Borat-buffer, Lysis-buffer) were all analytical grade salts from Fluka (Neu-Ulm, Germany). The detergents Triton-X-100 and sodiumdeoxycholate, the chromogenic horseradish peroxidase substrate 3, 3', 5, 5'-tetramethyl benzidine (TMB), fluorescence mounting buffer, paraformaldehyde, 65 mM phosphate standard, Folin-Ciocalteu reagent were obtained from Sigma-Aldrich (Deisenhofen, Germany). The TNF- α ELISA kit was obtained from Endogen (USA) and

the *in situ* Apoptag® *TUNEL* assay kit was from Chemicon (CA, USA). NuPage® Western Blot kit was obtained from Invitrogen (Karlsruhe, Germany).

2.2. Cell lines

Hybridoma cell line MK271 was from ATCC, Manassas, VA, USA; hybridoma cell line 390 was from S. Albelda, University of Pennsylvania, Philadelphia, PA, USA; hybridoma cell line Meca32 was from E. Butcher, Stanford University, Stanford, CA, USA. The murine brain endothelium cells, bEnd3, were obtained from B. Engelhardt, Theodor Kocher Institute, University of Bern, Switzerland. A2780, a human ovarian cancer cell line, was obtained from M. Wiese, Pharmaceutical Department, University of Bonn. Human tumor cell line Colo677, originally described as non-small cell lung cancer cell line, is a myeloma cell line from DSMZ, Braunschweig, Germany, which forms solid tumors with VCAM-positive vessels after subcutaneous injection [Dienst et al., 2005]. B16F10 are murine melanoma cells, which express tissue factor constitutively, came from R. Ludwig, University Clinic Frankfurt. All cell lines except bEnd3 and B16F10 were cultured in RPMI 1640 medium supplemented with 10 % fetal calf serum (FCS), 100U penicillin and 100 µg streptomycin at 37°C in a 5% CO₂ incubator. The bEnd3 and B16F10 cells were grown in Dulbecco's modified Eagle's medium (DMEM) supplemented with 10 % FCS, 100U penicillin, 100µg streptomycin and 4mM glutamine. All cell culture reagents were obtained from Sigma-Aldrich (Deisenhofen, Germany).

2.3 Synthesis of the cyanur-PEG-PE anchor

The synthesis of the cyanur-PEG-PE anchor was performed as previously described by Bendas et al. [1999], in one step. Briefly, 50 mg DSPE-PEG₂₀₀₀-NH₂ was dissolved in 18 ml chloroform, after which 5 mg cyanuric chloride and 2.5 mg N,N diisopropylethylamin were added. The reaction was allowed to run to the end for 72 hours under constant agitation at room temperature. The reaction product was checked using thin layer chromatography (TLC). A silicate TLC plate (Merck, Germany) was used. 2-5 µl of reaction solution was applied to the TLC plate. Furthermore, to identify the lipid spots, standards consisting of cyanuric chloride and DSPE-PEG-NH₂ were also applied. The lipids were eluted with chloroform: methanol: NH₃ (65:35:1 v/v/v) and visualized

with UV and molybdenum blue reaction [Dittmer and Lester, 1964] (solution 1: 4.011 g MoO₃, 100 ml H₂SO₄ boiled for 3-4 hours and cooled down overnight; solution 2: 0.178 g molybdenum, 50 ml solution boiled for 15 min; spray reagent: equal volumes of solution 1 and 2 to 4.5 volume parts H₂O). The reaction mixture was washed twice with methanol and after evaporation the Cyanur-PEG-PE was dissolved in chloroform to a concentration of 1 μmol/ml.

2.4. Liposome preparation

The liposomes used in this work, regardless of the different labels (fluorescence or radioactive) and different encapsulated drugs (TNF-α and DMXAA), were all prepared with the hydration method.

2.4.1 Preparation of empty liposomes

Liposomes were prepared from SPC/cholesterol/mPEG₂₀₀₀-PE/anchor/DiO in a ratio of 60/30/5/5/0.5 mol % and hydrated with a 0.9 % NaCl solution to a final lipid concentration of 30 mM. In some preparations, trace amounts of [³H]-cholesteryloleylether (Amersham, Buckinghamshire, U.K.) (0.25 μCi/μmol lipid) were added instead of the DiO label. To couple a protein to the liposomal surface, two different coupling-anchors were used; either the NgPE anchor or the cyanur-PEG₂₀₀₀-PE anchor, which couples the targeting device directly to the surface of the liposomes or to the terminal ends of the PEG chain, respectively [Bendas et al., 1999]. When preparing liposomes with the cyanur-anchor the mPEG₂₀₀₀-PE was omitted.

Unilamellar liposomes were prepared with a Mini-extruder (Avanti Polar Lipids, Alabaster, USA) from multilamellar vesicles extruded 19 times through a 200 nm polycarbonate membrane, 19 times through a 100 nm polycarbonate membrane and 10 times through a 50 nm polycarbonate membrane (Whatman Nuclepore 18 mm polycarbonate membrane, Richmond, USA).

2.4.2 Preparation of TNF- α and DMXAA liposomes

2.4.2.1 FITC-labeling of TNF- α

1 mg TNF- α was dissolved in 1 ml 0.9% NaCl solution. Before labeling, the buffer was replaced with a carbonate/bicarbonate buffer pH 8.8 using a Biospin 6 column (BioRad Laboratories, München, Germany). The amount of fluorescein isothiocyanate (FITC) labeling reagent (Pierce, IL, USA) to be added was calculated by using a 24-fold molar excess of the fluorescent dye to protein according to the manufacturer's recommendation. The FITC salt was dissolved in carbonate/bicarbonate buffer and added to the TNF- α , vortexed thoroughly and incubated for 1 hour at room temperature in the dark. Thereafter, excess FITC was removed by gel filtration using a BioSpin 6 column (cut-off: 6000 Da). The concentration and the degree of labelling were determined by measuring the absorbance at 280 nm and at the dye's maximum wavelength (494 nm for FITC, A_{494}). Thereafter equation 1 was used.

$$\text{Protein concentration (M)} = (A_{280} - (A_{494} \times \text{Correction factor})) / \epsilon \quad (1)$$

where A_{280} gives the protein concentration in the sample and the correction factor is used to correct for the absorbance of the fluorescence dye at 280 nm. ϵ is the molar extinction coefficient of the labeled protein (TNF- α , 17500) and A_{494} the absorbance at the dye's maximum wavelength.

The degree of labelling is then calculated with equation 2

$$\text{moles dye per mole protein} = A_{494} / \epsilon' \times \text{protein concentration (M)} \quad (2)$$

where ϵ' is the extinction coefficient of the fluorescence dye.

2.4.2.2 Liposomal encapsulation of TNF- α and DMXAA

TNF- α and DMXAA liposomes were prepared by hydration of a 10 μmol SPC/Cholesterol/cyanur-PEG₂₀₀₀-PE molar ratio 65/30/5/ film with 100 μl TNF- α (1 mg/ml) or 100 μl DMXAA (20 mg/ml), respectively. Unilamellar liposomes were formed by sonicating the liposomes 3 times for 5 seconds with 3 cycles. The particle size was thereafter determined as described in section 2.5.1. Non-encapsulated TNF- α or DMXAA

was removed by gel permeation chromatography using a Sepharose 4B column and a 0.9 % NaCl solution as eluant.

Encapsulation efficiency was given as $\mu\text{g TNF-}\alpha/\mu\text{mol lipid}$ and was established by measuring the amount of lipid using the phosphate assay (section 2.5.2) and the fluorescence of the FITC labeled TNF- α or by measuring protein concentration.

The amount of encapsulated DMXAA was determined by measuring the fluorescence of DMXAA. A calibration curve for DMXAA in 0.9 % NaCl solution was obtained using a LS 30 Fluorescence Spectrometer (Perkin-Elmer, Jügesheim, Germany) with an excitation wavelength of 350 nm and an emission of 412 nm, after which the fluorescence of the unknown sample was measured.

2.4.3 Coupling proteins to the liposomes

Two different anchor lipids (Ng-PE and Cyanur-PEG-PE anchor) were compared and used to couple proteins to the liposomes. Rat anti-mouse VCAM monoclonal antibody (mAb) (M/K-271) was used as homing devices. Control liposomes were coupled to an irrelevant IgG (human fractionated IgG with ~70% IgG₁ content or purified rat IgG₁) or to bovine serum albumin (BSA) (grade V). Coupling was performed in the optimal 1:1000 protein:lipid molar ratio [Hansen et al., 1995].

To form a protein linkage to liposomal Ng-PE, 6 mg EDC was added to 10 μmol liposomes in PBS (pH 7.4) followed by an incubation period of 4 h at room temperature. Antibodies were added and incubated overnight at room temperature. The ILs were separated from unbound antibodies by gel permeation chromatography using a Sepharose 4B column and 0.9 % NaCl solution as eluant.

To couple the proteins to the cyanur anchor the calculated amount of antibody was added to liposomes in borate buffer pH 8.8 (solution 1:4.77 g Borax in 250 ml H₂O; solution 2:0.1 M HCl; Borate buffer:75 ml solution 1, 25 ml solution 2) and incubated at room temperature for about 16 h. Unbound antibodies were separated by gel permeation chromatography using a Sepharose 4B column with a 0.9% NaCl solution as eluant.

2.5 Liposome characterization

Liposomes were characterized with respect to particle size by dynamic light scattering (Malvern autosizer IIc, Malvern, UK), and with respect to phospholipid concentration [Ames and Dubin, 1960]. The concentration of coupled proteins was determined with a modified Lowry assay [Peterson, 1977].

2.5.1 Particle sizing

Dynamic light scattering can be used to measure the size of small particles with a diameter of 5-5000 nm. Particles of this size are characterized by their constant random thermal movement. When monochromatic light hits a particle, the particle movement causes the intensity of light scattering to vary with time. The principle is that larger particles move slower than small particles, which causes the rate of fluctuation of the scattered light to be slower for large particles as compared to small particles [Malvern, 1993]. These properties make it possible to calculate the diffusion coefficient of a particle. The diffusion coefficient can be used to calculate the hydrodynamic radius by using the Stroke-Einstein equation (3)

$$r_H = k_B T / 6\pi\eta D \quad (3)$$

where k_B is Boltzmann's constant, T is temperature, η is the fluid viscosity and D is the diffusion time [Øgendahl, 2001]. After analysis the hydrodynamic diameter and the polydispersity is given. The polydispersity is a factor that describes the homogeneity of the sample and lies in the range of 0-1, with 0 being very homogenous [Constantinides and Yiv, 1995]. Polydispersity should be lower than 0.5, as samples with a higher polydispersity are not homogenous and not suited for the technique.

Measurements were carried out on a Malvern Autosizer 2c (Malvern Instruments, Worcestershire, UK). 1 ml 0.9 % NaCl solution was filtered sterile (Sterilfilter Satorius, 0,22 μ m), placed in a cuvette and approx. 30 μ l liposome suspension was added. Thereafter the size (nm) and polydispersity was given as a mean of 3 times 10 measurements.

2.5.2 Phospholipid concentration determination

Phosphate determination was performed as described by Ames and Dubin [1960]. Briefly, this method is based on a colorimetric determination of PO_4^{3-} . The liposomal phospholipids were oxidized with perchloric acid to produce inorganic phosphate, which reacts to phosphomolybdate acid. This can be converted quantitatively to a blue compound after being reduced by ascorbic acid while heated.

A calibration curve was made with a 65 mM phosphate standard. Known amounts of phosphate standard, from 2-65 nmol, were added to glass test tubes. Small amounts of the liposome solution (15-30 μl) were transferred to a glass test tube. Thereafter 0.2 ml perchloric acid was added to each tube, the tubes were covered with aluminum foil to prevent evaporation, and the mixtures were incubated for 30 min on a heating block at 180°C. The test tubes were cooled down and 2 ml hexa-ammoniummolybdate solution (2.2 g $(\text{NH}_4)_6\text{Mo}_7\text{O}_{24} \times 4\text{H}_2\text{O}$, 14.3 ml conc. sulfuric acid ad 1000 ml dH_2O) and 0.25 ml 10 % ascorbic acid solution (w/v) were added to each test tube. The mixture was vortexed, incubated for 10 min at 100°C in a water bath and thereafter cooled down in cold water. Absorbance was measured at 812 nm.

2.5.3 Protein concentration determination according to Peterson-Lowry

A modified Peterson-Lowry assay was used to determine the amount of protein coupled to the liposome. The advantage of this method is that the phospholipids only interfere minimally and that other interfering substances can be removed by precipitating the proteins prior to running the assay. The principle behind the Lowry method of determining protein concentrations lies in the reactivity of the peptide nitrogens with the copper [II] ions under alkaline conditions and the subsequent reduction of the Folin-Ciocalteu phosphomolybdic acid to heteropolymolybdenum blue by the copper-catalyzed oxidation of aromatic acids [Dunn, 1992]

Briefly, a calibration curve was produced with either human IgG or BSA as reference depending on the protein coupled to the liposome. Known amounts of protein between 2-12 μg were transferred to Eppendorf tubes. The protein concentration in the liposome samples was measured in 10-30 μl liposome suspension. dH_2O was added to each tube to give a final volume of 1 ml. The proteins were then precipitated. First, 50 μl 0.3% sodiumdeoxycholate was added to each tube; the samples were vortexed and

incubated for 10 min at room temperature. Then 100 μ l 70% trichloroacetic acid was added and the samples were vortexed and centrifuged for 20 min at 11.000 rpm at 4 °C in an Eppendorf centrifuge. The supernatant was discarded and the pellet was dissolved in 1 ml solution C consisting of 49 volume parts of solution A (4 g NaOH, 20 g Na₂CO₃, 1L milliQ H₂O) and 1 volume part of solution B (0.5 g CuSO₄ x 5 H₂O, 1 g Na-citrate, 100 ml milliQ H₂O) and vortexed and incubated for 10 min at room temperature. Finally, 50 μ l of Folin-Ciocalteu reagent was added and after vortexing, the samples were incubated for 30 min in the dark at room temperature. Absorbance was measured at 750 nm.

2.6 VCAM expression and liposome targeting to bEnd3 cells *in vitro*

2.6.1 VCAM expression and liposome binding using flow cytometry (FACS) analysis

Flow cytometry measures the fluorescence and optical characteristics of single cells by using the principles of light scattering, light excitation, and emission of fluorochrome molecules to generate specific multi-parameter data from particles and cells. Inside a flow cytometer, cells in suspension are drawn into a stream created by a surrounding sheath of isotonic fluid that creates laminar flow, allowing the cells to pass individually through an interrogation point. Lasers are most often used as a light source in flow cytometry. As the cells of interest intercept the light source they scatter light and fluorochromes are excited to a higher energy state. This energy is released as a photon of light with specific spectral properties unique to different fluorochromes. The emitted light signals are detected by photomultiplier tubes and digitized for computer analysis [Brown and Wittwer, 2000].

2.6.1.1 bEnd3 cells expression of VCAM

VCAM expression on activated bEnd3 cells was analyzed by flow cytometry. bEnd3 cells were incubated with 50 ng/ml TNF- α for 4 hours, rinsed twice in washing buffer (PBS containing 1% BSA), detached with 0.025% EDTA, and fixed in 4% neutral buffered paraformaldehyde for 10 min at room temperature. After two more washes, cells were stained with rat anti-mouse VCAM mAb MK271 (10 μ g/ml) for one hour on ice and

labeled with FITC-conjugated goat anti-rat secondary antibody for 30 min on ice, prior to analysis on a flow cytometer (BD Biosciences, San Jose, CA, USA).

2.6.1.2 Liposome binding to bEnd3 cells

Liposomal binding to the bEnd3 cells was determined by FACS analysis. bEnd3 cells were seeded in 96-well microtiter plates (density: 1×10^4 cells/well) 24 hours prior to the assay. The cells were activated with TNF- α (50 ng/ml) for 4 hours to ensure VCAM expression. Seven different liposome preparations carrying a DiO label were investigated: three with the NgPE anchor anti-VCAM mAb-liposomes (α VCAM-NL) human IgG (hIgG-NL) of irrelevant specificity and albumin-liposomes (Alb-NL) and four with the cyanur anchor; anti-VCAM mAb-liposomes (α -VCAM-CL), liposomes conjugated to rat IgG1 (rIgG-CL) or human IgG (hIgG-CL) of irrelevant specificity and albumin-liposomes (Alb-CL). The liposomes (75 nmol) were incubated with the cells for 1 hour at 4°C in normal cell medium. Unbound liposomes were removed by washing with 0.1 M PBS with 1 mM CaCl₂ and 0.5 mM MgCl₂. The cells were detached with 0.025% EDTA and liposomal binding was analyzed on the flow cytometer (BD Biosciences, San Jose, CA, USA).

2.6.2 Fluorescence- based cell assay

The binding of VCAM-directed liposomes to murine endothelial cells was measured using a fluorescence-based cell assay and compared to control liposomes. Murine bEnd3 endothelial cells were seeded and activated as described in section 2.6.2. Five different liposome preparations (see 2.4.) carrying a DiO label were investigated. The liposomes (75 nmol) were incubated with the cells for 1 hour at 4°C in normal cell medium. Unbound liposomes were removed by washing with 0.1 M PBS (pH 7.4) containing 1 mM CaCl₂ and 0.5 mM MgCl₂, and the liposomal binding was analyzed in a FLUOstar Optima micro plate reader (BMG Labtech, Offenburg, Germany).

To investigate whether the unspecific binding of control liposomes to endothelial cells was due to any interaction with the Fc receptor, a blocking assay was performed. 30 min prior to the addition of the liposomes, 2 μ g / 1×10^6 cells rat anti-mouse Fc-receptor antibody or 60 μ mol plain liposomes was added to the cells. Thereafter the liposomes were added and the same procedure as described above was followed.

2.6.2.1 Internalization of α -VCAM Cyanur-L

The internalization of VCAM-targeted liposomes was investigated using the acid wash method. This method uses the principle that the antigen/antibody binding is destroyed under acidic conditions and has the advantage that it straightforwardly discriminates and quantifies between cell surface bound and internalized antibody-coupled particles [Liu et al., 2007b].

To quantify the internalization of VCAM-directed liposomes upon binding to bEnd3 endothelial cells, the same procedure was followed as described above except that the cells were incubated with liposomes for 2 hours at 37°C. Thereafter, unbound liposomes were removed by washing with PBS containing 1 mM CaCl₂ and 0.5 mM MgCl₂ and liposome binding was measured. To determine the fraction of cell-associated liposomes that were internalized, the cells were stripped of their surface-bound liposomes by one wash for 5 min with citrate buffer (pH 3.0) followed by one wash with PBS. The remaining cell-associated liposomes were considered internalized.

2.6.3 Dynamic flow assay

In order to simulate the *in vivo* binding of the liposomes to the endothelial cells under shear force conditions, a dynamic flow assay was performed as previously described [Bendas *et al.*, 1998; Kessner *et al.*, 2001].

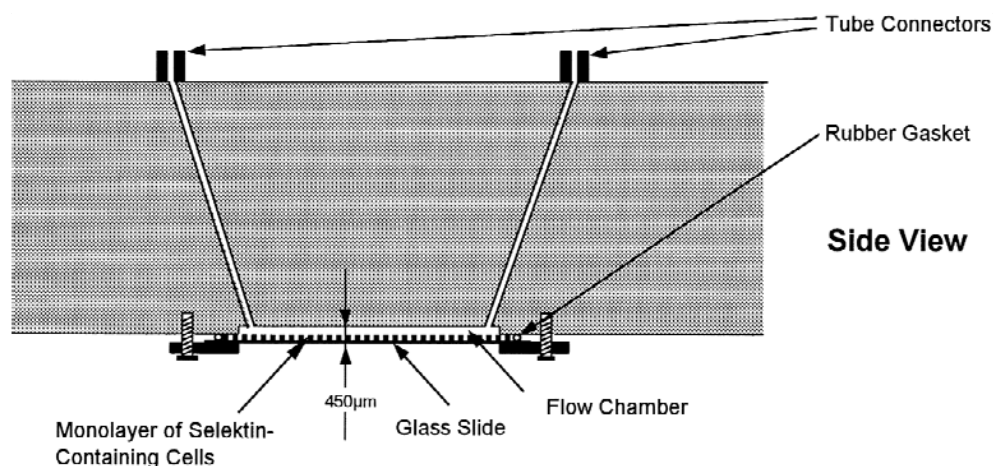


Figure 12. Schematic presentation of the laminar flow chamber. Immunoliposomes in the flow medium were rinsed through the chamber by hydrodynamic drag to interact with VCAM –expressing cells [Bendas *et al.*, 1998].

Briefly, the endothelial cells were seeded on circular (18 mm) coverslips (5×10^5 cells) 24 hours prior to the assay. The cells were activated with TNF- α (50 ng/ml) for 4 hours and subsequently washed once with PBS. The coverslips were inserted into a double flow chamber (Fig.12). Each chamber was perfused with 5 ml of RPMI 1640 medium containing 1% penicillin/streptomycin, 10% FCS and 0.5 μ M liposome dispersion for 20 hours at a shear rate mimicking capillary blood flow (about 200 s⁻¹) using a peristaltic pump at approx. 37°C. Two different liposome preparations carrying a rhodamine-label, were investigated; α -VCAM-CL and hIgG-CL. At different time points (t = 0, 1 hour, 2 hours and 20 hours), the flow was stopped and pictures of the liposomal binding to the cell layer were taken through an inverted fluorescence microscope Axiovert 200 equipped with an AxioCam MRc camera (Carl Zeiss, Germany).

2.7 α -VCAM IL targeting and biodistribution *in vivo*

2.7.1 *Xenograft mouse model and biodistribution studies*

Female CD1 nude mice (Charles River Laboratories, Germany) were housed in cages with free access to food and water with a 12 hour light/dark cycle. Human Colo 677 xenograft tumors were created by a subcutaneous co-injection of 1×10^6 Colo 677 cells with Matrigel (BD Science, Heidelberg, Germany) diluted 1:1 into one flank of 4 - 5 week-old mice. The tumor size was measured every second day with a caliper in three perpendicular directions a, b and c, and tumor volumes were calculated according to the formula $V = \pi/6 \times a \times b \times c$. When the tumors had grown to 200 - 500 mm³, the mice were injected with 0.5 μ mol liposomes into the tail vein. Three different liposome preparations were investigated; α -VCAM-Ls, irrelevant IgG-liposomes and Alb-L (n = 3 per group), all containing DiO as a fluorescent label. The mice were sacrificed either 30 min or 24 hours after liposome injection. Experiments were terminated by transcardial perfusion of deeply anesthetized mice with PBS for 10 min and major organs and tumors were snap frozen in dry ice/isopentane slush and stored at -80°C until further use. The organs and tumors were cut into 5 μ m sections on a Leica CM 3050 G cryostat (Leica, Wetzlar, Germany) and were either used directly or stored at -80°C.

Total liposome tumor accumulation and biodistribution were investigated using Tritium-labeled liposomes. [³H]-labeled liposomes coupled to either anti-VCAM

antibody or an irrelevant human IgG were injected i.v. at a dose of 0.5 μmol liposome/mouse ($n = 4\text{-}5$ mice per group). The animals were anesthetized after 24 hours and blood was collected by heart puncture. This was followed by a transcardial perfusion with PBS for 10 min before liver, spleen, kidney, lungs, heart, skin, muscle and tumor were removed, weighed and stored at -20°C until further use. To measure the amount of accumulated radioactive liposomes in the organs and tumor, the tissues were homogenized using a Potter Elvehjelm tube in 3 ml homogenization buffer per g tissue. Radioactivity was measured in 500 μl tissue homogenate after adding 100 μl of 10% SDS and 4 ml scintillation liquid (Ultima Gold). Blood samples were allowed to clot for 3 hours and centrifuged for 20 min at 13.520 g at 4°C .

2.7.2 Fluorescence microscopy of tissue sections

Cryosections of tumors and organs were thawed, fixed in 4 % paraformaldehyde for 10 min and incubated with one of the following primary antibodies: rat anti-mouse CD31 or rat anti-mouse Meca32 against endothelial cells; rat anti-mouse BM8 against macrophages; rat anti-mouse CD11b against macrophages and dendritic cells. Sections were incubated with primary antibodies for 1 hour at room temperature. Excess primary antibody was removed by three successive washes for 5 min with PBS. Thereafter, Alexa Fluor 568 conjugated secondary antibody was applied for one hour at room temperature, followed by three washes with PBS. Coverslips were mounted with a fluorescence-mounting medium (Dako, Glostrup, Denmark). The sections were stored in the dark at 4°C until further analysis. Overlay analysis was performed using AxioVision software (Carl Zeiss AxioVision release 4.6). Percentages of liposomes co-localized with the endothelium were determined in four randomized microscopic fields and calculated as the ratio between the amount of co-localised pixels $\times 100$ and the total number of green pixels. The co-localization percentages are given as mean \pm SD.

2.8 Cytotoxicity studies

Both TNF- α and DMXAA influence cells in many different ways. Therefore the two drugs themselves were tested for any cytotoxic effect that might act in synergy with the induction of coagulation in the tumor.

2.8.1 Propidium iodide (PI) assay

PI is a DNA-binding agent that is impermeable to the membranes of viable cells, but penetrates plasma membranes of dead cells and binds to the DNA of dead cells. PI is known as an indicator of necrosis or late-stage apoptosis. 5×10^4 bEnd3 cells / well were plated out in 6 well plates and allowed to attach overnight. The following day the cells were treated with TNF- α (50 – 200 ng/ml) for 24 and 48 hours in the incubator. Subsequently, PI solution (5 μ g/ml) was added to each well and the cells were incubated for 5 min at 37°C. Thereafter the cells were analyzed in a flow cytometer. PI has an excitation wavelength of 488 nm and an emission of 630 nm.

2.8.2 3-(4,5-dimethylthiazol-2-yl)-2,5-diphenyl tetrasodium bromide (MTT) assay

The MTT assay is a quantitative colorimetric assay used to measure mammalian cell survival and cell proliferation. The assay measures cellular respiration by determining the mitochondrial activity. MTT is a pale yellow substrate that is cleaved by living cells to yield a dark blue formazan product. The process requires active mitochondria, and the amount of formazan produced is proportional to the number of living cells present in a given culture [Hayton *et al.*, 2003].

The bEnd3 cells were seeded out with a density of 5×10^3 cells/ well and allowed to attach overnight. The cells were treated with TNF- α in a range of 1 – 10.000 ng /ml and with DMXAA in a range of 0.2 – 3000 μ g/ml for 24, 48 and 72 hours. One hour before assay termination, 20 μ l MTT solution (5mg/ml MTT in 0.1M PBS pH 7.4) was added to each well and the cells were incubated for 1 hour in the incubator. The reaction was then stopped by lysing the cells and dissolving the formazan salt by adding 150 μ l acidic isopropanol solution (160 μ l HCl in 50 ml isopropanol) to each well. After extensive mixing with a pipette, the formazan salt was allowed to dissolve completely at 4°C for 2 hours. Finally the absorbance was measured at 580 nm. The background absorbance was also measured at 690 nm and subtracted.

2.9 TNF- α induced TF expression and activity *in vitro*

2.9.1 TF cell-based enzyme-linked Immunosorbent Assay (ELISA)

A cell-based ELISA was developed to measure the relative amount of TF expressed on the endothelial cells after TNF- α stimulation. bEnd3 cells and/or B16F10 cells were seeded out with a density of 1×10^4 cells/well and allowed to attach overnight. B16F10 cells are melanoma cells that have been shown to express tissue factor constitutively and are therefore used as a positive control. The bEnd3 cells were activated with 50 ng/ml TNF- α for 6 hours after which a sandwich ELISA was carried out on top of the cells. The cells were washed twice with 0.1 M PBS (pH 7.4) and thereafter fixed with 1 % paraformaldehyde for 10 min at 4°C. The cells were rinsed twice with PBS; unspecific antibody binding was inhibited by incubating the cells with blocking solution (0.1 M PBS pH 7.4, 0.5 % BSA) for 15 min. The cells were stained with 10 μ g/ml rabbit anti-mouse tissue factor antibody for 45 min at room temperature, washed 3 times with PBS and labeled with 1:5000 goat anti-rabbit horse radish peroxidase conjugated secondary antibody for 30 min at room temperature. After three washes with PBS, 100 μ l of the peroxidase substrate TMB was added and the reaction was allowed to run for 10 min. Thereafter the reaction was stopped with 2 N H₂SO₄ and absorbance was measured at 450 nm.

2.9.2 TNF- α induced TF expression analyzed with flow cytometry

The cell-based ELISA does not analyze the TF expression on each single cell, but on the cells as a population. To investigate the TF expression on single cells, flow cytometry was used.

bEnd3 cells were incubated with 50 ng/ml TNF- α in serum depleted (normal medium with 1% FCS) for 6, 12 and 24 hours. After two washes in 0.1 M PBS (pH 7.4) containing 1 mM CaCl₂, cells were stained with rabbit anti-mouse tissue factor (200 μ g/ml) in incubation buffer (0.1 M PBS (pH 7.4), 1 mM CaCl₂, 1% BSA) for one hour on ice and labeled with FITC-conjugated goat anti-rat secondary antibody in incubation buffer for 30 min on ice. Before analysis the cells were detached from the plates by washing the cells twice with 0.1 M PBS (pH 7.4) and incubation with 0.025% EDTA for

15 min at 37°C. The cells were finally analyzed by flow cytometry (BD Biosciences, San Jose, CA, USA).

2.9.3 Western Blot

Western Blot analysis was used to investigate the total tissue factor expression by b.End.3 cells and in tumor tissue from animals treated with TNF- α encapsulated liposomes.

2.9.3.1 Cell lysis

bEnd3 cells were seeded in T25 flasks and activated with 50 ng/ml TNF- α for 6 hours. Thereafter the cells were rinsed twice with PBS. Protease inhibitor cocktail (Roche, Basel, Switzerland) was added to the lysis buffer (50 mM Tris/HCl; 100 mM NaCl, 1 mM EGTA, 10 mM, 1% triton X-100, 0.2 % SDS) in a dilution of 1:100 and 400 μ l was added to each flask. The cells were scraped off with a rubber scraper, transferred to an Eppendorf tube and kept on ice. To disperse any large aggregates, the cells were run through a 27 G needle 4-5 times. Thereafter the protein concentration was measured using a Bio-Rad D_c Kit (Bio-Rad, CA, USA) according to the manufacturer's instructions. The lysates could be used directly or stored at -20°C until later use.

2.9.3.2 Tissue homogenization

The tumor tissue was homogenized in a ratio of 1 g tumor tissue to 1 ml lysis buffer (50 mM Tris/HCl, 100 mM NaCl, 1 mM EGTA, 10 mM MgCl₂, 1 % Triton X-100, 0.1% SDS) added 1 complete[®] tablet (Roche, Basel, Switzerland) with protease inhibitors per 50 ml. First, the tissue was homogenized with a Potter Elvehjem tube (5 strokes) and thereafter with an Ultra-Turrax (KIA[®], Wilmington, USA) for 3 times 20 seconds. The protein concentration was then measured as described above.

2.9.3.3 SDS page

A SDS page is run to separate the sample proteins by size. The samples were prepared by mixing 20 μ g protein with NuPage LDS sample buffer (1:4) and reducing agent (0.25 % mercaptoethanol, 1:10), after which the samples were heated for 10 min at 70°C and then loaded. A NuPage[®] 4-12% Bis-Tris gel with MOPS running buffer was

prepared by washing the gel in distilled water, removing the comb and washing the wells. The samples were loaded and run, first, for 10 min at 150 V and then for 40 min at 200 V.

2.9.3.4 Immunoblotting

While the gel was running, the blotting pads, filter paper and nitrocellulose membrane were soaked in NuPAGE transfer buffer mixed with 10% methanol. The proteins were transferred to a 0.20 µm nitrocellulose membrane (LKB Diagnostics) using NuPAGE transfer buffer mixed with 10% methanol to provide optimal protein transfer at 30 V for 1 hour. Membranes were blocked for nonspecific immunoreactivity by incubation for 1 hour with 5 % skimmed milk powder dissolved in 0.1 M PBS, (pH 7.4). The membrane was thereafter incubated with primary antibody solution containing 5 µg/ml rabbit anti-mouse tissue factor in 0.1 M PBS, (pH 7.4) with 0.05% Tween 20, overnight at 4 °C. The membrane was washed 3 times 10 min with 0.1 M PBS containing 0.05 % Tween 20. Antibody binding was detected with horse radish peroxidase-coupled goat anti-rabbit immunoglobulin 1:10,000 in blocking buffer (5 % skimmed milk powder in 0.1 M PBS (pH 7.4)) for 1 hour at room temperature. The membrane was washed 3 times 10 min with PBS containing 0.05% Tween 20. The immunoreaction was visualized using the chemiluminescent ELC plus Western Blot reagent (GE Healthcare Life Sciences, Buckinghamshire, UK) and Amersham Hyperfilm ELC (Amersham, Buckinghamshire, UK).

2.9.4 TF induced coagulation

To investigate whether the up-regulated tissue factor was active, a simple coagulation assay was developed. A single-stage assay where CaCl₂ was added to a mixture of cell lysate and citrated mouse plasma was performed. The mouse plasma contains all the components except tissue factor needed for fibrin formation and clotting. Therefore clotting is dependent on the presence of the active tissue factor protein expressed by the cells. The clotting time was measured by detecting changes in the intensity of light scattered by the samples due to the increased turbidity caused by the clotting particles [Seetharam et al., 2003].

2.9.4.1 Coagulation assay cell lysates

The bEnd3 or B16F10 cells were seeded out in 6 well plates with a density of 5×10^4 cells/well. The cells were allowed to adhere overnight in normal medium. The next

day the cells were activated in serum-depleted cell medium containing 1% FCS and 50 ng/ml TNF- α or 800 μ g/ml DMXAA and stimulated for different time points 4 - 24 hours. The cell lysates were prepared according to Kim et al. [2001]. Briefly, the cells were washed twice with 0.1 M PBS (pH 7.4) and lysed in 100 μ l lysis buffer (15 mM octyl- β -D glucopyranoside in 25 mM HEPES buffer). The cell lysates were transferred to Eppendorf tubes, vortexed for 1 min and incubated at 37 °C for 15 min. Thereafter 200 μ l of 25 mM HEPES buffer was added to each tube and the cell lysates were ready for use.

2.9.4.2 Single-stage coagulation assay

The assay was carried out in a flat-bottomed 96 well plate. To each well 50 μ l cell lysate and 50 μ l citrated mouse plasma (Equitech Bio, Texas, USA) were added and the mixture was incubated for 1 min at 37°C. Thereafter 50 μ l 25 mM CaCl₂ was added to each well and the absorbance was measured continuously at 405 nm with intervals of 8 sec for 2 min using a FLUOstar Optima microplate reader (BMG Labtech, Offenburg, Germany). Negative controls were performed where citrated mouse plasma, cell lysate or CaCl₂ were omitted. Cell lysates from B16F10 cells were used as positive controls. Clotting could be delayed or completely inhibited by pre-incubating the cell lysates with a rabbit anti-mouse tissue factor antibody (10 μ g/ml) for 30 min prior to starting the assay.

2.10 Treatment of colo 677 tumors with DMXAA and TNF- α liposomes *in vivo*

2.10.1 Treatment with TNF-alpha and DMXAA liposomes

The Colo 677 tumors were grown as previously described in section 2.7.1. When the tumors reached a size of 150 - 200 mm the animals were treated with one bolus injection of TNF- α loaded α -VCAM-L or TNF- α -loaded rIgG-L in a concentration of 200 μ g/kg TNF- α . The tumor size was measured daily until the tumors reached a size of 900 - 1000 mm³, after which the animals were sacrificed. A control group of mice were not treated. Each group contained 10 animals. The tumors from four animals in each group were either fixed in 4 % formaldehyde overnight or embedded in paraffin, or snap frozen used for TNF- α ELISA.

2.10.1.1 Tissue factor expression in tumors treated with TNF-L after 24 and 72 hours

A small pilot experiment was carried out in which the expression of TF after treatment with VCAM targeted TNF-L and empty liposomes 24 hours and 72 hours after treatment. Western blot was used to investigate whether TF was upregulated.

The Colo 677 tumors were grown and when the tumors reached a size of 150 - 200 mm the animals were treated with one bolus injection of either TNF- α loaded α -VCAM-L or empty α -VCAM-L in a concentration of 200 μ g/kg TNF- α . After 24 and 72 hours the animals were sacrificed, the tumors immediately snap frozen and stored at -80°C until further use.

The tumors were then homogenized. First, 1 g tumor tissue was homogenized using 1 ml lysis buffer (50 mM Tris/HCl, 100 mM NaCl, 1 mM EGTA, 10 mM MgCl₂, 1 % Triton X-100) added one complete® tablet with protease inhibitors (Roche, Basel, Switzerland) per 50 ml. Secondly, the tissue was homogenized with a Potter Elvehjem tube (5 strokes) and then with an Ultra-Turrax for 3 times 10 seconds. Thereafter the same Western Blot procedure was followed as described in section 2.8.3.

2.10.2 TNF- α ELISA

A TNF- α ELISA was carried out to measure the amount of TNF- α accumulated in the tumors after treatment. First, 1 g tumor tissue was homogenized using 1 ml lysis buffer (50 mM Tris/HCl, 100 mM NaCl, 1 mM EGTA, 10 mM MgCl₂, 1 % Triton X-100) added one complete® tablet with protease inhibitors per 50 ml. Then the tissue was homogenized with a Potter Elvehjem tube (5 strokes) and further homogenized with an Ultra-Turrax for 3 times 10 seconds. The homogenate was centrifuged at 11000 rpm for 20 min at 4°C in a Eppendorf centrifuge. The supernatant was collected and the protein concentration was measured with a Bio-Rad Dc Kit according to the manufacturer's recommendations. The amount of TNF- α was measured in the supernatants using a TNF- α ELISA kit according to the manufacturer's instructions.

2.10.3 Immunohistochemistry and histology

2.10.3.1 Fluorescence microscopy of tissue sections

Cryosections of tumors were thawed, fixed in 4 % paraformaldehyde for 10 min and incubated with rabbit anti-mouse tissue factor (10 µg/ml). Sections were incubated with primary antibodies for 1 hour at room temperature. Excess primary antibody was removed by three successive washes for 5 min with PBS. Thereafter, Alexa Fluor 568 conjugated secondary antibody was applied for one hour at room temperature, followed by three washes with PBS. Coverslips were mounted with a fluorescence-mounting medium (Dako, Glostrup, Denmark). The sections were stored in the dark at 4°C until further analysis.

2.10.3.2 In situ TUNEL assay

In order to investigate whether treatment with TNF- α and DMXAA induced cell death in the tumor a terminal deoxynucleotidyl transferase dUTP nick end labeling (TUNEL) assay was employed.

Apoptosis is a well controlled process, which among other things, results in DNA fragmentation. The TUNEL assay takes advantage of the apoptosis-induced single and double strand breaks by labeling the free 3'OH DNA termini with digoxigenin-labeled and unlabeled nucleotides. The reaction is catalyzed by the enzyme deoxynucleotidyl transferase, which catalyses a template independent of the addition of nucleotide triphosphates to the 3'OH ends. The DNA fragments labeled with digoxigenin are then labeled with a peroxidase labeled anti-digoxigenin antibody, which enzymatically generates an intense localized staining of chromogenic substrates such as diaminobenzidine (DAB).

The TUNEL assay was carried out according to the manufacturer's recommendations. Briefly, 20 µm paraformaldehyde-fixed tumor cryosections were post-fixed in pre-cooled ethanol:acetic acid (2:1 v/v) for 5 min at -20°C. Thereafter the sections were washed two times 5 min in PBS. Endogenous peroxidase activity was quenched in 3 % H₂O₂ in PBS for 5 min at RT and thereafter washed twice with PBS for 5 min. The sections were equilibrated with EQUILIBRATION BUFFER for 10 seconds. Excess liquid was tapped off and immediately thereafter, working-strength TdT enzyme was added. The sections were incubated for 1 hour in a humid chamber at 37 °C. The reaction is stopped by washing the sections twice in stop/wash buffer for 15 sec agitation

and thereafter for 10 min. The sections are washed 3 times in PBS for 5 min and excess of liquid is removed. The sections were incubated with anti-digoxigenin peroxidase conjugated antibody for 30 min in a humid chamber at RT. The sections were washed 4 times in PBS for 2 min. Thereafter the substrate DAB was applied for 6 min. DAB was in 0.01% H₂O₂ 0.05 M Tris/HCl buffer. The sections were washed in demineralized water twice for 5 min. Tissue sections were placed on slides and coverslips were mounted with Pertex mounting medium. Some sections were not exposed to TdT and served as negative controls.

To investigate whether there was a quantitative difference in the amount of apoptotic cells within the different treatment groups, two different fields were counted from 4 tumors in each group. Both fields were in the periphery, one in a hot spot area and one in a normal area.

2.11 Statistical analysis

Statistical significance between groups in the *in vitro* binding assays and in the *in vivo* biodistribution experiment was calculated using unpaired Student's t-test. Significance was assumed at a p-value < 0.05. Statistical significance between multiple groups in the treatment experiment were calculated using one way analysis of variance (ANOVA), and post-hoc the Newman-Keuls test was used to test for significance between the individual groups.

3. Results and Discussion

The concept of targeting liposomes to tumor vasculature provides an opportunity for specific and effective delivery of drugs to the diseased sites and is an appealing strategy for therapy. The accessibility and stability of tumor endothelial cells makes them convenient targets, both for drug delivery and drug action. Targeting ILs against endothelial cell surface antigens has been used to target the endothelium [Kessner *et al.*, 2001; Voinea *et al.*, 2005]. The cell adhesion molecule VCAM is one promising target receptor and plays a role in the pathogenesis of inflammatory diseases such as atherosclerosis, rheumatoid arthritis and multiple sclerosis [Dienst *et al.*, 2005]. VCAM expression is inducible and is selectively expressed on activated endothelium, i.e. in human malignant tumors [Guccione *et al.*, 2004]. Firstly, the targetability of endothelial cells by VCAM-targeting liposomes was investigated *in vitro* and *in vivo*. Subsequently experiments were carried out to ensure that the liposomes targeted tumor vasculature selectively and not the vasculature in other organs.

3.1 *In vitro* targeting of VCAM-1

The first step in the development of an α -VCAM liposomal drug delivery system was to investigate the targetability of α -VCAM-coupled liposomes to activated endothelium *in vitro*.

3.1.1 VCAM-1 expression in two different endothelial cells

The two murine endothelial cell lines, 2F2B and bEnd3, were chosen for the establishment of an *in vitro* model of vascular liposomal targeting. 2F2B is a murine endothelial cell line isolated from a Kaposi tumor [Walter-Yohrlin *et al.*, 2004], while bEnd3 is a brain endothelial cell line that is used to study adhesion molecule expression because the cells responds well to cytokine activation. The two different cell lines were investigated to ensure that activated endothelium could be targeted in general.

Flow cytometry was used to establish that the two cell lines indeed expressed VCAM on their surface. Although the non-activated bEnd3 cells (A) and 2F2B cells (not shown) also exhibited some surface expression of VCAM, 4 hours of incubation with TNF- α increased VCAM expression on both bEnd3 cells (B) and 2F2B cells (C) as

illustrated in Fig. 13. Based on these data, all further experiments were carried out with cells activated for 4 hours with TNF- α .

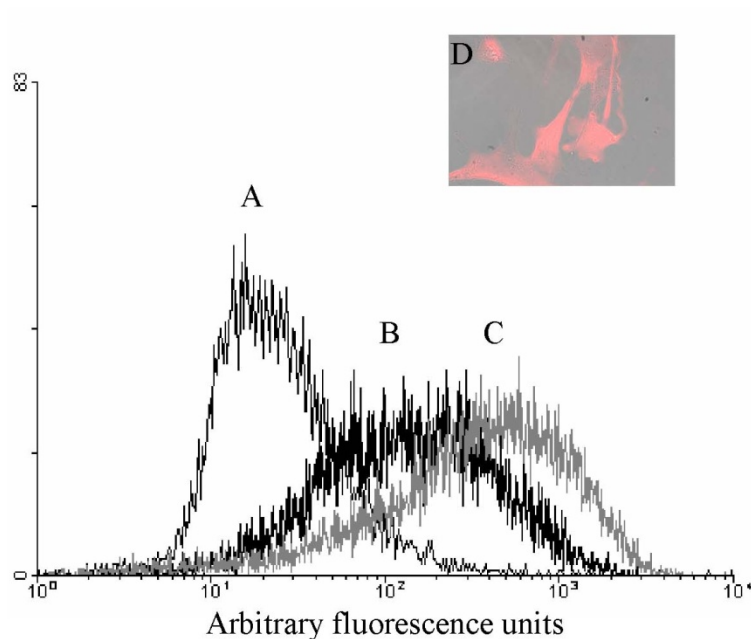


Figure 13. VCAM expression on bEnd3 cells and 2F2B cells after 4 hours. A: VCAM expression on non-activated bEnd3 cells; B: VCAM expression on TNF- α (50 ng/ml, 4 h) activated bEnd3 cells; C: VCAM expression on TNF- α (50 ng/ml, 4 h) activated 2F2B cells. D: VCAM staining of activated bEnd3 cells. The histograms A to C are representative for 3 or more similar diagrams.

3.1.2 Targeting VCAM on activated endothelium in vitro with α -VCAM liposomes

Fluorescence-labeled liposomes were prepared with various proteins coupled to their surface via an NgPE-anchor (Fig. 14). Liposomes carrying anti-VCAM mAb (α -VCAM-NL) were compared to liposomes carrying a human IgG of irrelevant specificity (hIgG-NL), or albumin-conjugated liposomes (Alb-NL) in a fluorescence-based cell assay using both cell lines. As illustrated in Fig. 14A, the binding of the α -VCAM-NL to 2F2B cells was higher than that of the two control liposome-formulations coupled to hIgG and albumin, respectively, although the differences were not statistically significant. The

same observation was made in bEnd3 cells, where the binding of α -VCAM-NL was higher than that of control liposomes and even reached statistical significance with the Alb-NL ($p < 0.05$) (Fig. 14B).

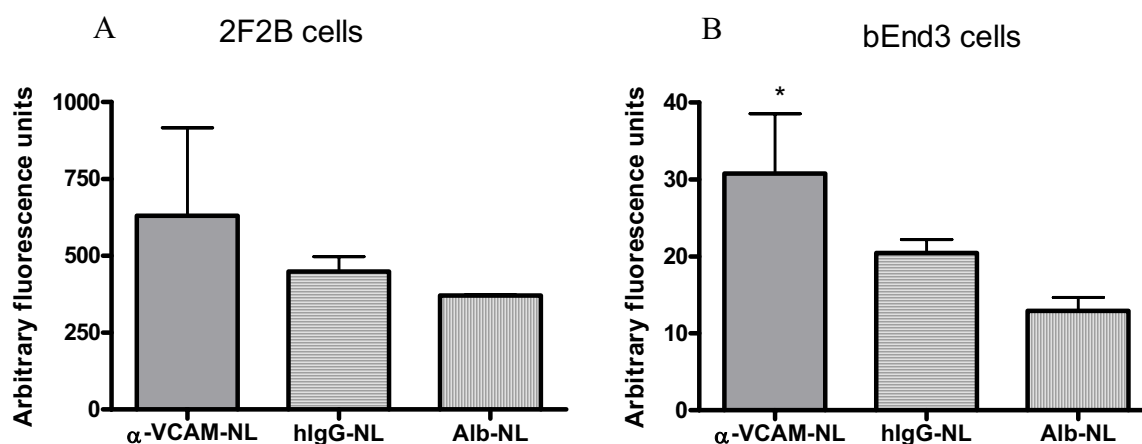


Figure 14. Targeting NgPE- liposomes to VCAM-1 expressing 2F2B cells and bEnd3 cells using plate reader analysis. A comparison of the binding efficiency of α -VCAM-NL and hIgG-NL or Alb-NL is made in 2F2B cells (A) and bEnd3 cells (B) * $p < 0.05$ α -VCAM-NL vs. Alb-NL. Data points represent the average of at least three experiments, error bars are SD.

To investigate whether the relatively high binding of the control hIgG-NL was mediated via Fc-receptors, which have been reported to be up-regulated on activated endothelium [Ryan, 1986; Pan *et al.*, 1998], the same assay was carried out in the presence of a Fc-receptor blocking antibody. The inhibition of binding FITC-labeled human IgG to activated 2F2B cells was investigated using the α -Fc-receptor antibody. As seen in Fig. 15A, 50 % of the binding was inhibited. However, when repeating the experiment with hIgG-NL instead of FITC-labeled human IgG, the binding was only partially inhibited (approximately 25 %) (Fig. 15B). The fact that the binding was not totally abolished suggests that other mechanisms could be involved in the unspecific binding of the hIgG-NL. Fc-receptors are mostly expressed by monocytes, macrophages and lymphocytes [Dasgupta *et al.*, 2000], where they are involved in activating and down-modulating immune responses and combining the humoral and cell mediated immunity [Takai, 2005]. The Fc-receptor-mediated uptake of liposomes by macrophages of the RES has been studied extensively [Koning *et al.*, 2001; Koning *et al.*, 2002; Koning *et al.*, 2003]. Pre-treatment of Kupfer cells with aggregated IgG resulted in a 30 % or 50 % reduction of unspecific IgG-liposome binding, depending on the grafted position of the

antibody; either to the tip of the PEG chain with a hydrazide anchor or randomly to the reactive bilayer lipid through MPB-PE, respectively [Koning *et al.*, 2002]. Apart from the Fc-receptor, a scavenger receptor was shown to be involved in the Kupfer cell uptake of ILs [Koning *et al.*, 2003]. In comparison, our results showed that 25% of the unspecific binding was reduced when the antibody was coupled directly to the activated lipid bilayer, indicating that other factors might be involved in the unspecific binding. This could be the presence of other scavenger receptors on the activated endothelium. Furthermore, the concentration of the blocking antibody could not have been sufficient to completely block the unspecific binding.

It was also investigated whether lipids could play a role in the unspecific binding by adding excess of lipid prior to addition of the liposomes. The results showed that this treatment did not reduce the binding of hIgG-CL to the activated endothelium, but on the contrary showed a tendency to increase the unspecific binding, indicating that excess lipid could render the cell surface stickier.

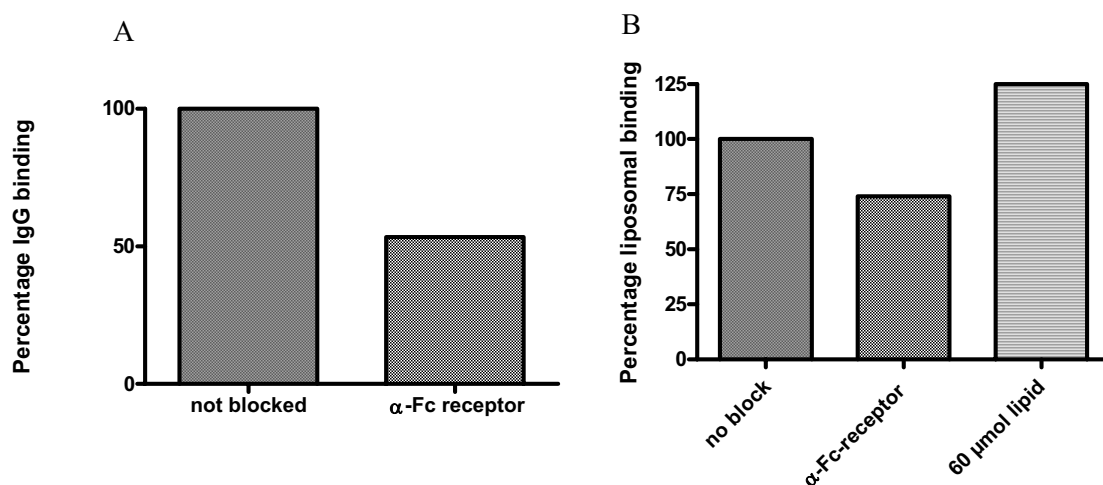


Figure 15. Inhibition of unspecific binding by blocking the Fc-receptor. A) Binding and inhibiting binding of FITC-labeled human IgG to activated bEnd3 cells. B) Binding of DiO labeled hIgG-NL to activated bEnd3 cells and inhibiting binding using a blocking anti-Fc-receptor antibody or 60 μmol of lipid to activated bEnd3 cells.

An alternative protein coupling technique was applied to improve binding selectivity. While the NgPE-anchor coupled the proteins directly to the surface of the liposome, the cyanur-PEG₂₀₀₀-PE anchor attached the protein to the terminal end of the PEG chain [Bendas *et al.*, 1999]. This grafted position of the homing device has been

shown to decrease the unspecific interactions at the membrane surface [Kessner *et al.*, 2001].

Liposomes were prepared with various proteins coupled to the PEG terminus via cyanur-PEG₂₀₀₀-PE anchor. First, the binding efficiency of liposomes carrying anti-VCAM mAb (α -VCAM-CL) to 2F2B cells was compared to liposomes carrying a human IgG of irrelevant specificity (hIgG-CL). The targetability of the two different liposomal preparations to activated 2F2B cells was analyzed in a fluorescence micro-plate assay. α -VCAM-CL bound with significantly higher intensity ($p < 0.001$) to the activated endothelial cells when compared to control liposomes, as illustrated in Fig. 16A. Binding was also analyzed by flow cytometry. Flow cytometry has the advantage that the interrogation of single cells in solution represents more accurate data and gives better signal-to-background ratios by eliminating background fluorescence remaining in the well after washes [Robinson, 2004].

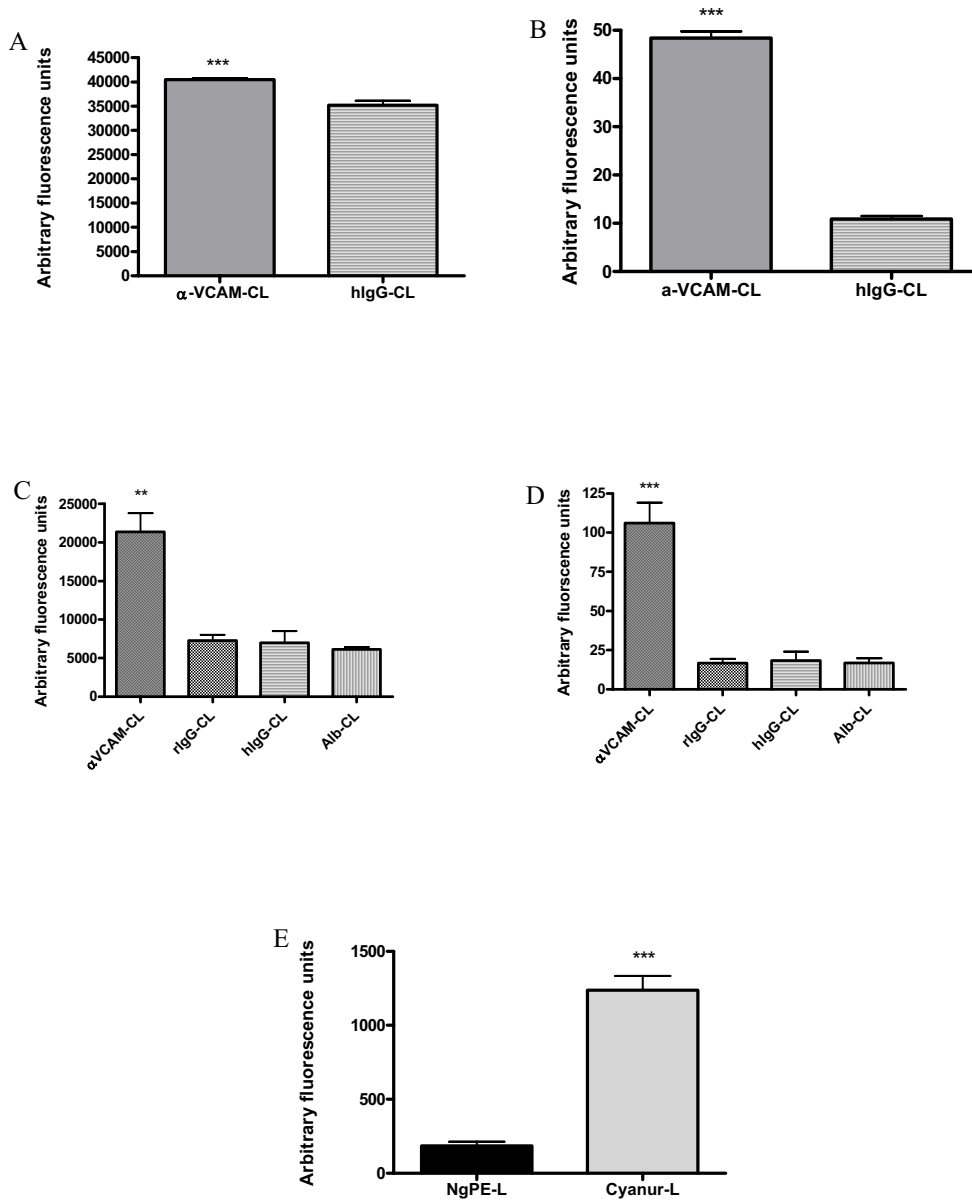


Figure 16. The *in vitro* targeting of cyanur liposomes to VCAM-1 expressing 2F2B cells and bEnd3 cells **A:** Plate reader analysis comparing the binding efficiency of α -VCAM directed IL with hIgG-IL to 2F2B cells. **B:** FACS analysis of the binding efficiency of anti-VCAM directed ILs (α -VCAM-CL), ILs with human IgG (hIgG-CL) of irrelevant specificity to 2F2B cells, *** $p < 0.001$ α -VCAM-CL vs. hIgG-CL. **C:** Comparison of the targetability of α -VCAM-CL, rIgG-CL, hIgG-CL and Alb-CL to activated bEnd3 cells analyzed by fluorescence based cell assay ** $p < 0.005$ α -VCAM-CL vs. all three control liposome populations. **D:** FACS analysis of the binding efficiency of anti-VCAM directed ILs (α -VCAM-CL), ILs with coupled rat IgG1 (rIgG-CL) or human IgG (hIgG-CL) of irrelevant specificity and albumin (Alb-CL) to bEnd3 *** $p = 0.001$ α -VCAM-CL vs. all three control liposome populations. **E:** Comparison of the binding efficiency of VCAM- targeted IL coupled with different anchors NgPE and cyanur-PEG-PE determined by fluorescence based cell assay *** $p = 0.001$ NgPE vs. the Cyanur anchor. Data points represent the average of at least three experiments, error bars are SD.

Indeed, the VCAM-mediated binding of α -VCAM-CL was confirmed and showed a 4-fold higher binding in comparison with the negative control (Fig. 16B). Coupling the antibody to the liposome via the cyanur anchor seemed to be the most successful. Therefore, the same experiments were repeated on activated bEnd3 cells. Additionally, two accessory controls that included albumin and isotype matched rat IgG₁ antibody conjugated to the liposomes were enrolled in the study. The fluorescence micro-plate assay showed that α -VCAM-CL bound with significantly higher intensity ($p < 0.005$) to the activated endothelial cells compared to all three types of control liposomes (Fig. 16C). The isotype matched rat IgG₁ is, compared to fractionated human IgG, a better control for the IgG mediated unspecific binding. There were no differences between binding of the purified rat IgG₁-conjugated liposomes (rIgG-CL) and the fractionated human IgG-conjugated liposomes (hIgG-CL) to the target cells. 60-70 % of fractionated human IgG has the IgG₁ subtype [Hamilton, 1987], and the mouse Fc receptor has been shown to bind all IgGs independent of the species [Ober *et al.*, 2001], indicating that the hIgG would behave similarly to rIgG₁ in circulation. Therefore, due to cost benefits, fractionated human IgG was used as a control.

As an additional negative control, it was shown that, α -VCAM-CL did not bind to a VCAM-negative control cell line (A2780, data not shown), suggesting that the VCAM-mediated targeting was specific. Flow cytometry analysis confirmed the VCAM-mediated binding and showed a higher binding in comparison to negative controls (Fig. 1D; $p < 0.001$).

Finally, α -VCAM liposomes with the two different anchors were compared against each other in a micro plate assay. As illustrated in Fig. 16E, the VCAM targeted cyanur-coupled liposomes showed a significantly higher binding efficiency compared to the NgPE liposomes ($p < 0.001$). The difference was not caused by differences in the amount of protein coupled to the liposomal surface. Table 1 shows that the liposome populations used were comparable in size and protein coupling. Therefore, it is unlikely that any differences in targeting behavior were related to liposomal physical characteristics.

	<i>Particle size (nm)</i>	<i>Polydispersity</i>	<i>μg protein/ μmol PL</i>	<i>Protein content/molecule per liposome</i>
<i>α-VCAM-NL</i>	<i>83.1 ± 14.4</i>	<i>0.13 ± 0.05</i>	<i>54.8 ± 35.5</i>	<i>63.1 ± 52.0</i>
<i>hIgG-NL</i>	<i>91.3 ± 13.2</i>	<i>0.12 ± 0.06</i>	<i>69.9 ± 51.6</i>	<i>70.1 ± 53.2</i>
<i>α-VCAM-CL</i>	<i>83.1 ± 14.4</i>	<i>0.13 ± 0.05</i>	<i>59.0 ± 17.9</i>	<i>52.3 ± 15.8</i>
<i>rIgG-CL</i>	<i>93.4 ± 12.0</i>	<i>0.15 ± 0.04</i>	<i>67.0 ± 51.8</i>	<i>68.2 ± 36.1</i>
<i>hIgG-CL</i>	<i>91.3 ± 13.2</i>	<i>0.12 ± 0.06</i>	<i>74.4 ± 40.2</i>	<i>71.1 ± 35.2</i>
<i>Alb-CL</i>	<i>84.5 ± 13.1</i>	<i>0.15 ± 0.06</i>	<i>70.3 ± 42.0</i>	<i>85.0 ± 4.31</i>

Table 1: Comparison of the liposomal characteristics with respect to particle size and protein coupling yield

The superior behavior of the cyanur liposomes could be explained by the position of the grafted protein. Proteins coupled to the tip of the PEG chain might have better access to the target compared to proteins that are coupled directly to the surface of the liposomes and therefore are partly masked by the PEG chains [Maruyama *et al.*, 1995]. Finally the cyanur anchor was chosen as the best in achieving a VCAM-mediated binding and all further IL preparations in this work contain this anchor. The data confirm specific targeting of ILs via VCAM in two different cell models. Since both cell lines displayed identical targeting behavior, one cell line was chosen for further experiments. bEnd3 cells were selected because of their easier cultivation conditions with respect to safety requirements.

3.1.2.1 Internalization of VCAM-targeted liposomes by activated endothelium

To gain further insight into the behavior of the liposomes after binding to the endothelial cells, liposomal internalization was investigated. As illustrated in Fig. 17 (upper panel) the total association of liposomes with the activated endothelial cells increased with time; from 30 min to 2 hours, whereas the amount of liposomes that were internalized reached a maximum after 1 hour.

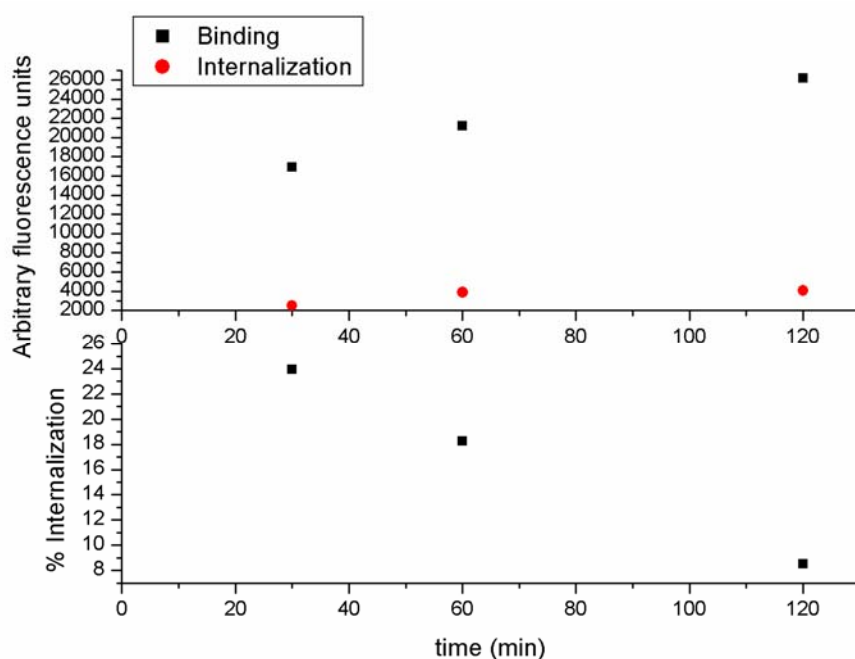


Figure 17. Internalization of DiO labeled α -VCAM liposomes by activated endothelial cells. The binding and internalization, depicted in the upper panel (top), and percentage endocytosis, in the lower panel (bottom), of α -VCAM liposomes was determined as a function of time at 37 °C.

Calculating the percentage of internalized liposomes showed that after 30 min approx. 24 % of the total liposomes associated with the cells were internalized, but after 2 hours the amount of internalized liposomes compared to total cell associated liposomes was reduced to 8 % (Fig. 17, lower panel). These results suggest that the α -VCAM-CL were initially internalized rapidly, but reached a plateau after 1 hour. The fate of the VCAM receptor after antibody binding is, as mentioned before, controversial [Kuijpers *et al.*, 1994; Ricard *et al.*, 1998]. One study showed that monoclonal antibodies against VCAM remained on the surface of HUVEC cells 20 min after binding [Kuijpers *et al.*, 1994], whereas another study found that α -VCAM antibodies were rapidly internalized and that 50% of the antibody was internalized after 11.2 min by HUVEC cells [Ricard *et al.*, 1998]. VCAM-targeted nanoparticles are also internalized. Voinea *et al.* [2005] showed that VCAM-targeted liposomes were internalized after binding to activated HUVECs [Voinea *et al.*, 2005] and a phage display-derived peptide with homology to the α -chain of VLA-4 was used to internalize nanoparticles into the endothelial cells via VCAM as a way to amplify signals (“biological amplification through intracellular trapping”) [Kelly *et al.*, 2005]. The bEnd3 cells internalized α -VCAM-CL and reached a plateau after 1 hour (Fig. 17, upper panel); in contrast, HUVECs were shown to increase

the amount of internalized liposomes from 1 to 24 hours [Voinea *et al.*, 2005]. The discrepancy between these two studies could be due to the different time frames. After 1 hour the internalizing mechanism might have been saturated, and the bEnd3 cells could after 24 hours have internalized a bigger fraction of the α -VCAM-CL. Another explanation could be that VCAM behaves differently in murine endothelial cells compared to human endothelial cells.

The experiment showed that a fraction of the liposomes were internalized after binding to the endothelium. Whether the internalization was a passive or active process was not investigated. However, previous studies have shown that VCAM internalization occurs via clatrin-mediated endocytosis [Ricard *et al.*, 1998; Voinea *et al.*, 2005].

The liposomes in this study are used to target TNF- α and DMXAA to the endothelium. TNF- α exerts its activity through TNFR60 which is expressed on the cell surface; the release of TNF- α at the endothelial surface is therefore preferable. However, a study showed that delivering TNF- α to the TNF- α resistant human cancer cells via internalizing ILs induced TNF- α cytotoxicity [Morishige *et al.*, 1993], suggesting that TNF- α is also cytotoxic when delivered intracellularly.

3.1.3 The targeting of activated endothelium in a dynamic flow assay

Static binding of liposomes to the cell surface does not mimic the vascular targeting of liposomes under physiological shear force conditions in circulation, especially considering the highly variable flow conditions in tumor vasculature [Denekamp *et al.*, 1985].

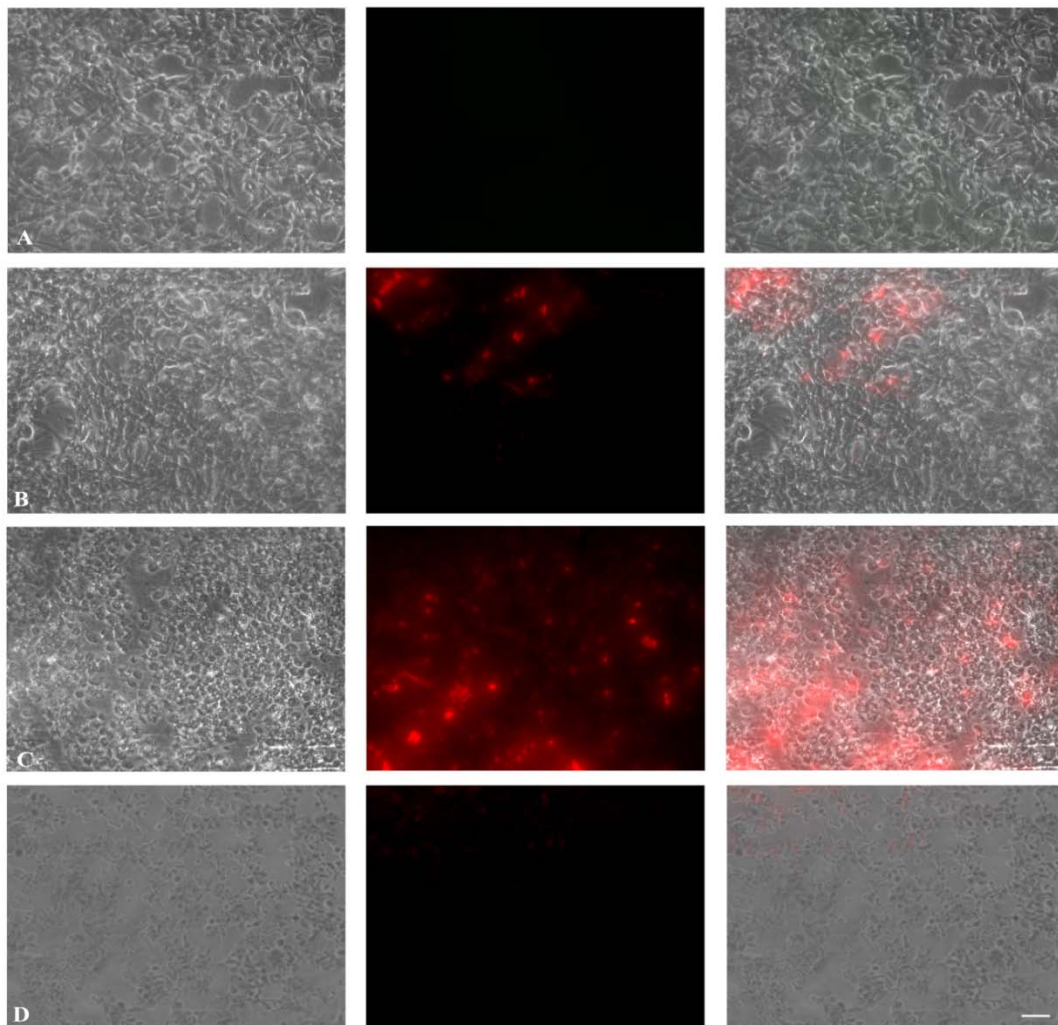


Figure 18. Binding of rhodamine-labeled α -VCAM-CL to stimulated bEnd3 cells under shear force conditions illustrated in a phase contrast image (left), as a fluorescence image (middle) and as an overlay image (right). The binding of rhodamine-labeled α -VCAM-CL to the cell monolayer was analyzed at 0, 1 and 20 hours (A-C) and compared to the binding of rhodamine-labeled hIgG-CL after 20 hours (D). The bar represents 50 μ m.

Therefore, we employed a flow chamber assay [Kessner *et al.*, 2001] to investigate whether liposome binding was sufficient to target bEnd3 cells under shear stress conditions similar to those found in capillary venules. The binding of α -VCAM-CL and hIgG-CL to endothelial cells was followed microscopically over a time period of 20

hours. As shown in Fig. 18 A-C, the binding of α -VCAM-CL to the cell layer increased in a sustainable manner illustrated by the increasing fluorescence intensity with time. In contrast, no binding was observed with the hIgG-CL (Fig. 18D). The staining of the bEnd3 cells (Fig. 18C) represents both internalized and surface-bound liposomes. The ratio of surface-bound and internalized ILs was not determined, and should be investigated further.

Dynamic flow based analysis of endothelial adhesion is mainly used to investigate the interactions between leukocytes and endothelial cells [Florey and Haskard, 2007]. However the technique has also been used to study liposomal interaction with endothelial cells. Previous studies targeted liposomes to the adhesion molecule, E-selectin, under shear stress conditions [Bendas *et al.*, 1998; Kessner *et al.*, 2001]. Antibody-based vascular targeting strategies are more advantageous because the antibody/antigen binding exhibits excellent bond dissociation constants; however it also has potential problems. One problem is the relatively low bond formation rates between antibody and antigen, which could hamper the attachment of rapidly transiting particles in shear stress where contact time is short [Kaufmann *et al.*, 2007]. The dynamic binding studies proved that α -VCAM-CLs were able to target VCAM on activated endothelium in a circulation relevant time range despite the shear stress. The dynamic flow assay also offers the advantage of being a method that mimics the conditions in circulation and reduces the number of animal experiments.

The *in vitro* studies showed that α -VCAM-CLs target activated endothelium successfully under both static and dynamic conditions. After binding, internalization of the α -VCAM-CLs was observed. Targeting ILs to VCAM on activated HUVEC cells has previously been investigated *in vitro* [Chiu *et al.*, 2003; Voinea *et al.*, 2005]. VCAM is a convenient target as it is found up-regulated on activated endothelium. Furthermore, α -VCAM nanoparticles have been used to detect areas of early inflammation [Tsourkas *et al.*, 2005] and *in vivo* detection of atherosclerotic lesions [Kelly *et al.*, 2005; Kaufmann *et al.*, 2007]. The VCAM nanoparticles could therefore be suitable candidates for a variety of therapies and as imaging agents.

3.2 *In vivo* targeting of VCAM-1 expressed on tumor endothelium

Since the *in vitro* results appeared promising, the vascular targeting of α -VCAM-CL was investigated in mice bearing human Colo 677 xenograft tumors.

3.2.1 VCAM expression on the vasculature of the human Colo 677 xenograft model

The Colo 677 tumor model has previously been investigated by Dienst *et al.* [2005] and has been shown to express VCAM on the endothelium. The Colo 677 cells form solid tumors when injected subcutaneously, although Colo 677 cells are myeloma cells that normally would not form solid tumors. However, in this model, ~30% of the tumor vasculature is VCAM-positive. The model was chosen because the expression of VCAM is generally low on blood vessels in other tumor mouse models, in contrast to tumor vascular VCAM expression in humans [Dienst *et al.*, 2005].

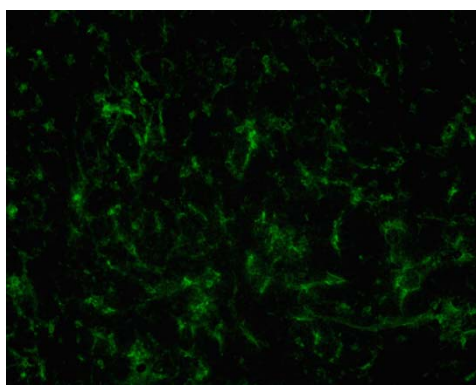


Figure 19. VCAM expression by tumor endothelial cells in a human Colo 677 xenograft tumor. Immunohistochemical staining showed that VCAM (Fig. 19) was expressed throughout the tumor in a vessel-like pattern confirming the previous results [Dienst *et al.*, 2005]. For our purpose the expression of VCAM on the endothelium is more important than the origin of cancer cell, therefore this tumor model was chosen for targeting and therapy experiments.

3.2.2 Tumor distribution of ^3H -labelled targeted and non-targeted liposomes

The intra-tumor accumulation of α -VCAM-CL versus hIgG-CL 30 min and 24 hours after i.v. injection, was quantified by detecting the [^3H]-labeled liposomes in the tumor tissue. The data given in Fig. 20 indicate that the accumulation of both liposomal populations increased with time. At 24 hours, about 2% of injected dose per gram of tissue was localized to the tumor, although – in contrast to human tumors - only ~30% of

tumor vessels show a medium strong expression of VCAM-1 in this mouse model [Dienst *et al.*, 2005].

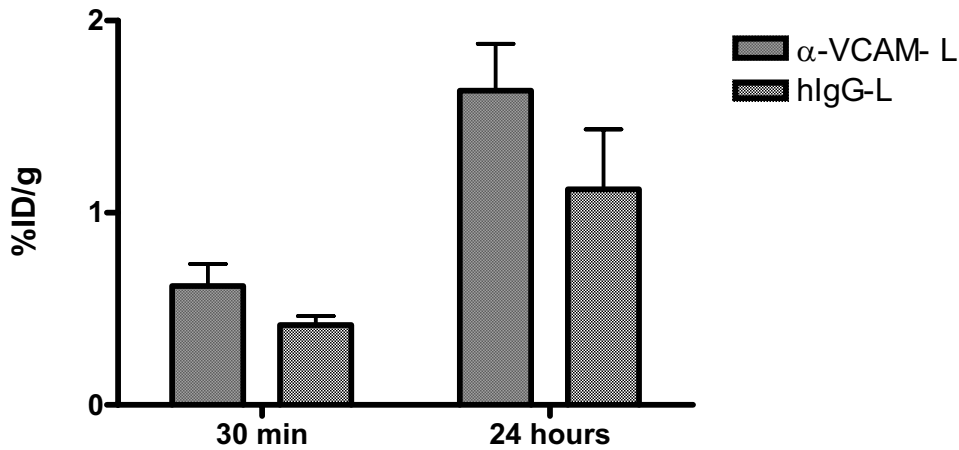


Figure 20. Comparison of the quantitative tumor accumulation of α -VCAM-CL and hIgG-CL. The [3 H]-activity in tumors was detected 30 min and 24 h after injection of the [3 H]-labeled liposomes into Colo 677 tumor xenograft mice (data are means \pm SD, $n \geq 4$).

The tumor accumulation of VCAM-directed ILs was slightly higher than that of control liposomes, but this difference did not reach statistical significance. This was not unexpected and should be related to unspecific tumor accumulation of the control liposomes. Unspecific accumulation of liposomes has been described previously [Huang *et al.*, 1992; Emanuel *et al.*, 1996; Charrois *et al.*, 2003] and is attributed to an EPR effect [Noguchi *et al.*, 1998].

The accumulation of doxorubicin-loaded liposomes targeted against polyoma virus-induced tumor associated antigen showed an accumulation of approximately 3 % ID/g tissue after 6 hours in mice bearing stage 1 A9 lung metastasis [Emanuel *et al.*, 1996], even though the time frame was different, this is comparable to the accumulation found in our study. However, other studies showed that approximately 5-8 % of both targeted and non-targeted liposomes accumulated in the tumor after 24 hours [Marty *et al.*, 2002; Maeda *et al.*, 2004; Kirpotin *et al.*, 2006; Pastorino *et al.*, 2006]. The difference might be attributed to the fact that the Colo 677 tumor model only expresses VCAM on approximately 30 % of the endothelium, resulting in a lower accumulation. It might also be case that different tumor model exhibit a different degree of EPR.

The differences between unspecific and specific tumor targeting of liposomes cannot be distinguished by quantitative evaluation. Therefore experiments were performed to investigate the specific localization of the liposomes after injection.

In order to evaluate whether vascular-directed versus unspecific ILs were localized to different compartments within the tumor, we investigated the targeting behavior of DiO-labeled ILs by fluorescence microscopy. The images, in Fig. 21 clearly indicate that tumor accumulation of α -VCAM-CL was evident after only 30 min (Fig. 21A1) and had increased by 24 hours (Fig. 21B1). At both time points the tumor accumulation of α -VCAM-CL was more intense than that of both control liposomes (Fig. 21C1-D1), which was unexpected when considering the data in Fig. 20. The lower fluorescence intensity of the control liposomes in the tumors could be related to a higher degree of extravasations and dilution of the liposomes throughout the tumor which renders their fluorescence below the detection level.

To confirm whether the different liposomes were localized to the tumor vasculature, tumor sections were counterstained with a fluorescent antibody against murine CD31 (Fig. 21A2-D2). This double labeling procedure (Fig. 21A3 and B3 low magnification, A6 and B6 high magnification) revealed a clear co-localization between the α -VCAM-CL and the endothelium after 30 min (91.7%) and after 24 hours (73.1%). In contrast, both types of control liposomes displayed a much lower degree of co-localization with vascular endothelium (30.3% and 23.7%, resp.; Fig. 21 C3-D3 low magnification, C6-D6 high magnification). Endothelial cells are known to express receptors for the Fc portion of antibodies [Olafsen *et al.*, 2006] as well as for albumin [Antohe *et al.*, 1991]. Labeling activated endothelial cells with a negative control IgG-antibody coupled to nanoparticles has been described in a mouse model for vascular inflammation [Tsourkas *et al.*, 2005]. This background binding could probably be decreased if recombinant antibody fragments devoid of the Fc portion, such as scFv, were to be used as a targeting moiety.

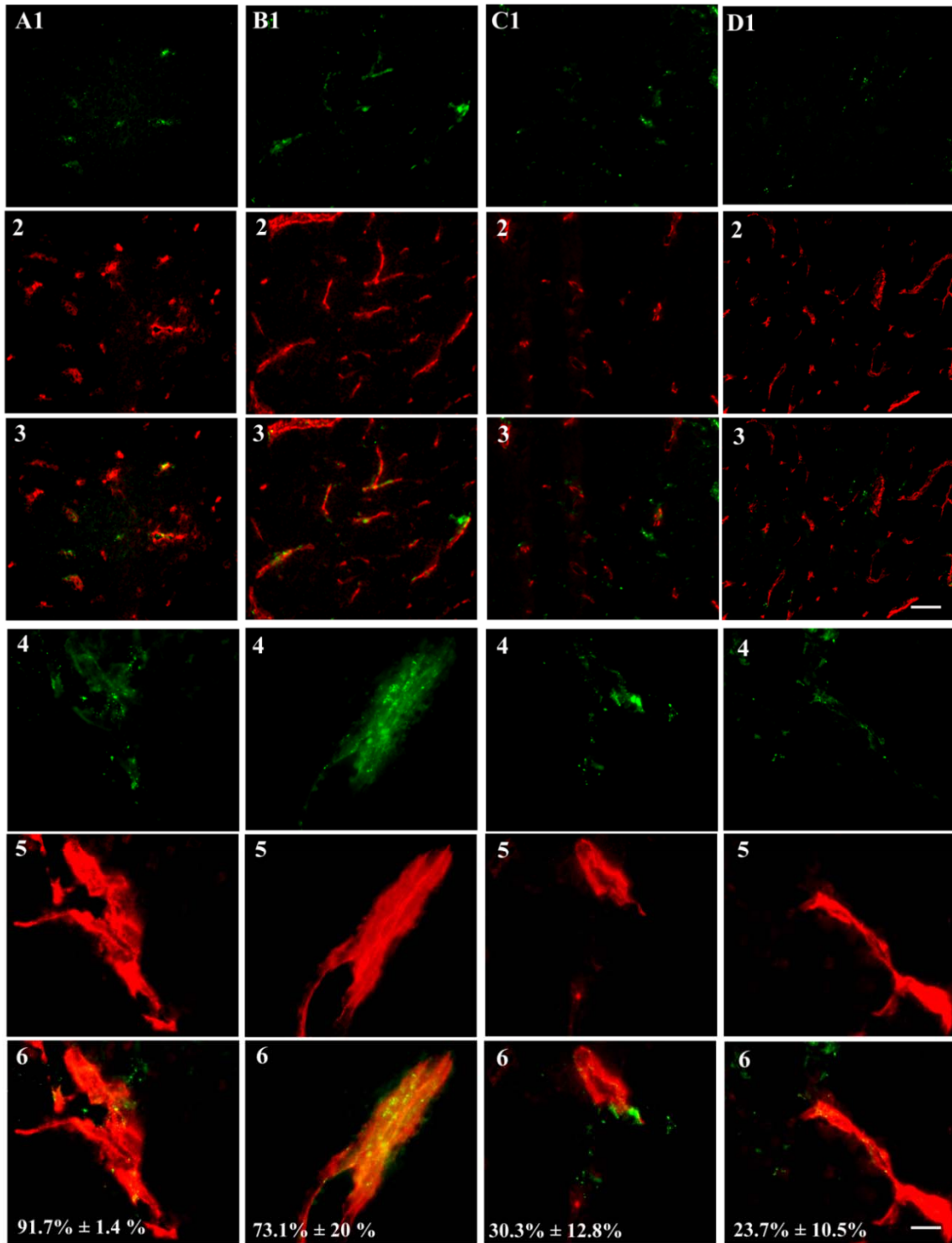


Figure 21. Localization of the different liposome populations within the tumors. (A1-6) α -VCAM-CL 30 min after i.v. injection; (B1-6) α -VCAM-CL 24 h after i.v. injection; (C1-6) hIgG-CL 24 h after i.v. injection; (D1-6) Alb-CL, 24 h after i.v. injection illustrating a high degree of co-localization for A and B, but not for C and D. 1) liposome distribution (green), 2) endothelial staining with CD31 (red), 3) overlay at low magnification, 4) liposome distribution (green), 5) endothelial staining with CD31 (red), 6) overlay at high magnification of liposome distribution (green) and endothelial marker CD31 (red). The bar in the low magnification images corresponds to 50 μ m. The bar in the high magnification images corresponds to 5 μ m.

Similar studies investigating the distribution of tumor vasculature targeting liposomes showed that the peptide SP5-52 accumulated in lung tumors by recognizing the tumor neo-vasculature [Lee *et al.*, 2007]. However, this study only investigated the localization of the homing peptide and lacked investigations of the whole liposomal particle. Another example is a nano-particle containing iron oxide that targeted clotted plasma proteins. This nano-particle was found localized to the tumor endothelium, but only after pretreatment with Ni²⁺-liposomes. Ni²⁺ and iron oxide are thought to attract plasma opsonins and deplete opsonins from circulation, thereby increasing the circulation time of the nanoparticles [Simberg *et al.*, 2007].

These data indicate that the α -VCAM-CLs behave differently from the unspecific tumor accumulation of non-targeted liposomes, supporting the effort to develop a specific and receptor-mediated vascular targeting. In a similar study, Kirpotin *et al.* [2006] investigated the distribution and localization of liposomes targeted against tumor cells compared to non-targeted liposomes. Their results showed that although approximately the same amounts of liposomes were found in the tumor, the specific localization of the liposomes differed. The non-targeted liposomes accumulated in the perivascular and extracellular space, whereas the targeted liposomes were found in the tumor cell cytosol [Kirpotin *et al.*, 2006]. Knowledge about the cellular distribution within the tumor is an important factor when choosing an appropriate effector molecule.

3.2.3 The localization of liposomes in organs

To investigate whether α -VCAM-CL would target vasculature outside the tumor, the localization of the liposomes in major organs, such as heart, lung, liver, spleen and kidney, was investigated. The biodistribution of the liposomes was quantitatively determined using both [³H]-labeled α -VCAM-CL and hIgG-CL with subsequent activity detection in the organs after 30 min and 24 hours. After 30 min, the majority of α -VCAM-CL was localized in the liver (16.3 % ID/g) and the spleen (11.5 % ID/g); whereas the organ distribution was much lower in the other organs. The same was seen for the hIgG-CL. Although there was a difference in the amount of liposomes accumulated in the liver and the spleen for the two types of liposomes it was not significant due to high standard deviations. There was also no difference observed for all other organs except the blood, where the difference between the levels of α -VCAM-CL

(15.7 %) and hIgG-CL (4.4 %) was statistically significant ($p = 0.008$). This was not expected and is most likely explained by technical difficulties in the 30 min series, which was also evident by the large standard deviation found in the liver and spleen. Heart puncture could have been the wrong blood sampling technique to use after 30 min or might have been carried out wrongly. Another explanation could be that the liposomes were still localized in the tail. In further experiments the radioactivity in the tail should be measured as a control.

	<i>Muscle</i>	<i>Skin</i>	<i>Heart</i>	<i>Lung</i>	<i>Kidney</i>	<i>Spleen</i>	<i>Liver</i>	<i>Blood</i>
α-VCAM-L	0.25 \pm 0.23	0.86 \pm 0.69	0.72 \pm 0.56	0.94 \pm 0.56	1.21 \pm 0.40	11.5 \pm 7.3	16.3 \pm 7.9	15.7 \pm 4.5
	0.25 \pm 0.18	0.69 \pm 0.45	1.03 \pm 0.67	1.85 \pm 0.94	3.59 \pm 2.14	3.40 \pm 2.32	8.11 \pm 1.24	1.02 \pm 0.82
hIgG-L	0.34 \pm 0.07	0.86 \pm 0.40	0.3 \pm 0.25	0.52 \pm 0.35	1.21 \pm 0.14	3.04 \pm 1.79	8.01 \pm 2.20	4.40 \pm 0.95
	0.46 \pm 0.14	0.99 \pm 0.53	0.97 \pm 0.37	1.66 \pm 0.13	2.65 \pm 1.73	3.30 \pm 0.3	6.72 \pm 2.20	1.11 \pm 0.39
Statistics								
($p \Rightarrow$)	0.55	1	0.302	0.293	1	0.140	0.135	0.008
30 min	0.130	0.42	0.893	0.747	0.546	0.931	0.285	0.864
24 hours								

Table 2: Biodistribution of α -VCAM-CL and hIgG-CL after 30 min and 24 hour as % injected dose per gram tissue.

The data given for the 24 hours point indicate that the majority of liposomes were accumulated in the liver (8% ID/g), followed by kidney, spleen, and lung, whereas other organs showed lower liposome accumulation. High uptake into liver, spleen and lung was not unexpected, since localization of liposomes into these organs is a well known phenomenon and is generally attributed to extraction via the RES [Emanuel *et al.*, 1996]. No statistically significant differences were seen between VCAM targeted liposomes and control liposomes after 24 hours, consistent with unspecific accumulation being part of the liposome elimination pathway. This is different from previous reports with both NGR-targeted and RGD-targeted liposomes, which accumulate in higher amounts in lung and/or spleen [Pastorino *et al.*, 2003; Schiffelers *et al.*, 2003].

To define the tissue compartments to which the liposomes localized within the different organs, a similar study as the one described above was carried out. Cryosections of lungs, kidneys, liver and spleen from mice injected with DiO labeled liposomes (Fig.

22A-D, left images) were counterstained with fluorescent antibodies detecting either endothelial cells (Fig. 22A-D, middle) or tissue resident macrophages (Fig. 22A-D, right). Liposome signals in the lung were rare and, if present, co-localized primarily with alveolar macrophages (Fig. 22A, right). Fluorescent signals in the kidney were observed in glomeruli, occasionally on endothelial cells, in tubuli and as scattered events. Glomerular staining could be explained by VCAM expression of mesangial cells [Seron *et al.*, 1991]. In contrast to human kidneys [Kuzu *et al.*, 1993], endothelial cells in murine kidneys show a low level of VCAM expression [Fries *et al.*, 1993 and Gottstein C., unpublished data]. The tubular stain appeared more diffuse possibly due to free dye reabsorbed by the tubuli after escaping into the glomerular filtrate. Scattered staining was found within tubular lumina, and also in co-localization with kidney macrophages (Fig. 22B, right).

The liver sections exhibited a clear co-localization between the liposomes and liver macrophages (Fig. 22C, right image), while virtually no co-localization was observed in sections stained against the endothelium (Fig. 22C, middle). Accumulation of liposomes in the liver has been studied extensively [Gabizon and Papahadjopoulos; 1988; Papahadjopoulos *et al.*, 1991] and the Kupfer cells have been shown to play an important role in removing liposomes from circulation [Huang *et al.*, 1992; Litzinger *et al.*, 1994]. In the spleen, liposome signals were prominent in the marginal zone, in accordance with previous studies [Litzinger *et al.*, 1994; Aichele *et al.*, 2003]. No co-localization with spleen vasculature was observed (Fig. 22D, middle). Instead, co-localization was observed with F4/80 positive macrophages in the red pulp (not shown) and with CD11b positive cells (Fig. 22D, right). CD11b is a marker for macrophages and also for dendritic cells, which are known to express VCAM.

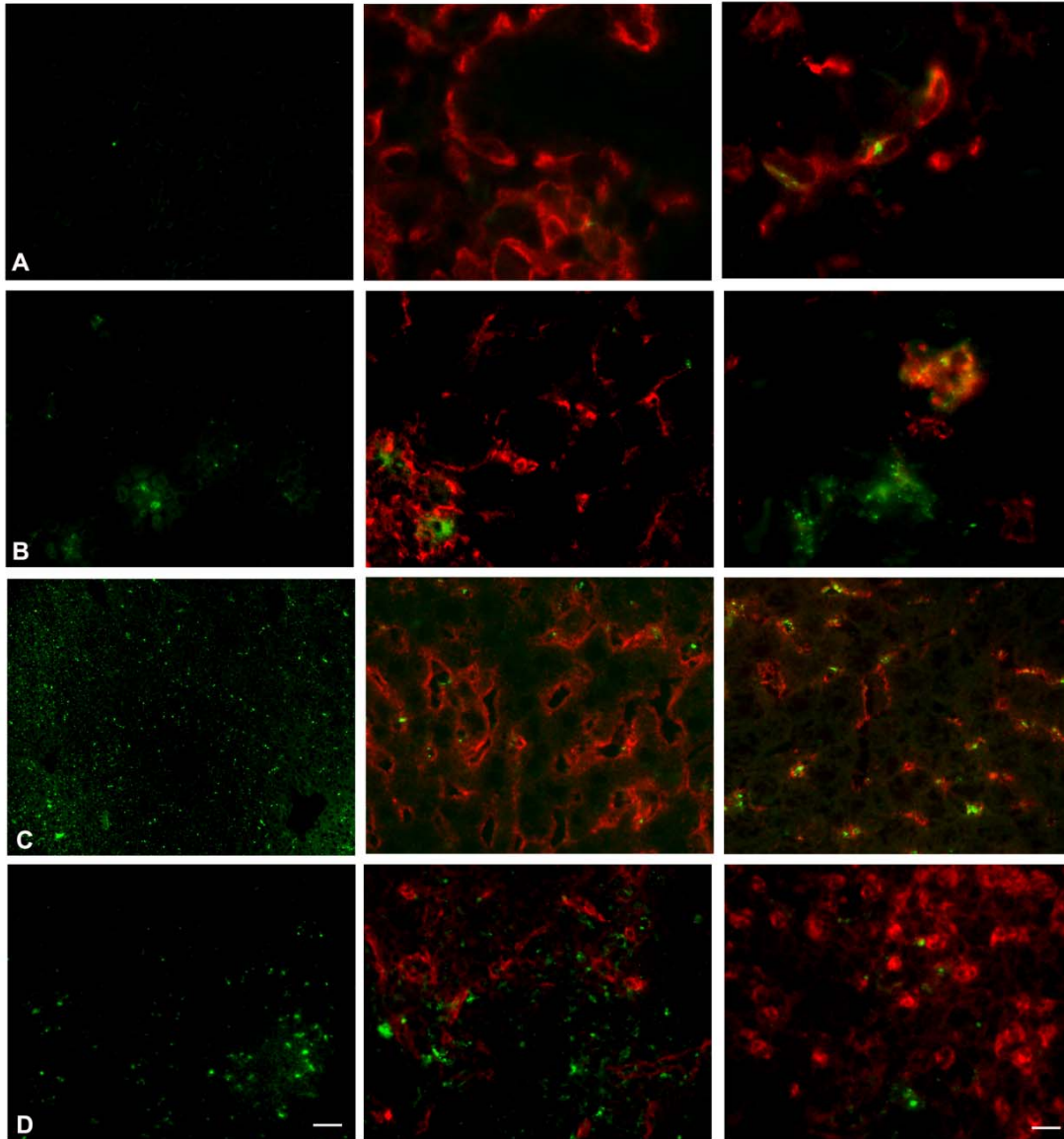


Figure 22. Distribution of liposomes in lung, kidney, liver and spleen from tumor bearing mice, 24 hours after i.v. injection. **A:** Lung section showing the α -VCAM-CL distribution (left), lung section double-stained against the endothelial marker Meca32 (middle) and double-stained against the macrophage marker CD11b (right). Note that the liposomes in the lung are co-localized with the lung macrophages. **B:** Kidney section showing the distribution of α -VCAM-CL (left); kidney section double-stained against the endothelial marker CD31 (middle); kidney section double-stained against the macrophage marker CD11b (right). **C:** Liver section illustrating the α -VCAM-CL (green) distribution (left). Liver section double-stained against the endothelial marker Meca32 (middle) and liver section double-stained against the macrophage marker F4/80 (right). Note the clear co-localization between the liver macrophages and liposomes. **D:** Spleen section showing the distribution of VCAM-CL (green) in the white pulp and marginal zone (left). Spleen section double-stained against the endothelial marker Meca32 (middle) and spleen section double-stained against the macrophage and dendritic cell marker CD11b (right). The bar in the low magnification images corresponds to 50 μ m. The bar in the high magnification images corresponds to 5 μ m.

The VCAM-targeted liposomes were shown to not co-localize with the endothelium in the major organs investigated in this study. The accumulation observed in the spleen and liver were excepted as these are the organs involved in the clearance of liposomes from circulation [Blume *et al.*, 1993; Maryama *et al.*, 1995]. Attempts have been made to reduce the RES-mediated clearance such as depleting the RES for macrophages by pretreatment with clodrate liposomes or opsonin chelating Ni²⁺-iron oxide nanoparticles [Simberg *et al.*, 2007]. Saturating the RES with lipid [Sharma and Sharma, 1997; Simberg *et al.*, 2007] or blocking the Fc receptors [Aragnol and Leserman, 1986] are other methods that were proven efficient in prolonging the circulation time of therapeutic liposomes [Aragnol and Leserman, 1986; Simberg *et al.*, 2007], resulting in a greater targeting potential. In our study the major concern was that the drugs encapsulated in the liposomes induce coagulation and vascular collapse and therefore a co-localization with the vasculature in other organs would not be desirable.

The VCAM-targeted liposomes were shown to target the tumor vasculature but not the vasculature of other organs, thereby the α -VCAM-CL show potential as a drug delivery system for drugs that are aimed at the tumor vasculature.

3.3 TNF- α and DMXAA induced cytotoxicity and TF expression and activation *in vitro*

The next step was to find the effector molecule(s) to encapsulate into the targeted liposomes. The cytokine, TNF- α , was chosen as a proof of concept drug, as it was shown to induce coagulation in tumors [Watanabe *et al.*, 1988]. The small molecule VDA, DMXAA, was also investigated as it is a TNF- α inducing drug that is currently undergoing clinical phase II trials. TNF- α is known to exhibit multiple effects such as permeabilizing the endothelium [Friedl *et al.*, 2002], inducing apoptosis [Pallerdy *et al.*, 1999; Deng *et al.*, 2003; Xia *et al.*, 2006] and inducing a pro-coagulative state by the induction of TF [Bevilacqua *et al.*, 1986; Conway *et al.*, 1989]. Therefore, *in vitro* studies were conducted to investigate the cytotoxic effect of TNF- α and DMXAA on murine endothelial cells. Thereafter the expression and activity of TF induced by TNF- α and DMXAA was studied.

3.3.1 TNF- α and DMXAA induced cytotoxicity on endothelial cells

The primary goal of our study was to induce TNF- α mediated clotting in tumors. However, TNF- α and DMXAA have also been shown to exert a direct cytotoxic effect on human endothelial cells [Xia *et al.*, 2006].

3.3.1.1 TNF- α induced cytotoxicity

A simple PI uptake assay and a MTT proliferation assay were used to study the TNF- α induced cytotoxicity. The cytotoxicity of TNF- α was first investigated using a crude assay that measures changes in the plasma membrane [Darzynkiewics *et al.*, 1997]. PI is a membrane impermeable dye, which only stains those cells whose membranes have become permeable by i.e. TNF- α induced cell damages. The PI method is based on the binding of the fluorescent PI to nucleic acids [Wrobel *et al.*, 1996].

As shown in the dot plots (Fig. 23B and D) the percentage of PI positive cells increased with time from 27.11% at 24 hours to 76.99% at 48 hours. These results indicate that TNF- α induces cell death in murine endothelial cells.

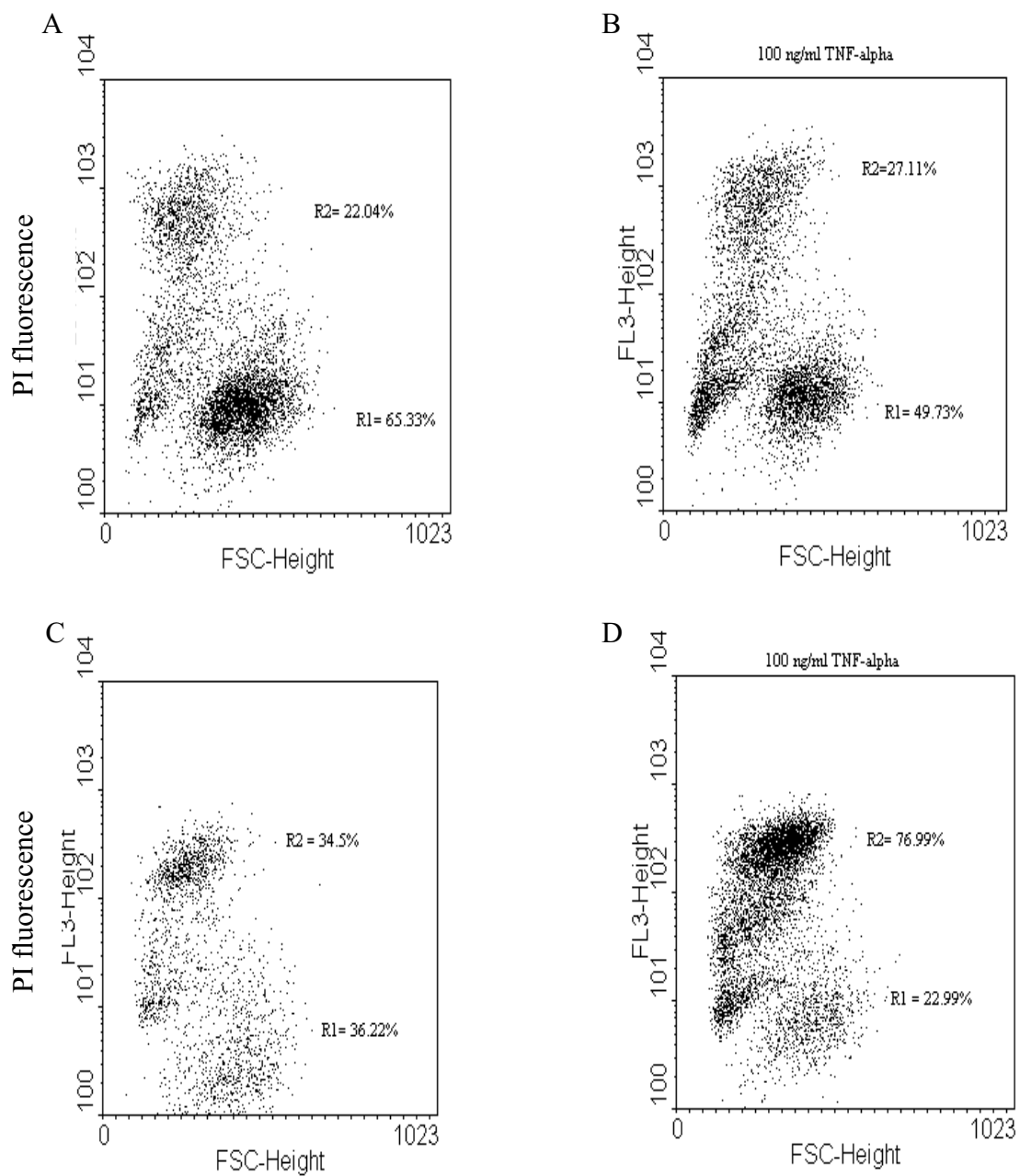


Figure 23. The uptake of PI after of TNF- α treatment on bEnd3 endothelial cells after 24 and 48 hours. A: PI stained not stimulated bEnd3 cells after 24 hour. B: PI stained bEnd 3 cells stimulated with 100 ng/ml TNF- α after 24 hours. C: PI stained not stimulated bEnd3 cells after 48 hour. D: PI stained bEnd 3 cells stimulated with 100 ng/ml TNF- α after 48 hours. R1 represents the still living, not stained cell fraction and R2 represents the dead or damaged (stained) cell fraction. The analyzed regions are representative for at least three similar experiments.

Apoptosis is generally regarded as the opposite of necrosis. Cell necrosis is a passive degeneration of cells characterized by swelling of cells and organelles and loss of electrolytes balance followed by rupture of the cell membrane [Darzynkiewics *et al.*, 1997]. Necrosis is often technically defined by the permeability of dyes such as PI and

trypan blue, due to membrane rupture. However, in *in vitro* assays the apoptotic cells are not phagocytosed by cells of the immune system, which in turn results in the degeneration of apoptotic cell membrane that thereby become permeable for these dyes, a process called “secondary necrosis” [Pallerdy *et al.*, 1999]. The PI positive cells in this experiment could therefore be both necrotic and late apoptotic cells. Another method to study apoptosis and necrosis using flow cytometry is given by analyzing the cell size using the forward scatter counts (FSC). During the process of apoptosis, the cells shrink, leading to a decrease in the FSC. As seen in Fig. 23B and D the PI positive cells have lower FSC, indicating cell shrinkage and thereby apoptosis. However, additional assays are necessary to more precisely differentiate between apoptosis and necrosis. This could simply be done by pre-incubating the cells with annexin V. Annexin V binds selectively to PS in the presence of Ca^{2+} , which is present on the outer membrane of early apoptotic cells [Vermes *et al.*, 1995].

The PI assay showed that the percentage of dead cells increased with time. To investigate the cytotoxicity of TNF- α in a dose dependent manner a MTT assay was employed. The MTT assay does not measure cell death directly but cell viability, thereby giving an indirect measure for cell killing.

The bEnd3 cells were treated with increasing concentrations of TNF- α for 6, 24 and 48 hours. After 6 hours (Table 3) nearly no cytotoxicity was seen independent of the concentration. After 24 hours, approximately 30% of the bEnd3 cells were killed by 100 ng/ml TNF- α , and after 48 hours the number of killed cells increased to 80%. Treatment with 10 ng/ml TNF- α was also cytotoxic towards the bEnd3 cells, after 24 hours 15% of the cells were killed and after 48 hours 70 % were killed.

<i>ng/ml</i>	<i>% survival 6 hours</i>	<i>% survival 24 hours</i>	<i>% survival 48 hours</i>
0	99.89 ± 28.72	99.88 ± 16.20	101.33 ± 15.65
10	100.50 ± 3.77	85.15 ± 4.30	33.68 ± 6.13
100	82.32 ± 8.90	71.13 ± 7.95	22.71 ± 10.17

Table 3: The cytotoxic effect of TNF- α on bEnd3 cells. The percentage of surviving cells at different concentration in the time range 6-48 hours

The MTT assay is widely used to measure cytotoxicity of agents used in anti-cancer treatment. TNF- α was previously shown to kill approximately 40% of bovine pulmonary arterial endothelial cells at a concentration of 20 ng/ml [Polunovsky *et al.*, 1994], or 40 % of HUVECs using 40 ng/ml TNF- α after 24 hours [Xia *et al.*, 2006]. After 24 hours the bEnd3 cells exhibited a lower degree of cytotoxicity (~15 % - 30%) compared to the two studies described above. However the use of different doses complicates a direct comparison. TNF- α is not cytotoxic to most cells, because activation of the TNFR60 also leads to the activation of NF- $\kappa\beta$ and JNK signaling pathway [Lee *et al.*, 1997], which protects the cells against the apoptotic effect of TNF- α [Deng *et al.*, 2003]. Co-treatment with inhibitors of protein synthesis by i.e. actinomycin D and cyclohexamide, which inhibits transcription and translation respectively, enhances the cytotoxicity of TNF- α [Polunovsky *et al.*, 1994]. Thus, de novo synthesis of apoptosis protecting proteins seems to be essential for the protective effect of NF- $\kappa\beta$. Treatment with TNF- α for 48 hours seems to be cytotoxic independent of the dose. The results presented here give no explanation for this. However, it might be that after 48 hour the amount of TNF- α induced ROS has increased to such a degree leading to a ROS mediated inactivation of NF- $\kappa\beta$ [Deshpande *et al.*, 2000]. This is very speculative and the mechanism is not known, however another study showed that approx 78 % of bovine adrenal cortex-derived microvascular endothelial cells were apoptotic after 48 hours of exposure to 1 $\mu\text{g/ml}$ TNF- α [Lucas *et al.*, 1998] corresponding well with the results in the present study. Further studies are needed to clarify the mechanism.

The two assays, PI and MTT, showed the same tendency namely that after 24 hours about 30% and after 48 hours about 70 % of the cells are killed, confirming that both assay can be used to study the TNF- α induced cytotoxicity.

3.3.1.2. DMXAA induced cytotoxicity

The cytotoxic effect of DMXAA on endothelial cell was also studied using the bEnd3 cells. The cytotoxicity assays of TNF- α on bEnd3 cells showed that TNF- α did not induce cell death after 6 hours. Therefore, the DMXAA induced cytotoxicity was studied after 24 and 72 hours of treatment. DMXAA showed a dose dependent cytotoxicity on bEnd3 after 24 and 72 hours (Table 4).

<i>DMXAA</i> ($\mu\text{g/ml}$)	<i>% survival</i> <i>24 hours</i>	<i>% survival</i> <i>72 hours</i>
0	100 \pm 3.77	100 \pm 6.18
100	50.97 \pm 1.34	76.49 \pm 11.14
1000	34.89 \pm 2.81	43.09 \pm 6.68

Table 4: The cytotoxic effect of DMXAA on bEnd3 cells. The percentage of surviving cells at different concentration after 24 and 72 hours

The greatest cytotoxic effect was seen after 24 hours. Treatment with 100 $\mu\text{g/ml}$ DMXAA resulted in killing of approx. 50% of the cells, and 1 mg/ml resulted in 65% dead cells. However, after 72 hours the percentage of viable cells was increased, indicating that especially for low doses of DMXAA, the cells recover from 24 to 72 hours. The cytotoxicity of DMXAA on endothelial cells *in vitro* has been investigated using the TUNEL assay in another study. After 24 hours a dose of 400 $\mu\text{g/ml}$ DMXAA induced apoptosis in approximately 40% of murine endothelial cells [Ching *et al.*, 2002]. Two different methods were used to determined cell death, which might be the reason for the discrepancy between these two studies. The TUNEL assay labels apoptotic cells, whereas the MTT assay illustrates the cell viability but does not distinguish between apoptotic and necrotic cells.

Apart for being cytotoxic against endothelial cells, the cytotoxic effects of DMXAA on tumor cells are controversial. DMXAA was not cytotoxic against RIF-1 cells [Bellnier *et al.*, 2003], but approx 10 $\mu\text{g/ml}$ DMXAA was shown to inhibit cell growth in 70Z/3 and 1.3E2 pre-B lymphoma cells [Woon *et al.*, 2003]. In both cases the cytotoxicity of TNF- α on the tumor cells was investigated and it was found that the tumor cell death was not affected by TNF- α [Bellnier *et al.*, 2003; Woon *et al.*, 2003]. The cytotoxic effects of DMXAA seen in the two pre-B lymphoma cell lines was independent of TNF- α , indicating that DMXAA might exhibit some direct cytotoxic activities dependent on the tumor cell.

3.3.2 TNF- α induced TF expression and activity

Among several effects, TNF- α is known to induce the expression of TF. Since the expression of TF is of central importance in our targeting approach, we first wanted to study the TNF- α effect on TF expression in the bEnd3 cell system. The relationship between TNF- α and TF up-regulation has been described before, but most studies were carried out on human endothelial cells [Rehemtulla *et al.*, 1991; Kim *et al.*, 2001; O'Reilly *et al.*, 2003]. In this work a murine model was used and therefore an investigation of the effect of TNF- α on murine endothelial cells was needed.

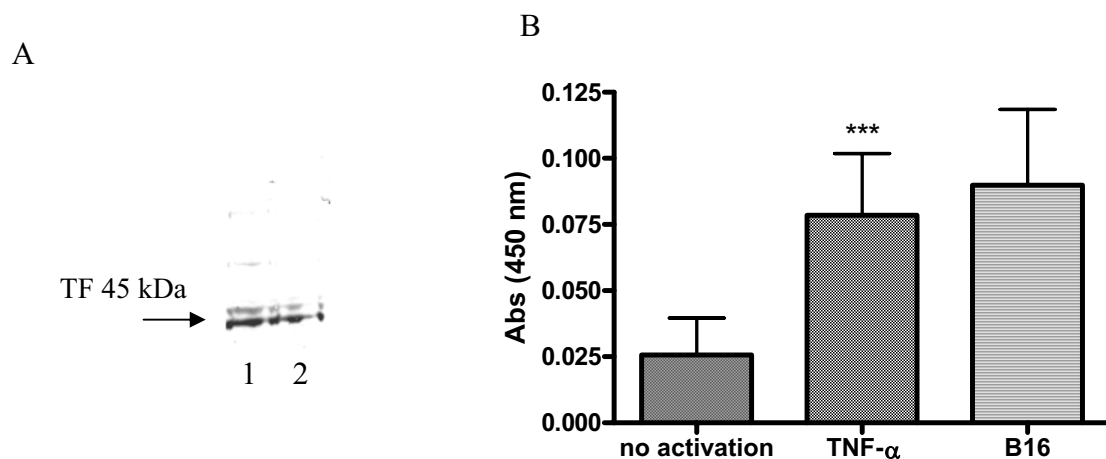


Figure 24. TNF- α induced tissue factor expression on bEnd3 cells investigated by Western blot and cell-based ELISA. A: Immunoblot of bEnd3 cells either stimulated (1) with 50 ng/ml TNF- α for 6 hours or not treated (2). B: tissue factor expression on bEnd 3 cells that were either not activated or treated with 50 ng/ml TNF- α for 6 hours; compared to B16 cells that constitutively express tissue factor. *** p = 0.001 no activation vs. TNF- α treated cells. Data points represent the mean of at least three experiments, error bars are SD.

Western Blot analysis of stimulated and not stimulated bEnd3 cells showed that both treatments resulted in an expression of TF protein. The band representing the activated cells (Fig. 24A) seems to be stronger than the band representing the control cells, when taking into account that the same amount of total protein was added to each well. However, to be able to quantify the increase, a cell-based ELISA was developed where the immunoreaction was carried out on top of fixed cells. As illustrated in Fig. 24B, the stimulated bEnd3 cells showed a 3-fold increase in the TF expression. Untreated cells showed a basal level of TF expression, which was not unexpected as previous studies on human endothelial cells also found that the same [Kim *et al.*, 2001; O'Reilly *et al.*, 2003]. B16F10 myeloma cells (B16 cells) have previously been shown to express TF constitutively [Amarzguoiu *et al.*, 2006]. Therefore, they were included as a positive control and were shown to express a slightly increased amount of TF compared to the TNF- α treated bEnd3 cells.

Cell-based ELISAs have previously been used for detection and quantification of molecules expressed on the cell surface [Wewetzer *et al.*, 1996; Liu *et al.*, 2000; Yang *et al.*, 2006]. The advantages of cell-based ELISA are that it is a rapid method for screening for surface antigens [Arunachalam *et al.*, 1990; Sedgwick and Czerkinsky, 1992; Liu *et al.*, 2000], it is convenient for large scale screening [Wewetzer *et al.*, 1996] and a quick test prior to further analysis by more discriminating methods, such as flow cytometry [Sedgwick and Czerkinsky, 1992]. In addition, another advantage is that adherent cells are not detached from the plate by trypsination or other detachment methods, which might enzymatically remove epitopes crucial for antibody binding [Gaffar *et al.*, 1989] or induce cellular stress and thereby reducing or increasing the antibody binding. Fixation of cells is also known to interfere with the antigen/antibody binding [Wewetzer *et al.*, 1996]. In this study the cells were fixed with 1% paraformaldehyde, which was found to be optimal with respect to keeping the cells bound to the plate and at the same time retaining antigen/antibody binding. The cell-based ELISA has the disadvantage of not directly measuring the TF expression on every single cell, but instead gives an average of the total increase in TF for the whole cell population. Therefore, to investigate the TF expression on single cells, flow cytometry analysis was carried out.

As shown in Fig. 25, FACS analysis confirmed that TNF- α induced TF expression at a significant level. Furthermore, TF expression was again observed on the control cells. To assure that the TF antibody binds specifically to the TF protein, the reaction was

spiked with recombinant mouse tissue factor protein (50 $\mu\text{g/ml}$). This resulted in a blockage of the TF antibody/antigen reaction confirming that the detected binding was specific towards the TF protein. However, blockage did not completely abolish binding, which could indicate that the TF antibody also exhibited unspecific binding.

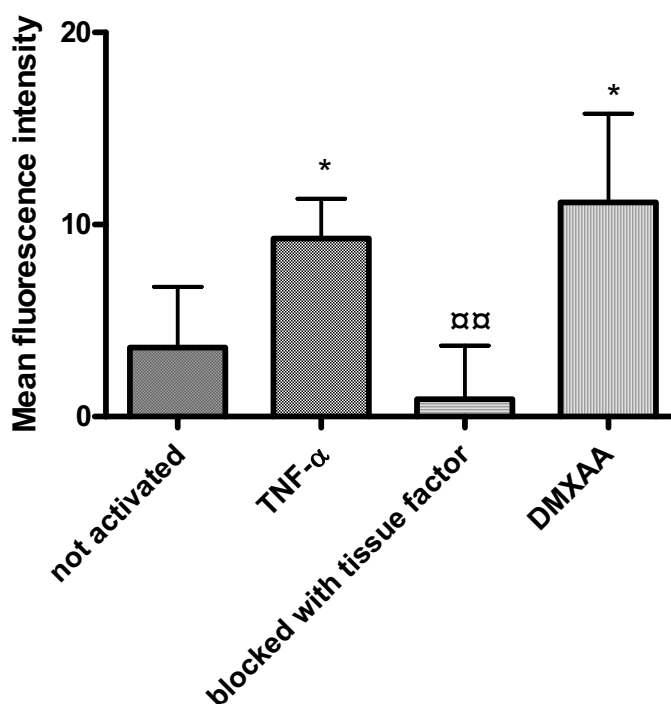


Figure 25. Tissue factor expression on bEnd3 cells treated with TNF- α or DMXAA. bEnd3 cells treated with plain medium, TNF- α (50 ng/ml) for 6 hours or DMXAA (100 $\mu\text{g/ml}$) for 12 hours were subjected to flow cytometry analysis. The specificity of the TF antibody/TF antigen was tested by spiking the reaction with excess TF protein. * $P < 0.05$ not treated vs. TNF- α and DMXAA treated. □□ $p < 0.001$ TNF- α vs. blocked. Data points represent the mean of at least three experiments, error bars are SD.

For further control, a similar experiment was carried out using the human ovarian cancer cell line (A2780Adr), which is negative for mouse TF. Only a slight unspecific binding was detected (results not shown). The antibody towards murine TF was of polyclonal nature. Polyclonal antibodies are known to exhibit a higher background binding compared to monoclonal antibodies [Lipman *et al.*, 2005] and this might explain the unspecific binding seen in these experiments.

In addition, the expression of TF on bEnd3 cells after treatment with DMXAA was studied. The biochemical target of DMXAA is unknown but it has been shown to induce the synthesis of TNF- α , which might lead to the up-regulation of TF either as a primary or secondary effect. The cells were treated with DMXAA for 12 hours and a

significant up-regulation of the TF expression, comparable to that TNF- α , was seen (Fig. 25). This is the first study showing that treatment of endothelial cells with DMXAA results in an up-regulation of TF. However, this was expected as DMXAA is known to induce the synthesis of TNF- α . The question is whether the induced TF is the result of TNF- α dependent or independent action of DMXAA. Further studies are needed to clarify this.

The protocols for both cell-based ELISA and flow cytometry have been thoroughly optimized. It was previously shown in mouse 3T3 cells [Gregory *et al.*, 1989] and COS-7 cells transfected with human TF [Mackman *et al.*, 1990] that expression of the TF gene was induced by serum through the regulatory element called serum response element [Mackman *et al.*, 1990]. Therefore, the experiments were carried out with cells in serum starved medium (1% FCS), which was found to reduce the expression of TF in the control cells (not shown). Another problem was that the detachment process seemed to activate the cells. It was previously hypothesized that the detachment induces stress in cultured cells thereby resulting in a rapid up-regulation or decryption of TF expression [Maynard *et al.*, 1975]. Subsequently, all TF expression experiments were carried out on attached cells, which were detached after the immunoreaction and right before flow cytometry measurement.

TF is the primary cellular inducer of coagulation and acts as a high affinity receptor for factor VII /VIIa. Apart from inducing coagulation, TF also has other distinct functions such as participating in inflammation [Mackman, 1995], metastasis [Bromberg *et al.*, 1995; Hjortoe *et al.*, 2004], tumor associated angiogenesis [Zhang *et al.*, 1994; Contorino *et al.*, 1996] and embryonic development [Carmelit *et al.*, 1997]. The TNF- α induced TF expression is regulated by the TNFR60, which in turn activates the transcription factors NF- κ B [Moll *et al.*, 1995; Matschurat *et al.*, 2003]. Cytokine activation might induce changes in cell surface expression of TF by changing gene transcription, mRNA stability, translation and protein trafficking [Hansen *et al.*, 2001]. The TNF- α mediated TF up-regulation was found to be dependent on an increased transcription of TF mRNA in HUVECs [Conway *et al.*, 1988] and human dermal micro endothelial cells (HDMEC) [O'Reilly *et al.*, 2003]. An enhanced transcription might be assumed as the mechanism involved in the TNF- α induced up-regulation in bEnd3 cells. The signaling pathway involved in the induction of TF after TNF- α treatment varies

depending on the cell line [O'Reilly *et al.*, 2003] but it is beyond the scope of this study to investigate the signaling pathways involved in TNF- α mediated TF in bEnd3 cell.

It has been hypothesized that cells express encrypted TF protein, which does not have full clotting activity and needs to be decrypted to regain full activity [Bach and Rifkin, 1990; Bogdanov *et al.*, 2005]. Therefore a simple coagulation assay was developed to roughly validate that the up-regulated TF indeed was active.

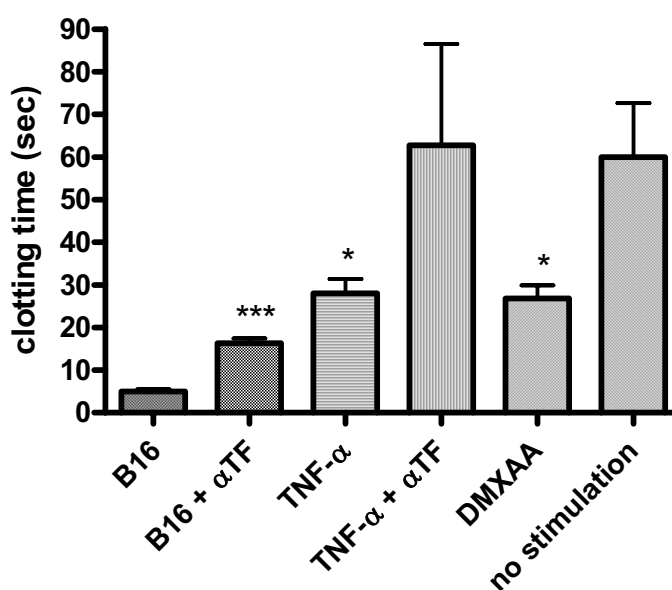


Figure 26. Coagulation time induced by tissue factor activity on bEnd3 cells treated with TNF- α or DMXAA or on B16 cells. B16 cells were used as positive control cell line. bEnd3 cells were treated with TNF- α (50 ng/ml) for 6 hours, DMXAA (100 μ g/ml) for 12 hours or plain medium. TF mediated clotting was abolished with a TF antibody. *** $p=0.0006$ B16 vs. B16 + α -TF. * $P<0.05$ no stimulation vs. TNF- α and DMXAA. Data points represent the mean of at least three experiments, error bars are SD.

The cells were stimulated with TNF- α for 6 hours or with DMXAA for 12 hours before cell lysis. The cell lysate was mixed with citrated mouse plasma and after addition of Ca^{2+} the change in absorption at 405 nm was observed. As illustrated in Fig. 26, clotting time decreased when stimulating the bEnd3 cells with DMXAA (26.8 sec.) or TNF- α (28.0 sec.) compared to non-stimulated endothelial cells (60 sec.). This indicates that the up-regulated TF indeed was active. Again the B16F10 cells were included in the experiment as a positive control and also showed a strong clotting potential that could be delayed by blocking with a TF antibody. This also confirms that the rapid clotting activity indeed was TF specific. Blocking the bEnd3 cells activated with TNF- α also resulted in an increased clotting time. However, the deviation in these experiments was rather high

and the differences between the clotting times for blocked and not blocked were not statistically significant.

Although this clotting assay has several restrictions and only allows for a crude evaluation of the clotting intensity, it confirms the active state of the TF protein expressed by the bEnd3 cells. Blood clotting induced by bEnd3 cells has previously been investigated [Dienst *et al.*, 2005; Bhattacharjee *et al.*, 2007]. The targeting of truncated TF to the bEnd3 cell surface induced coagulation in a cell-free two-stage coagulation assay [Dienst *et al.*, 2005] confirming that bEnd3 cells could be made pro-coagulant. Also, LPS stimulated bEnd3 cells were subjected to a cell-free single-stage clotting assay, which resulted in a clotting time of 145 sec, whereas non-treated cells exhibited a clotting time of 200 sec [Bhattachajee *et. al.*, 2007]. Compared to the presented results, the clotting times obtained in the other study were considerably longer, however this could be due to the different treatments (TNF- α and LPS) and different measurement methods. Other assays which directly determine the activity of factor VII or X were not performed, but could have been useful to more fully characterize the TF activity.

The TNF- α and DMXAA induced clotting time reduction correlates well with the up-regulation of TF. The normal bEnd3 cells were shown to express a basal level of TF. TF is thought to exist encrypted on the surface of endothelial cells also in culture [Bach and Rifkin, 1990; Pendurthi *et al.*, 2007]. Decryption of TF is thought to be mediated by modulation of the cell surface in a calcium dependent manner. The precise mechanism of TF-decryption is unclear, but the presence of PS on the outer cell membrane [Bach and Rifkin, 1990; Henriksson *et al.*, 2005] and changes to the TF protein itself [Henriksson *et al.*, 2005; Pendurthi *et al.*, 2007] have been suggested as the mechanism. As shown above TNF- α and DMXAA induce cell death, which results in the translocation of PS from the inner leaflet to the outer leaflet of the membrane, indicating that activation of the endothelium both leads to cell death and at the same time to the induction of a pro-coagulant state. There is evidence that apoptosis correlates with a pro-coagulant state and TF activity [Bombeli *et al.*, 1997; Matschurat *et al.*, 2003], which together might lead to the induction of endothelial apoptosis and vascular collapse.

In conclusion, TNF- α upregulated and activated TF protein on bEnd3 cells. At sites of inflammation and in tumors the cells produce VEGF, which in synergy with TNF- α have been shown to up-regulate TF expression [Kim *et al.*, 2001; Shen *et al.*, 2001]. Preliminary studies showed that cells treated with both TNF- α and VEGF expressed a

higher amount TF on the cell surface (data not shown). The delivery of TNF- α to the tumor endothelium, could therefore together with the endogenous tumor VEGF lead to increased TF expression and clotting.

3.4 Combing VCAM-targeted liposomes and induction of TF activity

Specific targeting of α -VCAM liposomes to the tumor vasculature was achieved and it was shown that both, TNF- α and DMXAA are capable of inducing an increased TF expression and pro-coagulant activity in murine endothelial cells. The next step was therefore to combine the two parts and to investigate the anti-tumor effect of α -VCAM targeted liposomes carrying either TNF- α or DMXAA *in vivo*. First, the encapsulation of the two agents was investigated.

3.4.1 Encapsulation of TNF-alpha and DMXAA into ILs

Liposomes encapsulated with TNF- α and DMXAA were formulated and characterized. In order to encapsulate sufficient amount of drugs, another method of liposome preparation was used. A 100 mM concentration combined with small volumes excluded the use of extrusion. The liposomes were instead sonicated to achieve the right size. However, this method has a lower reproducibility with respect to particle size. As seen in Table 5, the particle size was slightly increased and so was the polydispersity, compared to the empty liposomes used in the targeting studies (Table 1).

	<i>Particle size(nm)</i>	<i>Polydispersity</i>	<i>Encapsulation efficiency (%)</i>
<i>TNF-α-L</i>	<i>109 \pm 2.3</i>	<i>0.294 \pm 0.027</i>	<i>33.04 \pm 10</i>
<i>DMXAA-L</i>	<i>110 \pm 1.8</i>	<i>0.306 \pm 0.04</i>	<i>18.02 \pm 3.7</i>

Table 5: Comparison of the liposomal characteristics with respect to particle size and encapsulation efficiency.

The amount of encapsulated TNF- α was determined with FITC-labeled TNF- α , whereas the determination of the DMXAA concentration was based on direct measurements of the fluorescent drug. A fluorescence spectrum was obtained and the optimal wavelength for excitation and emission were 350 nm and 412 nm, respectively. This was nearly identical to the wavelengths used by Zhou *et al.* [2001] who used an excitation wavelength of 345 nm and an emission wavelength of 409 nm.

Fluorescence measurements showed that about 33% of TNF- α was encapsulated, which is in agreement with other studies, where encapsulation efficiencies were around 24% [ten Hagen *et al.*, 2002]. Using the reverse phase evaporation method to prepare the liposomes, a much higher encapsulation efficiency of 63 % was achieved [Morishige *et al.*, 1993]. Former studies focused whether the liposomal TNF- α was partly bound non-covalently to the outer membrane of the liposome. The association efficiency of native TNF- α to preformed liposomes was 3.9 % [Utsumi *et al.*, 1991], suggesting that TNF- α also might unspecifically associate with the liposomal membrane. However, this fraction appears tolerable and should not significantly influence the liposomal behavior. Modifications of the cytokine itself, by i.e. increasing its lipophilicity, can also increase the encapsulation efficiency, as shown in a study by Utsumi *et al.* [1991].

The encapsulation efficiency of DMXAA was approximately 18 %, which was lower compared to the encapsulation efficiency of TNF- α , but not unexpected. DMXAA is a small molecule and a weak acid that is ionized at pH 7.4 [Rewcastle *et al.*, 1991; Zhou *et al.*, 2001]. DMXAA has therefore a low tendency to associate with the membrane and subsequently a lower percentage load of DMXAA is expected. Permeability studies in Caco-2 cells showed that DMXAA had a high permeability coefficient and that it was transported by passive diffusion over the cell membrane [Zhou *et al.*, 2005]. This makes DMXAA a difficult drug to encapsulate in liposomes, as it will leak out of the liposomes following its concentration gradient. This explains the low encapsulation efficiency. New DMXAA derivatives are under investigation, where lipophilic groups are added to the molecule [Gobbi *et al.*, 2006]; more lipophilic molecules might display a higher encapsulation efficiency.

3.4.2 Treatment of tumor xenografts with TNF- α and DMXAA loaded VCAM-targeted liposomes

After successfully targeting α -VCAM liposomes to the tumor vasculature, experiments were designed to combine the targeting with the clotting potential of TNF- α or DMXAA. VCAM targeted and non-targeted TNF- α or DMXAA loaded liposomes were injected into mice bearing Colo 677 xenografts.

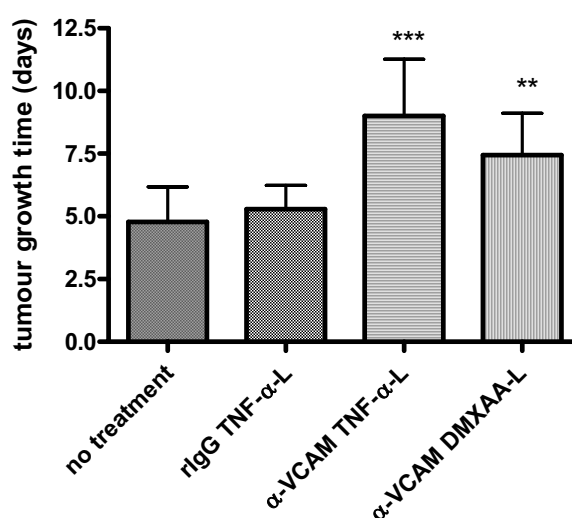


Figure 27. Effect of different treatments with targeted and non-targeted TNF- α and DMXAA encapsulated liposomes on tumor growth of Colo 677 xenografts in mice. 10 animals per group were treated with either rIgG TNF-L (0.5 mg TNF- α / kg), α -VCAM TNF-L (0.5 mg TNF- α / kg) or α -VCAM DMXAA-L (7 mg DMXAA/kg). One group was not treated. One-way analysis of variance resulted in $P < 0.001$ *** $P < 0.001$ not-treated and rIgG TNF- α -L vs. α -VCAM TNF- α -L; ** $P < 0.05$ not treated vs. α -VCAM DMXAA-L and $P < 0.01$ rIgG TNF- α -L and α -VCAM DMXAA-L. Each data point is an average of at least 9 mice; error bars are SD.

The two drugs have previously been shown not to induce complete tumor regression, but a delay in tumor growth or shrinkage of the tumor volume. The delay in tumor growth was selected as the experimental read-out, and the time was recorded which was needed for the tumor to reach 5 times its original size at treatment. As illustrated in Fig. 27 the treatment with α -VCAM TNF- α -CL and α -VCAM DMXAA-CL delayed the tumor growth time compared to that of tumors treated with rIgG-TNF- α -CL and animals that received no treatment. The growth delay was greatest for tumors treated with targeted TNF- α -CL (approximately 4 days longer than control), but the difference between the two targeted treatments was not significant (DMXAA 2.7 days). Subsequently, the growth

time for the non-targeted TNF- α liposomes was only slightly increased compared to the control group, suggesting that targeting the liposomes to tumor vasculature is necessary for TNF- α to have an effect i.e. by inducing a collapse of the tumor vasculature.

This is the first study investigating the anti-tumor effect of targeted TNF- α liposomes on xenograft tumors. Previous studies have used sterically stabilized liposomes loaded with TNF- α in the treatment of solid tumors [van der Veen *et al.*, 1998; Yuyamaa *et al.*, 2000; Kim *et al.*, 2002a; ten Hagen *et al.*, 2002]. The encapsulation of TNF- α in PEGylated liposomes resulted in an increased circulation time of TNF- α and an enhanced TNF- α accumulation in the tumor [van der Veen *et al.*, 1998]. TNF- α loaded liposomes were also shown to reduce tumor growth in rats transplanted with T9 gliosarcoma cells in the time span of 14 days after two treatments [Wakabayashi *et al.*, 1997] and in mice bearing Meth A sarcoma tumors [Yuyamaa *et al.*, 2000]. However others found that treatment with TNF- α loaded PEGylated liposomes had no effect on tumor growth alone, but enhanced the anti-tumor effect of radiation [Kim *et al.*, 2002b] or doxorubicin [ten Hagen *et al.*, 2002] in a synergistic manner. Our results show that one bolus injection of VCAM targeted TNF- α loaded liposomes resulted in a tumor growth delay compared to control tumors and tumors treated with non-targeted TNF- α liposomes. It seems that the localization of the liposome in the tumor is of importance to the anti-tumor effect, thus this could explain why, in some studies, unspecific accumulation of sterically stabilized liposomes had no effect on tumor growth.

After VCAM binding, the TNF- α -CL might either release TNF- α , thereby inducing an endothelial effect via the TNFR60 or be internalized and induce endothelial cell cytotoxicity [Morishige *et al.*, 1993]. In addition to the direct effect on tumor endothelial cells, liposomal TNF- α has been shown to also have an immuno-modulatory effect [Kedar *et al.*, 1997]. Liposomal TNF- α exhibits an altered biodistribution compared free TNF- α and is eliminated through the liposomal elimination pathway, which leads to accumulation in i.e. the spleen and liver. Especially, the accumulation of TNF- α -liposomes in the spleen was found to result in a sustained leukocyte recruitment [Kim *et al.*, 2002b] and activation, which might be an important factor in the additive or synergistic anti-tumor effect of liposomal TNF- α in combination with other cancer therapies [Kim *et al.*, 2002a].

The dose of DMXAA used in this study was considerably lower than the optimal dose (7 mg/kg vs. 25 mg/kg). DMXAA is known to have a narrow therapeutic window

ranging from 15- 25 mg/kg [Siemann *et al.*, 2002]. However, targeting and encapsulation of drugs in liposomes has previously been shown to expand the therapeutic window, which could also be the case here. More studies are needed where higher concentrations of liposomal DMXAA are administered to investigate, whether a dose above 25 mg/kg is tolerated and the therapeutic window expanded.

When comparing these results with the results obtained from the distribution experiments with radiolabeled and DiO-labeled targeted and non-targeted liposomes, the significance of targeting is emphasized. The difference in tumor growth time could not be attributed to the physical properties of the liposomes used in this experiment (Table 6).

	Particle size(nm)	Polydispersity	Drug $\mu\text{g}/\text{ml}$	Coupling $\mu\text{g Ab}/\mu\text{mol PL}$
α -VCAM TNF- α -L	168.5 \pm 9.3	0.302 \pm 0.07	41.01	181
rIgG TNF- α -L	154.3 \pm 3.2	0.350 \pm 0.05	39.35	199
α -VCAM DMXAA-L	161.0 \pm 15.4	0.352 \pm 0.04	504.00	96

Table 6: Characteristics of liposomes used in the treatment experiment. Particle size, amount of drug and the coupling efficiency are described.

The liposome populations used were comparable in size and protein coupling, except for the α -VCAM DMXAA-L which exhibit a lower amount of antibodies coupled to the liposomal surface. The particle size of these liposomes was slightly increased compared to the liposomes used in the targeting study. This could have an effect on the biodistribution of the liposomes but should not interfere with the targeting.

The tumor xenograft model Colo 677 has previously been used to study tumor growth delay in mice treated with truncated TF targeted to VCAM on the tumor endothelium. This showed that the Colo 677 model was suited for long-term treatment experiments. Tumor growth was moderately delayed when mice were treated with the truncated TF conjugate alone, but in combination with multiple doxorubicin treatments tumor growth was inhibited for 14 days [Dienst *et al.*, 2005]. The success of VDAs in

anti-cancer treatment is more pronounced when VDAs are used in combination with conventional anticancer treatments.

3.4.2.1 The side effects of liposomal TNF- α and DMXAA

The use of TNF- α in cancer treatment is often hampered by multiple side effects due to the cytokines systemic effect. The use of liposomal encapsulation has the advantage that it may reduce the systemic effect of the drug by altering their organ distribution [Debs *et al.*, 1990; Kim *et al.*, 2002a; ten Hagen *et al.*, 2002]. The severe side effects seen in mice treated with free TNF- α result in changes in blood pressure, shock-like syndrome and death [ten Hagen *et al.*, 2002]. It was therefore important to examine the toxic effect of TNF- α and DMXAA loaded liposomes. One study showed that the body weight of rats injected with 0.2 mg/kg free TNF- α was reduced > 30% [ten Hagen *et al.*, 2002]. Body weight is a sensitive parameter of systemic TNF- α induced toxicity. The body weight was monitored throughout the whole study and is illustrated in Fig. 28. Body weight loss was not detected for any of the TNF- α treatments, indicating that the mice were not suffering from systemic toxicity.

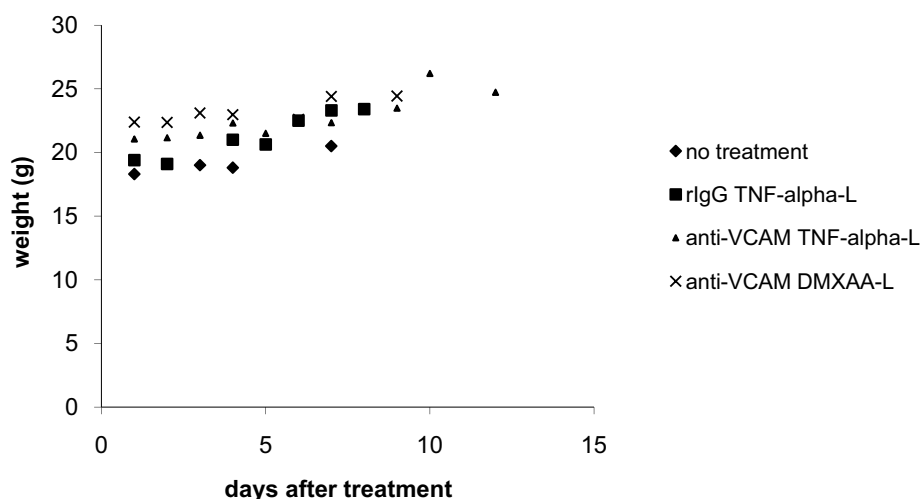


Figure 28. Side effect monitoring by following the body weight of the mice during TNF- α treatment. Each data point is an average of at least 4 animals.

The dose of DMXAA administered in this study was relatively low and therefore no toxicity was expected. Based on the body weight, mice treated with DMXAA liposomes did not develop toxicities.

3.4.2.2 Distribution of TNF- α and TF in the tumors

To understand the mechanism behind the tumor growth delay and to examine the amount of accumulated TNF- α in the tumor after treatment, a TNF- α ELISA was applied. The TNF- α ELISA should also quantify the amount of TNF- α induced by the DMXAA treatment.

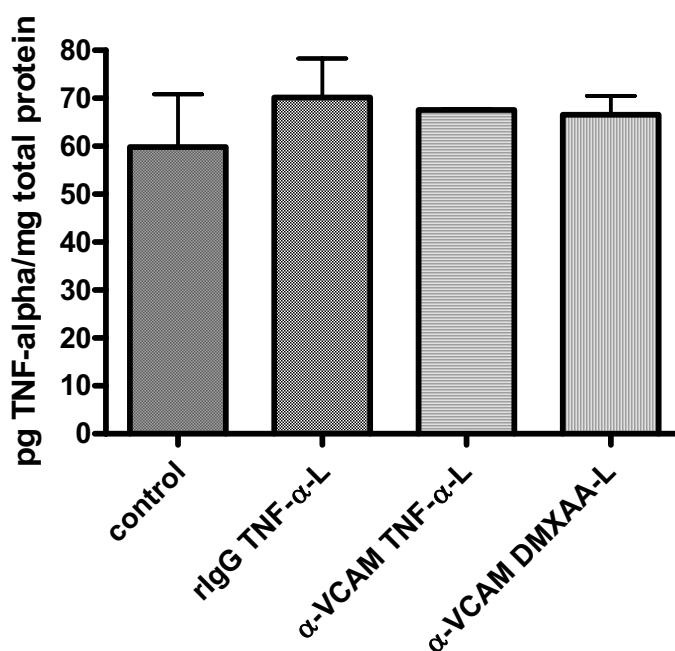


Figure 29. Distribution of murine TNF- α in the tumors using a TNF- α ELISA. The amount of TNF- α in the tumors was determined after the tumor reached the maximal size. Each data point is an average of at least 9 mice; error bars are SD

The amount of TNF- α in tumors from treated-mice, independent of the treatment, was shown to be slightly elevated compared to the control group that received no treatment (Fig. 29). However, the differences were not statistically significant. This was most likely due to the time point of investigation. All animals were sacrificed after their tumors reached a tumor size 5-fold to the treatment size. Therefore, some animals were sacrificed after 4 days, and other after 10 days. Thus, it is difficult to compare the groups. Another study is needed where animals are sacrificed at certain pre-defined time points after injection of TNF- α or DMXAA loaded liposomes. The accumulation of sterically stabilized TNF- α loaded liposomes in tumors was investigated in a time range of four days. The amount of TNF- α in the tumors was higher in animals receiving liposomal TNF- α compared to animals receiving free TNF- α and remained elevated for up to 4 days

[Kim *et al.*, 2002a]. Confirming that experiments carried out within shorter time intervals after treatment are needed.

Administration of DMXAA results in an increase in TNF- α synthesis [Pang *et al.*, 1998; Joseph *et al.*, 1999]. In the time range of 0 - 4 hours, tumor bearing mice treated with DMXAA showed a time-dependent increase in the intratumoral TNF- α activity [Joseph *et al.*, 1999]. Another study found the same increase in TNF- α protein, which peaked after 4 hours, in tumors using a TNF- α ELISA [Seshadri *et al.*, 2007]. Our results showed that there was no difference in the accumulation of TNF- α between the non-treated control and DMXAA treated groups either indicating that the dose was too low to induce a TNF- α response or that a too long time had passed since the synthesis of TNF- α was peaked. The latter explanation is most likely, as a tumor growth delay was observed suggesting that DMXAA had exerted its action the tumor.

Our hypothesis focused on administration of TNF- α or DMXAA to induce blood coagulation via TF at the tumor endothelium. Therefore immunohistochemistry was employed to investigate whether a treatment specific up-regulation of TF on tumor endothelium was found. However, the immunohistochemical detection of the TF expression in the tumor endothelium was not successful. This is due to the fact that the available antibodies were not suited for immunohistochemistry on paraffin embedded and paraformaldehyde fixed tissues. Thus, it was not possible to determine the localization of TF in tumor sections.

A pilot experiment was performed where Colo 677 bearing mice were treated with VCAM-targeted TNF- α -CL and sacrificed after 0, 24 or 72 hours. Thereafter, Western Blot analysis was used to investigate the TF expression in the tumors. As illustrated in Fig. 30, a clear up-regulation of TF protein was seen in tumors after 72 hours (Fig. 30, lane 1 and 2) compared to the control tumors (Fig. 30, lane 4 and 5). After 24 hours (Fig. 30, lane 3) a slight increase in the expression of TF was seen, indicating that treatment with TNF- α loaded liposomes indeed leads to an increased TF expression.

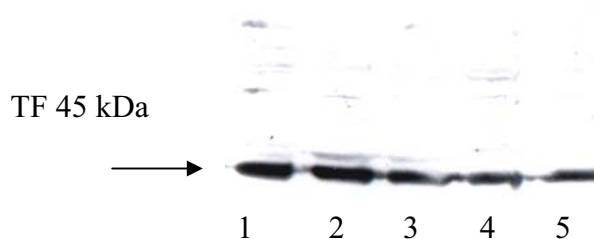


Figure 30. TNF- α induced tissue factor expression in Colo 677 xenograft tumors 0, 24 and 72 hours cells after treatment with α -VCAM TNF- α -L investigated by Western blot A: Immunoblot Colo 677 tumors either after treatment (1-2) for 72 hours, (3) for 24 hours and (4-5) for 0 hours.

This study was only preliminary and the amount of mice used was not sufficient to exclude coincidences. Despite of that, these results indicate that TF was upregulated after TNF- α -CL treatment, although the specific localization of TF could not be determined. TNF- α is known to induce thrombus and fibrin formation in tumor vasculature in mice [Watanabe *et al.*, 1988]. We were not able to show thrombus formation in this study as the end-point of the treatment study was tumor growth delay and the tumors had recovered from the damages induced by the treatment at the time of scarification. However, it was important first to investigate whether the treatments had any effect on tumor growth before looking for a molecular reason. The performed pilot experiment showed that TF was up-regulated in a time-dependent fashion, which correlates well with previous studies. Indirectly, this might indicate that the tumor growth delay could have correlated with an up-regulation of TF and induction of coagulation.

3.4.2.3 Induction of apoptosis in tumors treated with TNF- α or DMXAA-L

The anti-tumor activity of TNF- α and DMXAA is based on the selective destruction of the tumor vasculature leading to a secondary ischemic necrosis of the tumor cells [Baguley and Ching, 2002]. Both TNF- α [Xia *et al.*, 2006] and DMXAA [Ching *et al.*, 2002] have been shown, in previous studies and in this study, to have a direct cytotoxic activity against endothelial cells. TNF- α also induces changes in the vascular permeability, and after DMXAA treatment, an increased tumor vascular permeability was strongly correlated with the induction of TNF- α [Seshadri *et al.*, 2007]. The vascular permeability was associated with changes in cell shape and motility, as well as and the expression of TF and adhesion molecules [Friedl *et al.*, 2002]. All together, these changes result in vascular collapse.

In order to get a further insight into the mechanism behind the tumor growth delay, apoptosis was investigated using a TUNEL assay. As illustrated in Fig. 31 (A-D) all four types of tumors obtained from mice treated with either, nothing, rIgG TNF- α -CL, α -VCAM TNF- α -CL, and α -VCAM DMXAA-CL contained TUNEL positive cells. Control sections that were not treated with the TdT enzyme, were included as negative controls for unspecific peroxidase activity (Fig. 31E), implying that the positive reactions seen in other sections indeed TdT activity specific. The staining pattern showed a hot spot area in the middle of the tumor (Fig 31A-D1; §), corresponding to the necrotic core of the tumor. In the periphery of the tumor occasionally similar hot spots were seen. To investigate whether there was a quantitative difference in the amount of apoptotic cells within the different treatment groups, two different fields were counted from 4 tumors in each group. Both fields were in the periphery, one in a hot spot area (*) and one in a normal area (#). Counting the positive cells in the cores of the tumors was difficult due to the exceeding number of positive cells (Fig. 31A-D 2). As illustrated by the graphs (Fig. 31 F and G), the amount of TUNEL positive cells was elevated in the hot spot area of the tumor periphery in tumors treated with α -VCAM TNF- α -L. In addition, the amount of TUNEL positive cells was increased in all groups except the control group in fields from the periphery without hot spots. These results indicate that treatment with all liposome preparations induced cell death in the tumors. However, the α -VCAM TNF- α -CL induced more hot spots, which could be due to an increased shut down of in the vasculature after this treatment. The results correlate well with the tumor growth delay, where the α -VCAM TNF- α -CL liposomes also induced the greatest response.

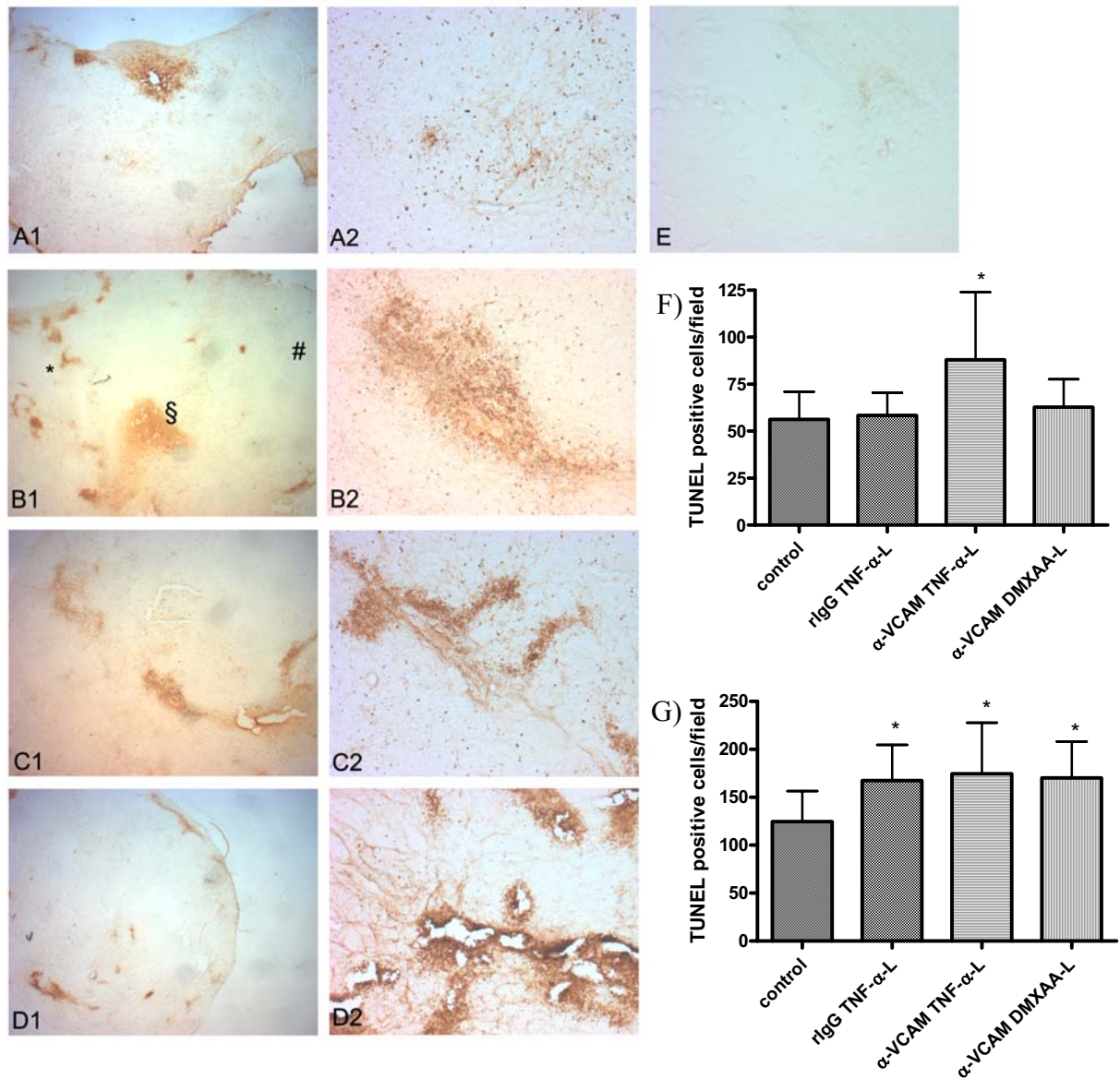


Figure 31: Apoptosis induced in Colo 677 xenografts after treatment with targeted and non-targeted TNF- α or DMXAA loaded liposomes. A) TUNEL stained tumor section from a control mouse 1) at low magnification 2) the core of the tumor at high magnification (§). B) TUNEL stained tumor section from a rIgG TNF- α -L 1) at low magnification 2) the core of the tumor at high magnification. C) TUNEL stained tumor section from α -VCAM TNF- α -L 1) at low magnification 2) the core of the tumor at high magnification. D) TUNEL stained tumor section from α -VCAM DMXAA-L 1) at low magnification 2) the core of the tumor at high magnification. E) Control staining without addition of TdT enzyme. F) Quantification of TUNEL positive cells per field in fields like the one marked by (*) $p < 0.05$ α -VCAM TNF- α -L vs. the rest. G) Quantification of TUNEL positive cells per field in fields like the one marked by (#); $p < 0.05$ control vs. the rest.

The TUNEL assay was employed to investigate the apoptotic state of the endothelial cells and the tumor cell after administration of the different liposome

preparations. It was not possible to determine the origin of apoptotic cells, without double staining against i.e. CD31 or a tumor cell antigen. The TUNEL assay sensitively stains cells with damaged DNA primarily apoptotic cells, however necrotic cells also exhibit DNA fragmentation and the TUNEL assay fails to distinguish between apoptotic and necrotic cells [Gras-Kraupp *et al.*, 1995]. Therefore staining represents both the necrotic and apoptotic cells. As expected, most tumors were shown to have a necrotic area in the middle of the tumor. Stainings in the periphery correlated well with the increased amount of TNF- α found in Fig. 29, indicating that this was not associated with the tumor growth delay. On the other hand, treatment with α -VCAM TNF- α -CL resulted in an elevated number of hotspots in the tumors and an increase in apoptotic cells, which might be treatment specific. However, as previously discussed this experiment was performed too late and the tumors had properly recovered from most of the TNF- α and DMXAA-induced cell damage and death. DMXAA induced apoptosis was determined after 3 hour in Colon 38 tumors, where a 12-fold increase compared to tumors in untreated animals was found [Ching *et al.*, 2002]. Another study directly investigated the effect of DMXAA on the endothelial cells and showed that 4 hours after DMXAA treatment a strong TUNEL reactivity was seen in CD31 positive cells, which was virtually absent after 24 hours [Seshadri *et al.*, 2007].

Summarized, treatment with α -VCAM liposomes loaded with either TNF- α or DMXAA were shown to induce a tumor growth delay after one bolus injection. Thus, the effect of vascular targeting was clearly evident. It was difficult to determine the mechanism for the treatment induced growth delay, as the tumors were excised to late after treatment. However, an increase in total tumor TF in mice treated with TNF- α was shown using Western Blot analysis and the amount of apoptotic/necrotic cells was also increased in this treatment group, indicating that coagulation might be the mechanism behind the tumor growth delay.

4. Conclusions

The tumor vasculature has been recognized as an attractive drug target, and means for efficient delivery of payloads to tumor vascular markers are demanded. First, the development of a drug carrier system that specifically targets tumor endothelium was investigated. We have generated long-circulating ILs targeted to VCAM. The *in vitro* targeting studies provides evidence that α -VCAM-CLs, compared to VCAM-targeted-NLs, specifically bound to activated endothelial cells *in vitro* under static and flow conditions. The non-targeted NgPE-coupled liposomes exhibited some unspecific binding, which could be inhibited by blocking the Fc-receptor. Investigation of the vascular targeting *in vivo* revealed that α -VCAM-CLs, but not controls liposomes, effectively targeted tumor endothelial cells. The localization of VCAM-targeted-CLs in non-target organs was primarily found in phagocytic cells and not co-localized to the vasculature. The RES uptake of the targeted ILs was not significantly higher compared to non-targeted ILs. Thus, PEGylated α -VCAM-CLs are candidate drug carriers for delivery of vascular specific payloads to tumor vasculature.

TNF- α and the TNF- α inducing drug, DMXAA, were chosen as they both are vascular disrupting agents, which act on the tumor endothelial cells instead of the tumor cells themselves. Their anti-tumor action is mediated through occlusion of tumor vessels. It was proposed that TNF- α and DMXAA had a pro-coagulative effect on murine endothelial cells *in vitro*. After 24 hours treatment with both agents, 30 to 50% of the murine endothelial cells were killed providing evidence that both agents exhibit a direct cytotoxic effect on endothelial cells. The hypothesis that TNF- α induced a pro-coagulative state in endothelial cells through the up-regulation of TF was investigated. Stimulation of murine endothelial cells was shown to induce a TNF- α and DMXAA mediated up-regulation of TF expression and activity *in vitro*. TNF- α and DMXAA were therefore accepted as candidate drugs for the VCAM-targeted liposomes.

TNF- α and DMXAA loaded α -VCAM liposomes were formulated and reasonable encapsulation efficiencies of 33% and 18%, respectively, were obtained. Treatment of Colo 677 tumors with VCAM-targeted TNF- α or DMXAA loaded liposomes resulted in a delay in tumor growth time compared to control mice and mice treated with non-targeted

TNF- α loaded liposomes. The mechanism responsible for the tumor growth delay was hypothesized be tumor vessel clotting due to an up-regulation of TF expression and activity. Investigation of the tumor tissues from mice used in the growth delay experiments with respect to the intra-tumor TNF- α levels, tumor cell apoptosis and TF localization could not sufficiently provide insights into the mechanism behind the tumor growth delay. However, clotting induced by up-regulated TF might be assumed. Experiments with a different endpoint would have been necessary. However, a pilot experiment showed that TF protein was upregulated after 24 and 72 hours and together with the *in vitro* data, this indicates that clotting through the up-regulation of TF could have been responsible for the VCAM- targeted TNF- α or DMXAA liposome induced tumor growth delay.

In summary, sterically stabilized VCAM targeted liposomes loaded with either TNF- α or DMXAA specifically target the tumor vasculature and induce a tumor growth delay in mice bearing human xenografts, which might be due to an up-regulation of TF expression and activity. Therefore, the vascular targeting of liposomal drugs aiming at interfering with the tumor vascular function appears as very attractive therapeutic approach in the anticancer research and will be continued in further studies.

5. References

Adams, G.P., Schier, R., McCall, A.M., Simmons, H.H., Horak, E.M., Alpaugh, R.K., Marks, J.D., Weiner, L.M. High Affinity Restricts the Localization and Tumor Penetration of Single-Chain Fv Antibody Molecules, *Cancer Res* 61 (2001) 4750-4755

Aggerwal, B.B. Signalling pathways of the TNF superfamily: A double-edged sword, *Nature Rev* 3 (2003) 745-756

Aichele, P., Zinke, J., Grode, L., Schwendener, R.A., Kaufmann, S.H.E., Seiler, P. Macrophages of the splenic marginal zone are essential for trapping of blood-borne particulate antigen but dispensable for induction of specific T cell responses, *J Immunol* 171 (2003) 1148-1155

Amarzguioui, M., Peng, Q., Wiiger, M.T., Vasovic, V., Babaie, E., Holen, T., Nesland, J.M., Prydzl, H. *Ex vivo* and *in vivo* delivery of anti-tissue factor short interfering RNA inhibits mouse pulmonary metastasis of B1 6 melanoma cells, *Clin Cancer Res* 12 (2006) 4055-4061

Ames, B., Dubin, D. The role of polyamines in the neutralization of bacteriophage deoxyribonucleic acid, *J Biol Chem* 235 (1960) 769-775

Angelini, D.J., Hyun, S-W., Grigoryev, D.N., Garg, P., Gong, P., Singh, I.S., Passaniti, A., Hasday, J.D., Goldblum, S.E. TNF α increases tyrosine phosphorylation of vascular endothelial-cadherin and opens the paracellular pathway through fyn activation in human lung endothelia, *Am J Physiol Lung Cell Mol Physiol* 291 (2006) L1232-1245

Antohe, F., Heltianu, C., Simionescu, M. Albumin-binding proteins of endothelial cells: immunocytochemical detection of the 18 kDA peptide, *Eur J Cell Biol* 56 (1991) 34-42.

Allen, T.M., Chonn, A., Large unilamellar liposomes with low uptake into the reticulendothelial system, *FEBS Letters* 223 (1987) 42-46

Allen, T., Brandeis, E., Hansen, C., Kao, G., Zalipsky, S. A new strategy for attachment of antibodies to sterically stabilized liposomes resulting in efficient targeting to cancer cells, *BBA* 1237 (1995) 99-108

Aragnol, D., Leserman, L.D. Immune clearance of liposomes inhibited by an anti-Fc receptor antibody in vivo, *PNAS* 83 (1986) 2699-2703

Arap, W., Pasqualini, R., Ruoslahti, E. Cancer treatment by targeted drug delivery to tumor vasculature in a mouse model, *Science* 279 (1998) 377-380

Arora, N., Masood, R., Zheng, T., Cai, J., Smith, D.L., Gill, P.S. Vascular endothelial growth factor chimeric toxin is highly active against endothelial cells, *Cancer Res* 59 (1999) 183-188

Arunachalam, B., Talwar, G.P., Raghupathy, R. A simplified cellular ELISA (CELIS) for detection of antibodies reacting with cell-surface antigens, *J Immunol Methods* 135 (1990) 181-189

Bach, R., Rifkin, D.B. Expression of tissue factor procoagulant activity: Regulation by cytosolic calcium, *PNAS* 87 (1990) 6995-6999

Baguley, B.C., Zhuang, L., Kestell, P. Increased plasma serotonin following treatment with flavone-8-acetic acid, 5,6-dimethylxanthenone-4-acetic acid, vinblastine, and colchicine: relation to vascular effects, *Oncol Res* 9 (1997) 55-60

Baguley, B.C., Ching, L.M. DMXAA: an antivascular agent with multiple host responses, *Int J Radiat Oncol Biol Phys* 54 (2002)1503-1511

Bazan-Peregrino, M., Seymour, L.W., Harris, A.L. Gene therapy targeting to tumor endothelium, *Cancer Gene Therapy* 14 (2007) 117-127

Bellnier, D.A., Gollnick, S.O., Camacho, S.H., Greco, W.R., Cheney, R.T. Treatment with the tumor necrosis factor- α inducing drug 5,6dimethylxanthenone-4-acetic acid

enhances the antitumor activity of the photodynamic therapy of RIF-1 mouse tumors, *Cancer Res* 63 (2003) 7584-7590

Belting, M., Dorrel, M.I., Sandgren, S., Aguilar, E., Ahamed, J., Dorfleutner, A., Carmeliet, P., Mueller, B.M., Friedlander, M., Ruf, W. Regulation of angiogenesis by tissue factor cytoplasmic domain signaling, *Nature Med* 10 (2004) 502-509

Bemelmans, M.H., van Tits, L.J., Buurman, W.A. Tumor necrosis factor: function, release and clearance, *Crit Rev Immunol* 16(1996) 1-11

Bendas, G., Krause, A., Schmidt, R., Vogel, J., Rothe, U. Selectins as new targeted for immunoliposome-mediated drug delivery a potential way of anti-inflammatory therapy, *Pharmaceutica Acta Helvetiae* 73 (1998) 19-26

Bendas, G., Krause, A., Bakowsky, U., Vogel, J., Rothe, U. Targetability of novel immunoliposomes prepared by a new antibody conjugation technique, *Int J Pharm* 181 (1999) 79-93

Bendas, G., Rothe, U., Scherphof, G.L., Kamps, J.A.A.M. The influence of repeated injections on pharmacokinetics and biodistribution of different types of sterically stabilized immunoliposomes, *BBA* 1609 (2003) 63-70

Benzinger, P., Martiny-Baron, G., Reusch, P., Siemeister, G., Kley, J.T., Marme, D., Unger, C., Massing, U. Targeting of endothelial KDR receptors with 3G2 immunoliposomes in vitro, *BBA* 1466 (2000) 71-78

Bevilacqua, M.P., Pober, J.S., Majeau, G.R., Fiers, W., Cotran, R.S., Gimbrone, M.A. Jr. Recombinant tumor necrosis factor induces procoagulant activity in cultured human vascular endothelium: Characterization and comparison with the actions of interleukin 1, *PNAS* 83 (1986) 4533-4537

- Bhattacharjee, G., Ahamed, J., Pedersen, B., El-Sheikh, A., Mackman, N., Ruf, W., Liu, C., Edgington, T.S. Regulation of tissue factor-mediated initiation of the coagulation cascade by cell surface Grp78, *Arterioscler Thromb Vasc Biol* 25 (2005) 1737-1743
- Bloemen, P.G.M., Henricks, P.A.J., van Bloois, L., van den Tweel, M.C., Bloem, A.C., Nijkamp, F.P., Crommelin, D.J.A., Storm, G. Adhesion molecules: a new target for immunoliposome-mediated drug delivery, *FEBS Letters* 357 (1995) 140-144
- Blume, G., Cevc, G., Crommelin, M.D.J.A., Bakker-Woudenberg, ImA.J.M., Kluft, C., Storm, G. Specific targeting with poly(ethylene glycol)-modified liposomes: coupling of homing devices to the ends of the polymeric chains combines effective target binding with long circulation times, *BBA* 1149 (1993) 180-184
- Boehm, T., Folkman, J., Browder, T., O'Reilly, M.S. Antiangiogenic therapy of experimental cancer does not induce acquired drug resistance, *Nature* 390 (1997) 404-407
- Bogdanov, V.Y., Kirk, R.I., Miller, C., Hathcock, J.J., Vele, S., Gazdoui, M., Nemerson, Y., Taubman, M.B. Identification and characterization of murine alternatively spliced tissue factor, *J Thromb Haemost* 4 (2006) 158-167
- Bombeli, T., Karsan, A., Tait, J.F., Harlan, J.M. Apoptotic vascular endothelial cells become procoagulant, *Blood* 89 (1997) 2429-2442
- Boucher, Y., Baxter, L.T, Jain, R.K. Interstitial pressure gradients in tissue-isolated and subcutaneous tumors: Implications for therapy, *Cancer Res* 50 (1990) 4478-4484
- Brandwijk, R.J.M.G.E., Mulder, W.J.M., Nicolay, K., Mayo, K.H., Thijssen, V.L.J.L., Griffioen, A.W. Anginex-conjugated liposomes for targeting for targeting of angiogenic endothelial cells, *Bioconjugate Chem* 18 (2007) 785-790
- Braun, S., Hepp, F., Kentenich, C.R.M, Janni, W., Pantel, K., Riethmüller, G., Willgeroth, F., Sommer, H.L. Monoclonal antibody therapy with edrecolomab in breast

cancer patients: monitoring of elimination of disseminated cytokeratin positive tumor cells in bone marrow, *Clin Cancer Res* 5 (1999) 3999–4004

Brem, S., Brem, H., Folkman, J., Finkelstein, D., Patz, A. Prolonged tumor dormancy by prevention of neovascularization in the vitreous, *Cancer Res* 36 (1976) 2807-2812

Bromberg, M.E., Konigsberg, W.H., Madison, J.F., Pawashe, A., Garen, A. Tissue factor promotes melanoma metastasis by a pathway independent of blood coagulation, *PNAS* 92 (1995) 8205-9

Browder, T., Butterfield, C.E., Kräling, B.M., Shi, B., Marshall, B., O'Reilly, M.S., Folkman, J. Antiangiogenic scheduling of chemotherapy improves efficacy against experimental drug-resistant cancer, *Cancer Res* 60 (2000) 1878-1886

Brown, M., Wittwer, C. Flow cytometry: principles and clinical applications in hematology, *Clin Chem* 46 (2000) 1221–1229

Burrows, F.J., Watanabe, Y., Thorpe, P.E. A murine model for antibody-directed targeting of vascular endothelial cells in solid tumors, *Cancer Res* 52 (1992) 5954-5962

Burrows, F.J., Thorpe, P.E. Vascular targeting -a new approach to the therapy of solid tumors, *Pharmacol Ther* 64 (1994) 155-174

Cairns, R., Papandreou, I., Denko, N., Overcoming physiologic barriers to cancer treatment by molecularly targeting the tumor microenvironment, *Mol Cancer Res* 4 (2006) 61-70

Camby, I., Le Mercier, M., Lefranc, F., Kiss, R. Galectin-1: a small protein with major functions, *Glycobiology* 16 (2006) 137R-157R

Carmeliet, P., Moons, L., Dewerchin, M., Mackman, N., Luther, T., Breier, G., Ploplis, V., Muller, M., Nagy, A., Plow, E., Gerdard, R., Edgington, T., Risau, W., Collen, D. Insights in vessel development and vascular disorders using targeted inactivation and

transfer of vascular endothelial growth factor, the tissue factor receptor , and the plasminogen system, *Ann NY Acad Sci* 8 (1997) 191-206

Carmeliet, P., Mechanisms of angiogenesis and arteriogenesis, *Nature Med* 6 (2000) 389-395

Carnemolla, B., Borsi, L., Balza, E., Castellani, P., Maezza, R., Berndt, A., Ferrini, S., Kosmehl, H., Neri, D., Zardi, L. Enhancement of the antitumor properties of interleukin-2 by its targeted delivery to the tumor blood vessel extracellular matrix, *Blood* 99 (2002) 1659-1665

Carroll, N.M., Elaraj, D.M., Puhlmann, M., Weinreich, D.M., Turner, E.M., Xu, H., Alexander, H.R.Jr. Alterations in tumor necrosis factor-induced endothelial cell procoagulant activity by hyperthermia, *Int J Cancer* 111 (2004) 457-462

Carson, S.D., Ross, S.E., Bach, R., Guha, A. An inhibitory monoclonal antibody against human tissue factor, *Blood* 70 (1987) 490-493

Carswell, E.A., Old, L.J., Kassel, R.L., Green, S., Fiore, N., Williamson, B. An endotoxin-induced serum factor that causes necrosis of tumors, *PNAS* 72 (1975) 3666-3670

Charpin, C., Garcia, S., Andrac, L., Horschowski, N., Choux, R., Lavaut, M-N. VCAM (IGSF) adhesion molecule expression in breast carcinomas detected by automated and quantitative immunocytochemical assays, *Hum Pathol* 29 (1998) 869-903

Charrois, G.J.R., Allen, T.M., Multiple injections of pegylated liposomal doxorubicin: pharmacokinetics and therapeutic activity, *J Pharmacol Exp Ther* 306 (2003) 1058-1067

Carroll, N.M., Elaraj, D.M., Puhlmann, M., Weinreich, D.M., Turner, E.M., Xu, H., Alexander, H.R. Jr. Alterations in tumor necrosis factor-induced endothelial cell procoagulant activity by hyperthermia, *Int J Cancer* 111 (2004) 457-462

Ching, L-M., Zwain, S., Baguley, B.C. Relationship between tumour endothelial cell apoptosis and tumour blood flow shutdown following treatment with the antivascular agent DMXAA in mice, *British J Cancer* 90 (2004) 906-910

Chiu, G.N.C., Bally, M.B. Mayer, L.D. Targeting of antibody conjugated, phosphatidylserine-containing liposomes to vascular cell adhesion molecule 1 for controlled thrombogenesis, *BBA* 1613 (2003) 115-121

Christiansen, J., Rajasekaran, A.K. Biological impediments to monoclonal antibody-based cancer immunotherapy, *Mol Cancer Ther* 3 (2004) 1493-1501

Chung, F., Liu, J., Ching, L-M., Baguley, B.C. Consequences of increased vascular permeability induced by treatment of mice with 5.6-dimethylxanthenone-4-acetic acid (DMXAA) and thalidomide, *Cancer Chemother Pharmacol* 61 (2007) 497-502

Clauss, M., Grell, M., Fangmann, C., Fiers, W., Scheurich, P., Risau, W. Synergistic induction of endothelial tissue factor by tumor necrosis factor and vascular endothelial growth factor: functional analysis of the tumor necrosis factor receptors, *FEBS Letters* 390 (1996) 334-338

Cobleigh, M.A., Vogel, C.L., Tripathy, D. Multinational study of the efficacy and safety of humanized anti-HER2 monoclonal antibody in women who have HER-2 overexpressing metastatic breast cancer that has progressed after chemotherapy for metastatic disease, *J Clin Oncol* 17 (1999) 2639-2648

Constantinides P., Yiv, S.I. Particle size determination of phase-inverted water-in-oil microemulsions under different dilution and storage conditions, *Int J Pharmaceut* 115 (1995) 225-234

Contorino, J., Hair, G., Kreutzer, D.L., Ricklers, F. *In situ* detection of tissue factor in vascular endothelial cells: Correlation with the malignant phenotype of human breast disease, *Nature Med* 2 (1996) 209-215

Conway, E.M., Bach, R., Rosenberg, R.D., Konigsberg, W.H. Tumor necrosis factor expression of tissue factor mRNA in endothelial cells, *Thrombosis Res* 53 (1989) 231-241

Corti, A., Ponzoni, Tumor vascular targeting with tumor necrosis factor α and chemotherapeutic drugs, *Vascular targeting and chemotherapy, Ann NY Acad Sci* 1028 (2004) 104-112

Dams, E., Laverman, P., Oyen, W., Storm, G., Scherphof, G., van Der Meer, J., Corstens, F., Boerman, O. Accelerated blood clearance and altered biodistribution of repeated injections of sterically stabilized liposomes, *J Pharmacol Exp Ther* 292 (2000) 1071-1079

Darzynkiewics, Z., Juan, G., Li, X., Gorczyca, W., Murakami, T., Tranganos, F. Cytometry in cell necrobiology: Analysis of apoptosis and accidental cell death (necrosis), *Cytometry* 27 (1997) 1-20

Dasgupta, D., Charraborty, P., Basu, M.K. ligation of Fc receptor of macrophages stimulates protein kinase C and anti-leishmanial activity, *Mol Cell Biochem* 209 (2000) 1-8

Davie, E.W., Fujikawa, K., Kisiel, W. The coagulation cascade: Initiation, maintenance, and regulation, *Biochemistry* 30 (1991) 10363-10370

Debs, R.J., Fuchs, H.J., Philip, R., Brunette, E.N., Düzgünes, N., Shellito, J.E., Liggitt, D., Patton, J.R. Immunomodulatory and toxic effects of free and liposome-encapsulated tumor necrosis factor α in rats, *Cancer Res* 50 (1990) 375-380

Dedrick, R.L., Bodary, S., Garovoy, M.R. Adhesion molecules as therapeutic targets for autoimmune diseases and transplant rejection, *Exp Opin Biol Ther* 3 (2003) 85-95

Denekamp, J. Vascular attack as a therapeutic strategy for cancer, *Cancer and Meta Rev* 9 (1990) 267-282

Denekamp, J. The tumor microcirculation as a target in cancer therapy: a clearer perspective, *Euro J Clin Invest* 29 (1999) 733-736

Deng, Y., Ren, X., Yang, L., Lin, Y., Wu, X. A JNK-dependent pathway is required for TNF- α -induced apoptosis, *Cell* 115 (2003) 61-70

Deshpande, S.S., Angkeow, P., Huang, J., Ozaki, M., Irani, K. Rac 1 inhibits TNF- α -induced endothelial cell apoptosis: dual regulation by reactive oxygen species, *FASEB J* 14 (2000) 1705-1714

Devin, A., Cook, A., Lin, Y., Rodriguez, Y., Kelliher, M. Liu, Z. The distinct roles of TRAF2 and RIP in IKK activation by TNF-R1: TRAF2 recruits IKK to TNF-R1 while RIP mediates IKK activation, *Immunity* 12 (2000) 419-429

Dewhirst, M.W., Kimura, H., Rehmus, S.W., Braun, R.D., Papahadjopoulos, D., Hong, K., Secomb, T.W. Microvascular studies on the origins of perfusion-limited hypoxia, *British J Cancer Suppl* 27 (1996) S247-251

Dienst, A., Grunow, A., Unruh, M. Rabausch, B., Nor, J.E., Fries, J.W., Gottstein, C. Specific occlusion of murine and human tumor vasculature by VCAM-1-targeted recombinant fusion proteins, *J Natl Cancer Inst* 97 (2005) 733-747

Dittmer, J.C., Lester, R.C. A simple, specific spray for the detection of phospholipids on thin-layer chromatograms, *J Lipid Res* 5 (1964) 126-127

Dunn, M. J. Protein determination of total protein concentration. Harris, E. L. V., Angal, S., [Eds], *Protein Purification Methods* (1992) Oxford: IRL Press

Dvorak H.F., Dvorak A.M., Manseau, E., Wiberg, L., Churchill, W. J. Fibrin gel investment associated with line 1 and line 10 solid tumor growth, angiogenesis, and fibroplasia in guinea pigs. Role of cellular immunity, myofibroblasts, microvascular damage, and infarction in line 1 tumor regression, *Natl Cancer Inst* 62 (1979) 1459-1472

Emanuel, N., Kedar, E., Bolotin, E., Smorodinsky, N., Barenholz, Y. Targeted delivery of doxorubicin via sterically stabilized immunoliposomes: pharmacokinetics and biodistribution in tumor-bearing mice, *Pharm Res* 13 (1996) 861-868

Everts, M., Koning, G.A., Kok, R.J., Asgeirsdottir, S.A., Vestweber, D., Meijer, D.K., Storm, G., Molema, G., In vitro cellular handling and in vivo targeting of E-selectin-directed immunoconjugates and immunoliposomes used for drug delivery to inflamed endothelium, *Pharm Res* 20 (2003) 64-72

Fleck, R.A., Rao, L.V.M., Rapaport, S.I., Varki N. Localization of human tissue factor antigen by immunostaining with monospecific, polyclonal anti-human tissue factor antibody, *Thromb Res* 57 (1990) 765-781

Florey, O., Haskard, D.O. Analysis of flow-based adhesion in vitro, *Methods Mol Med* 135 (2007) 323-331

Folkman, J. How is blood vessel growth regulated in normal and neoplastic tissue? - G.H.A. Clowes memorial award lecture, *Cancer Res* 46 (1986) 467-473

Friedl, J., Puhlman, M., Bartlett, D.L., Libutti, S.K., Turner, E.N, Gnant, M.F.X., Alexander, H.R. Induction of permeability across endothelial cell monolayers by tumor necrosis factor(TNF) occurs via a tissue factor-dependent mechanism: relationship between the procoagulant and permeability effects of TNF, *Blood* 100 (2002) 1334-1339

Fries, J., Williams, A., Atkins, R., Newman, W., Lipscomb, M., Collins, T. Expression of VCAM-1 and E-selectin in an in vivo model of endothelial activation, *Am J Pathol* 143 (1993) 725-737

Gabizon, A., Papahadjopoulos, D. Liposome formulations with prolonged circulation time in blood and enhanced uptake by tumors, *PNAS* 85 (1988) 6949-6953

Gabizon, A., Papahadjopoulos, D. The role of surface charge and hydrophilic groups on liposome clearance in vivo, *BBA* 1103 (1992) 94-100

Gabra, H. Phase II study of DMXAA combined with carboplatin and paclitaxel in recurrent ovarian cancer, *J Clin Oncol* 24 (2006) 5032

Gaffar, S.A., Li, Z., Epstein, A.L. A live cell enzyme-linked immunosorbent assay for detecting human hepatoma membrane antigens, *Hybridoma* 8 (1989) 331-336

Garmy-Susini, B., Jin, H., Zhu, Y., Sung, R.-J., Hwang, R., Varner, J., Integrin $\alpha 4\beta 1$ -VCAM-1-mediated adhesion between endothelial and mural cells is required for blood vessel maturation, *J Clin Invest* 115 (2005) 1542-1551

Gobbi, S., Belluti, F., Bisi, A., Piazzzi, L., Rampa, A., Zampiron, A., Barbera, M., Caputo A., Carrarab, M. New derivatives of xanthenone-4-acetic acid: Synthesis, pharmacological profile and effect on TNF- α and NO production by human immune cells, *Bioorganic Med Chem* 14 (2006) 4101–4109

Gosk, S., Gottstein, C., Bendas, G. Targeting of immunoliposomes to endothelial cells expressing VCAM: a future strategy in cancer therapy, *Int J Clin Pharmacol Ther* 43 (2005) 581-582

Gras-Kraupp, B., Ruttkay-Nedicky, B., Koudeka, H. In situ detection of fragmented DNA (TUNEL assay) fails to discriminate among apoptosis, necrosis and autolytic cell death, a cautionary note, *Hepatology* 21 (1995) 4465-4468

Gregory, S.A., Morrissey, J.H., Edgington, T.S. Regulation of tissue factor gene expression in the monocyte procoagulant response to endotoxin, *Mol Cell Biol* 9 (1989) 2752-2755

Grunhagen D.J, de Wilt J.H, Graveland W.J, Verhoef C, van Geel A.N, Eggermont A.M. Outcome and prognostic factor analysis of 217 consecutive isolated limb perfusions with tumor necrosis factor-alpha and melphalan for limb-threatening soft tissue sarcoma. *Cancer* 106 (2006) 1776-84

Guccione, S., Li, K.C., Bednarski, M.D. Molecular imaging and therapy directed at the neovasculature in pathologies. How imaging can be incorporated into vascular-targeted delivery systems to generate active therapeutic agents, *IEEE Eng Med Biol Mag* 23 (2004) 50-56

Halin, C., Rondini, S., Nilsson, F., Berndt, A., Kosmehl, B.H., Zardi, L., Neri, D. Enhancement of the antitumor activity of interleukin-12 by targeted delivery to neovasculature, *Nature Biotechnol* 20 (2002) 264-269

Hamilton, R.G. Human IgG subclass measurements in the clinical laboratory, *Clin Chem* 33 (1987) 1707-1725

Hanahan, D., Bergers, G., Bergsland, E. Less is more, regularly: metronomic dosing of cytotoxic drugs can target tumor angiogenesis in mice, *J Clin Invest* 105 (2000) 1045-1047

Hansen, C., Kao, G.Y., Moase, E.H., Zalipsky, S., Allen, T.M., Attachment of antibodies to sterically stabilized liposomes: evaluation, comparison and optimization of coupling procedures, *BBA* 1239 (1995) 133-144.

Hansen C.B., Pyke, C., Petersen, L.C., Rao, L.V. Tissue factor-mediated endocytosis, recycling, and degradation of factor VIIa by clatrin-independent mechanism not requiring the cytoplasmic domain of tissue factor, *Blood* 97 (2001) 1712-1720

Harding, J.A., Engbers, C.M., Newman, M.S., Goldstein, N.I., Zalipsky, S. Immunogenicity and pharmacokinetic attributes of poly(ethylene glycol)-grafted immunoliposomes, *BBA* 1327 (1997) 181-192

Hayes, A.J., Neuhaus, S.J., Clark, M.A., Thomas, J.M. Isolated limb perfusion with melphalan and tumor necrosis factor α for advanced melanoma and soft-tissue sarcoma, *Annals Surgical Oncol* 14 (2006) 230-238

Hayon, T., Dvilansky, A., Shpilberg, O., Nathan, I. Appraisal of the MTT-based assay as a useful tool for predicting drug chemosensitivity in leukemia, *Leuk Lymphoma* 44 (2003) 1957-62

- Henriksson, C.E., Klingenberg, O., Øvstebø, R., Westvik, Å-B., Kierulf, P. Discrepancy between tissue factor activity and tissue factor expression in endotoxin-induced monocytes is associated with apoptosis and necrosis, *Thromb Haemost* 94 (2005) 1236-1244
- Hinnen, P., Eskens, F.A.L.M. Vascular disrupting agents in clinical development, *British J Cancer* 96 (2007) 1159-1165
- Hjortoe, G.M., Petersen, L.C., Albrektsen, T., Sorensen, B.B., Norby, P.L., Mandal, S.K., Pendurthi, U.R., Rao, L.V.M. Tissue factor-factor VIIa-specific up-regulation of IL-8 expression in MDA-MB-231 cells is mediated by PAR-2 and results in increased cell migration, *Blood* 103 (2004) 3029-3037
- Hoffman, R.M. Unbalanced transmethylation and perturbation of the differentiated state leading to cancer, *BioEssays* 12 (1990) 163-166
- Hölig, .P, Bach, M., Völkel, T., Nahde, T., Hoffmann, S., Müller, R., Kontermann, R.E. Novel RGD lipopeptides for the targeting of liposomes to integrin-expressing endothelial and melanoma cells, *Protein Eng Des Sel* 17(2004) 433-441
- Hood, J.D., Bednarski, M., Frausto, R., Guccione, S., Reisfeld, R.A., Xiang, R., Cheresch, D.A. Tumor regression by targeted gene delivery to the neovasculature, *Science* 296 (2002) 2404-2407
- Horsman, M.R., Siemann, D.W. Pathophysiological effects of vascular-targeting agents and the implication of combination with conventional therapies, *Cancer Res* 66 (2006) 11520-11539
- Hoving, S., Seynhaeve, A.L.B., van Tiel, S.T., Eggermont, A.M.M., ten Hagen, T.L.M Addition of low-dose tumor necrosis factor- α to systemic treatment with STEALTH liposomal doxorubicin (DOXIL) improved anti-tumor activity⁶ in osteosarcoma-bearing rats, *Anti-Cancer Drugs* 16 (2005) 667-674

Huang, S.K., Lee, K.D., Hong, K., Friend, D.S., Papahadjopoulos, D. Microscopic Localization of Sterically Stabilized Liposomes in Colon Carcinoma-bearing Mice, *Cancer Res* 52 (1992) 5135-5143

Huang, X., Molema, G., King, S., Watkins, L., Edgington, T.S., Thorpe, P.E. Tumor infarction in mice by antibody-directed targeting of tissue factor to tumor vasculature, *Science* 275 (1997) 547-550

Hurwitz, H., Fehrenbacher, L., Novotny, W., Cartwright, T., Hainsworth, J., Heim, W., Berlin, J., Baron, A., Griffing, S., Holmgren, E., Ferrara, N., Fyfe, G., Rogers, B., Ross, R., Kabbinavar, F. Bevacizumab plus irinotecan, fluorouracil, and leucovorin for metastatic colorectal cancer, *N Engl J Med* 350 (2004) 2335-2342

Ishada, T., Harashima, H., Kiwada, H. Liposome clearance, *Biosci Reports* 22 (2002) 197-224

Jain, R.K., Transport of molecules on the tumor interstitium: A review, *Cancer Res* 47 (1987) 3039-3051

Jain, R., Baxter, L. Mechanisms of heterogeneous distribution of monoclonal antibodies and other macromolecules in tumors: Significance of elevated interstitial pressure, *Cancer Res* 48 (1988) 7022-7032

Jain, R.K. Normalization of tumor vasculature: an emerging concept in antiangiogenic therapy, *Science* 307 (2005) 58-62

Jamerson, M.B., Thompson, P.I., Baguley, B.C., Evans, B.D., Harvey, V.J., Porter, D.J., McCrystal, M.R., Small, M., Bellenger, K., Gumbrell, L., Halbert, G.L., Kestell, P. Clinical aspects of a phase I trial of 5,6dimethylxanthenone-4-acetic acid (DMXAA), a novel antivasculature agent, *British J Cancer* 88 (2003) 1844-1850

Jimenez, J.J., Jy, W., Mauro, L.M., Soderland, C., Horstman, L.L., Ahn, Y.S. Endothelial cells release phenotypically and quantitatively distinct microparticles in activation and apoptosis, *Thromb Res* 109 (2003) 175-180

Jin, H., Su, J., Garmy-Susini, B., Kleeman, J., Varner, J. Integrin $\alpha_4\beta_1$ Promotes monocyte trafficking and angiogenesis in tumors, *Cancer Res* 66 (2006) 2146-2152

Joseph, W.R., Cao, Z., Mountjoy, K.G., Marshall, E.S., Baguley, B.C., Ching, L-M. Stimulation of tumors to synthesize tumor necrosis factor- α *in situ* using 5,6dimethylxanthenone-4-acetic acid: a novel approach to cancer therapy, *Cancer Res* 59 (1999) 633-638

Juweid, M., Neumann, R., Paik, C., Perez-Bacete, M.J., Sato, J., van Osdol, W., Weinstein, J.N. (1992) micropharmacology of monoclonal antibodies in solid tumours: direct experimental evidence for binding site barriers, *Cancer Res* 52, 5144-5153

Kaufmann, B.A., Sanders, J.M., Davis, C., Xie, A., Aldred, P., Sarembock, I.J., Lindner, J.R. Molecular imaging of inflammation in atherosclerosis with targeted ultrasound detection of vascular cell adhesion molecule-1, *Circulation* 116 (2007) 276-284

Kedar, E., Palgi, O., Golod, G., Babi, I., Barenholz, Y. Delivery of cytokines by liposomes. III. Liposome-encapsulated GM-CSF and TNF- α show improved pharmacokinetics and biological activity and reduced toxicity in mice, *J Immunother* 20 (1997) 180-193

Kelly, K.A., Allport, J.R., Tsourkas, A., Shinde-Patil, V.R., Josephson, L., Weissleder, R. Detection of vascular adhesion molecule-1 expression using a novel multimodal nanoparticle, *Circ Res* 96 (2005) 327-336

Kennel, S.J., Falcioni, R., Wesley J.V.V. Microdistribution of specific rat monoclonal antibodies to mouse tissues and human tumor xenografts, *Cancer Res* 51 (1991) 1529-1536

Kerr, D.J., Kaye, S.B. Flavone acetic acid -preclinical and clinical activity, *Eur J Cancer Clin Oncol* 5 (1989) 1271-1272

Kerble, R.S. Inhibition of tumor angiogenesis as a strategy to circumvent acquired resistance to anti-cancer therapeutic agents, *BioEssays* 13 (1991) 31-36

Kerble, R., Folkman, J., Clinical translation of angiogenesis inhibitors, *Nature Rev* 2 (2002) 727-739

Kessner, S., Krause, A., Rothe, U., Bendas, G. Investigation of the cellular uptake of E-Selectin-targeted immunoliposomes by activated human endothelial cells, *BBA* 1514 (2001) 177-190

Kim, I., Oh, J-L, Ryu, T.S., So, J-N., Sessa, W.C., Walsh, K., Koh, G.Y. Angiopoetin-1 negatively regulates expression and activity of tissue factor in endothelial cells, *FASEB J* (2001) 126-128

Kim, D.W., Andres, M.L., Kajioka, E.H., Dutta-Roy, R., Miller, G.M., Seynhaeve, A.L., ten Hagen, T.L.M., Gridley, D.S. Modulation of innate immunological factors by STEALTH® liposome-encapsulated tumor necrosis factor- α in a colon tumor xenograft model, *Anticancer Res* 22 (2002a) 777-788

Kim, D.W., Andres, M.L., Miller, G.M., Cao, J.D., Green, L.M., Seynhaeve, A.L., ten Hagen, T.L., Gridley, D.S. Immunohistological analysis of immune cell infiltration of a human colon tumor after treatment with stealth liposome-encapsulated tumor necrosis-alpha and radiation, *Int J Oncol* 21 (2002b) 973-979

Kirpotin, D.B., Drummond, D.C., Shao, Y., Shalaby, M.R., Hong, K., Nielsen, U.B., Marks, J.D., Benz, C.C., Park, J.W. Antibody targeting of long-circulating lipidic nanoparticles does not increase tumor localization but does increase internalization in animal models, *Cancer Res* 66 (2006) 6732-6740

Klemke, M., Weschenfelder, T., Konstandin, M.H., Samstag, Y. High affinity interaction of integrin $\alpha_4\beta_1$ (VLA-4) and vascular cell adhesion molecule 1 (VCAM-1) enhances migration of human melanoma cells across activated endothelial cell layers, *J Cell Physiol* 212 (2007) 368-374

Klibanov, A.L., Maruyama, K., Beckerleg, A.M., Torchilin, V.P., Huang, L. Activity of amphipathic poly(ethylene glycol) 5000 to prolong the circulation time of liposomes depends on the liposome size and is unfavourable for immunoliposome binding to target, *BBA* 1062 (1991) 142-148

Kobayashi, H., Boelte, K.C., Lin, P.C. Endothelial cell adhesion molecules and cancer progression, *Current Med Chem* 14 (2007) 377-386

Koch, A.E., Halloran, M.M., Haskell, C.J., Shah, M.R., Polverini, P.J. Angiogenesis mediated by soluble forms of E-selectin and vascular cell adhesion molecule-1, *Nature* 376 (1995) 517-519

Kondo, M., Asai, T., Katanasaka, Y., Sadzuka, Y., Tsukada, H., Ogino, K., Taki, T., Baba, K., Oku, N., Anti-neovascular therapy by liposomal drug targeted to membrane type-1 matrix metalloproteinase, *Inter J Cancer* 108 (2004) 301-306

Koning, G.A. Morselt, H.W.M., Gorter, A., Allen, T.M., Zalipsky, S., Kamps, J.A.A.M., Scherphof, G.L. Pharmacokinetics of differently designed immunoliposome formulations in rats with or without hepatic colon cancer metastases, *Pharmaceut Res* 18 (2001) 1291-1298

Koning, G.A., Kamps, J.A.A.M., Scherphof, G.L. Interference of macrophages with immunotargeting of liposomes, *J Liposome Res* 12 (2002) 107-119

Koning, G.A., Morselt, H.W.M., Gorter, A., Allen, T.M., Zalipsky, S., Scherphof, G.L., Kamps, J.A.A.M. Interaction of differently designed immunoliposomes with colon cancer cells and kupffer cells. An *in vitro* comparison, *Pharmaceutical Res* 20 (2003) 1249-1257

-
- Koning, G.A., Fretz, M.M., Woroniecka, U., Storm, G., Krijger, G.C. Targeting liposomes to tumor endothelial cells for neutron capture therapy, *Appl Radiat Isot* 61 (2004) 963-967
- Kontermann, R. Immunoliposomes for cancer therapy, *Curr Opin Mol Ther* 8 (2006) 39-45
- Kuldo, J.M., Westra, J., Asgeirsdottir, S.A., Kok, R.J., Oosterhuis, K., Rots, M.G., Schouten, J.P., Limburg, P.C., Molema, G. Differential effects of NF- κ B and p38 MAPK inhibitors and combinations thereof on TNF- α and IL-1 β induced pro-inflammatory status of endothelial cells *in vitro*, *Am J Physiol Cell Physiol* 289 (2005) C1229-1239
- Kuijpers, T.W., Raleigh, M., Kavanagh, T., Janssen, H., Calafat, J., Roos, D., Harlan, J.M. Cytokine-activated endothelial cells internalize E-selectin into lysosomal compartment of vesiculotubular shape, *J Immunol* 152 (1994) 5060-5069
- Kumagai, Y., Toi, M., Inoues, H. Dynamism of tumour vasculature in the early phase of cancer progression: outcomes from oesophageal cancer research, *Lancet Oncol* 3 (2002) 604-610
- Kuzu, I., Bicknell, R., Fletcher, C., Gatter, K. Expression of adhesion molecules on the endothelium of normal tissue vessels and vascular tumors, *Lab Invest* 69 (1993) 322-328
- Lankelma, J., Dekker, H., Luque, R.F., Luykx, S., Hoekman, K., van der Valk, P., van Dienst, P.J., Pinedo, H.M. Doxorubicin gradients in human breast cancer, *Clin Cancer Res* 5 (1999) 1703-1707
- Larbouret, C., Robert, B., Linard, C., Teulon, I., Gourgou, S., Bibeau, F., Martineau, P., Santoror, L., Pouget, J-P., Pelegrin, A., Azria, D. Radiocurability by targeting tumor necrosis- α using a bispecific antibody in carcinoembryonic antigen transgenic mice, *Int J Radiat Oncol Biol Phys* 69 (2007) 1231-1237

Lasic, D.D., Martin, F.J., Gabizon, A., Huang, S.K., Papahadjopoulos, D., Sterically stabilized liposomes*: a hypothesis on the molecular origin of the extended circulation times, *BBA* 1070 (1991) 187-192

Lee, S.Y., Reichlin, A., Santana, A., Sokol, K.A., Nussenzweig, M.C., Choi, Y. TRAF2 is essential for JNK but not NF-kappaB activation and regulates lymphocyte proliferation and survival, *Immunity* 7 (1997) 703-713

Lee, T-Y., Lin, C-T., Kuo, S-Y., Chang, D-K., Wu, H-C. Peptide-mediated targeting to tumor blood vessels of lung cancer for drug delivery, *Cancer Res* 67 (2007) 10958-10965

Leu, A.J., Berk, D.A., Lymboussaki, A., Alitalo, K., Jain, R.K. Absence of functional lymphatics within a murine sarcoma: A molecular and functional evaluation, *Cancer Res* 60 (2000) 4324-4327

Li, S., Peck-Radosavljevic, M., Kienast, O., Preitfellner, J., Havlik, E., Schima, W., Traub-Weidinger, T., Graf, S., Beheshti, M., Schmid, M., Angelberger, P., Dudczak, R. Iodine-123-vascular endothelial growth factor-165 (123I-VEGF165). Biodistribution, safety and radiation dosimetry in patients with pancreatic carcinoma, *Q J Nucl Med Mol Imaging* 48 (2004) 198-206.

Lipman, N.S., Jackson, L.R., Trudel, L.J., Weis-Garcia, F. Monoclonal versus polyclonal antibodies: distinguishing characteristics, applications, and information resources, *ILAR J* 46 (2005) 258-268

Litzinger, D.C., Buiting, A.M.J., van Rooijen, N., Huang, L. Effect of liposome size on the circulation time and intraorgan distribution of amphipathic poly(ethylene glycol)-containing liposomes, *BBA* 1190 (1994) 99-107

Liu, Z., Gurlo, T., von Grafenstein, H. Cell-ELISA using β -galactosidase conjugated antibodies, *J Immunol Methods* 234 (2000) P153-P167

Liu, C., Huang, H., Donate, F., Dickinson, C., Satucci, R., El-Sheikh, A., Vessella, R., Edgington, T.S. Prostate-specific membrane antigen directed selective thrombotic infarction of tumors, *Cancer Res* 62 (2002) 5470-5475

Liu, J.J., Ching, L-M., Goldthorpe, M., Sutherland, R., Baguely, B.C., Kirker, J.A., McKeage, M.J. Antitumour action of 5,6dimethylxanthenone-4-acetic acid in rats bearing chemically induced primary mammary tumours, *Cancer Chemother Pharmacol* 59 (2007a) 661-669

Liu, G., Dou, S., Yin, D., Squires, S., Liu, X., Wang, Y., Rusckowski, Hnatowich, D.J. A novel pretargeting method for measuring antibody internalization in tumor cells, *Cancer Biother Radiopharmaceut* 22 (2007b) 33-39

Lucas, R., Holmgren, L., Garcia, I., Jimenez, B., Mandriota, S.J., Borlat, F., Sim, B.K.L., Wu, Z., Grau, G.E., Shing, Y., Soff, G.A., Bouck, N., Pepper, M.S. Multiple forms of angiostatin induce apoptosis in endothelial cells, *Blood* 92 (1998) 4730-4741

Mackman, N., Fowler, B.J., Edgington, T.S., Morrissey, J.H. Functional analysis of the human tissue factor promoter and induction by serum, *PNAS* 87 (1990) 2254-2258

Mackman, N. Regulation of the tissue factor gene, *FASEB J* 9 (1995) 883-889

Maeda, N., Takeuchi, Y., Takada, M., Sadzuka, Y., Namba, Y., Oku, N. Anti-neovascular therapy by use of tumor neovasculature-targeted long-circulating liposome, *J Control Release* 100 (2004) 41-52

Malvern Ltd. (1993) MalvernZetaSizer 4 hardware reference manual Na MAN 0057(1.2)

Mamot, C., Drummond, D.C., Noble, C.O., Kallab, V., Guo, Z., Hong, K., Kirpotin, D.B., Park, J.W. Epidermal growth factor receptor-targeted immunoliposomes significantly enhance the efficacy of multiple anticancer drugs in vivo, *Cancer Res* 65 (2005) 11631-11638

Marty, C., Odermatt, B., Schott, H., Neri, D., Ballmer-Hofer, K., Klemenz, R., Schwendener, R.A. Cytotoxic targeting of F9 tetratocarcinoma tumours with anti-ED-B fibronectin scTv antibody modified liposomes, *British J Cancer* 87 (2002) 106-112

Maruyama, K., Taksizawa, T., Yuda, T., Kennel, S.J., Huang, L., Iwatsuru, M. Targetability of novel immunoliposomes modified with amphipatic poly(ethylene glycol)s conjugated at their distal terminals to monoclonal antibodies, *BBA* 1234 (1995) 74-80

Maruyama, K., Takahashi, N., Tagawa, T., Nagaike, K., Iwatsuru, M. Immunoliposomes bearing polyethyleneglycol-coupled Fab' fragment show prolonged circulation time and high extravasation into targeted solid tumors in vivo, *FEBS Letters* 413 (1997) 177-180

Mastrobattista, E., Koning, G.A., Storm, G. Immunoliposomes for the targeted delivery of antitumor drugs, *Adv Drug Delivery Rev* 40 (1999) 103-127

Matschurat, S., Blum, S., Mitnacht-Kraus, R., Dukman, H.B.P.M., Kanal, L., de Waal, R.M.W., Clauss, M. Negative regulatory role of PI3-kinase in TNF-induced tumor necrosis, *Int J Cancer* 107 (2003) 30-37

Matsumura, Y., Maeda, H. A new concept for macromolecular therapeutics in cancer chemotherapy: Mechanism of tumortropic accumulation of proteins and the antitumor agent Smancs, *Cancer Res* 46 (1986) 6387-6392

Matsuno, F., Haruta, Y., Kondo, M., Tsai, H., Barcos, M., Seon, B.K. Induction of lasting complete regression of preformed distinct solid tumors by targeting the tumor vasculature using two new anti-endoglin monoclonal antibodies, *Clin Cancer Res* 5 (1999) 371-382

Maynard, J.R., Heckman, C.A., Pitlick, F.A., Nemerson, Y. Association of tissue factor activity with the surface of cultured cells, *J Clin Invest* 55 (1975) 814-824

McKeage, M.J. The potential of DMXAA (ASA404) in combination with docetaxel in advanced prostate cancer, *Expert Opin Investig Drugs* 17 (2008) 23-29

Mechtcheriakova, D., Schabbauer, G., Lucerna, M., Clauss, M., De Martin, R., Binder, B.R., Hofer, E., Specificity, diversity, and convergence in VEGF and TNF- α signaling events leading to tissue factor upregulation via EGR-1 in endothelial cells, *FASEB J* 15 (2001) 230–242

Miller, K.D., Sweeney, C.J., Sledge, G.W. Jr. Redefining the target: chemotherapeutics as antiangiogenics, *J Clin Oncol* 19 (2001)1195-1206

Moll, T., Czyz, M., Holzmüller, H., Hofer-Warbinek, R., Wagner, E., Winkler, H., Bach, F.H., Hofer, E. Regulation of the tissue factor promoter in endothelial cells, *J Biol Chem* 270 (1995) 3849-3857

Morishige, H., Ohkuma, T., Kaji, A. In vitro cytostatic effect of TNF (Tumor necrosis factor) entrapped in immunoliposomes on cells normally insensitive to TNF, *BBA* 1151 (1993) 59-68

Morrissey, J.H. Tissue factor: and enzyme cofactor and a true receptor, *Thromb Haemost* 86 (2001) 66-74

Murate, R., Siemann, D.W., Overgaard, J., Horsman, M.R. Improved tumor response by combining radiation and the vascular-damaging drug 5,6-dimethylxanthenone-4-actaic acid, *Radiation Res* 156 (2001) 503-509

Nagy, J.A., Brown, L.F., Senger, D.R., Lanior, N., Van de Water, L., Dvorak, A.M., Dvorka, H.F. Pathogenesis of tumor stroma generation: a critical role for leaky blood vessels and fibrin deposition, *BBA* 984 (1988) 305-326

Nallamothe, R., Wood, G.C, Pattillo, C.B., Scott, R.C., Kiani, M.F., Moore, B.M., Thoma, L.A., A tumor vasculature targeted liposome delivery system for combretastatin A4: design, characterization, and in vitro evaluation, *AAPS Pharm Sci Tech* 7 (2006) E1-E10

Nawroth , P., Handley, D., Matsueda, G., de Waal, R., Gerlach, H., Blohm, D., Stern, D. Tumor necrosis factor/cachectin-induced intravascular fibrin formation in meth A fibrosarcomas, *J Exp Med* 168 (1988) 637-647

Nemerson, Y., Repke, D. Tissue factor accelerates the activation of coagulation factor VII: the role of a bifunctional coagulation cofactor, *Thromb Res* 40 (1985) 351-358

Neumann, P., Gertzberg, N., Vaughan, E., Weisbrot, J., Woodburn, R., Lambert, W., Johnson, A. Peroxynitrite mediates TNF- α -induced endothelial barrier dysfunction and nitration of actin, *Am J Physiol Lung Cell Mol Physiol* 290 (2006) 674-684

New, R.R.V. (1990) *Liposome: a practical approach*; New York: University Press

Nilsson, F., Kosmehl, H., Zardi, L., Neri, D. Targeted delivery of tissue factor to the ED-B domain of fibronectin, a marker of angiogenesis, mediates the infarction of solid tumors in mice, *Cancer Res* 61 (2001) 711-716

Noguchi, Y., Wu, J., Duncan, R., Strohm, J., Ulbrich, K., Akaike, T., Maeda, H. Early phase tumor accumulation of macromolecules: a great difference in clearance rate between tumor and normal tissues, *Jpn J Cancer Res* 89 (1998) 307-314

Ober, R.J., Radu, C.G., Ghetie, V., Ward, S. Differences in promiscuity for antibody-FcRn interactions across species: implications for therapeutic antibodies, *Inter Immunol* 13 (2001) 1551-1559

Oh, P., Li, Y., Yu, J., Durr, E., Krasinska, K.M., Carver, L.A., Testa, J.E., Schnitzer J.E. Subtractive proteomic mapping of the endothelial surface in lung and solid tumours for tissue-specific therapy, *Nature* 429 (2004) 629-635

Oku, N., Namba, Y., Long-circulating liposomes, *Crut Rev Ther Drug Carrier Systems* 11 (1994) 231-270

Olafsen, T., Kenanova, V.E., Wu, A.M. Tunable pharmacokinetics: modifying the in vivo half-life of antibodies by directed mutagenesis of the Fc fragment, *Nat Protoc* 1 (2006) 2048-2060

O'Reilly, F.M., Casper, K.A., Otto, K.B., Sexton, S.A., Swerlick, R.A. Regulation of tissue factor in microvascular dermal endothelial cells, *J Invest Dermatol* 120 (2003) 489-494

Osborn, L., Hession, C., Tizard, R., Vassallo, C., Luhowskyj, S., Chi-Rosso, G., Lobb, R. Direct expression cloning of vascular cell adhesion molecule 1, a cytokine-induced endothelial protein that binds to lymphocytes, *Cell* 59 (1989) 1203-1211

Osterud, B., Bjørklid, E. The tissue factor pathway in disseminated intravascular coagulation, *Semin Thromb Hemost* 27 (2001) 605-617

Pan, L.-F., Kreisle, R., Shi, Y.D. Detection of Fc-gamma receptors on human endothelial cells stimulated with cytokines tumour necrosis factor-alpha (TNF-alpha) and interferon-gamma (IFN-gamma), *Clin Exp Immunol* 112 (1998) 533-538

Pang, J.-H., Cao, Z., Joseph, W.R., Baguley, B.C., Ching, L.-M., Antitumour activity of the novel immune modulator 5,6 dimethylxanthenone-4-acetic acid (DMXAA) in mice lacking the interferon-gamma receptor, *Euro J Cancer* 34 (1998) 1282-1289

Pallardy, M., Biola, A., Lebrec, H., Bréard, J. Assessment of apoptosis in xenobiotic-induced immunotoxicity, *Methods* 19 (1999) 36-47

Papahadjopoulos, D., Allen, T.M., Gabizon, A., Mayhew, E., Huang, S.K., Lee, K.-D. Woodle, M.C., Lasic, D.D., Redemann, C., Martin, F.J. Sterically, stabilized liposomes: Improvements on pharmacokinetics and antitumor therapeutic efficacy, *PNAS* 88 (1991) 11460-11464

Pastorino, F., Brignole, C., Marimpietri, D., Cilli, M., Gambini, C., Ribatti, D., Longhi, R., Allen, T.M., Corti, A., Ponzoni, M. Vascular damage and anti-angiogenic effects of tumor vessel-targeted liposomal chemotherapy, *Cancer Res* 63 (2003) 7400-7409

Pastorino, F., Brignole, C., Di Paolo, D., Nico, B., Pezzolo, A., Marimpietri, D., Pagnan, G., Piccardi, F., Cilli, M., Longhi, R., Ribatti, D., Corti, A., Allen, T.M., Ponzoni, M. Targeting liposomal chemotherapy via both tumor cell-specific and tumor vasculature-specific ligands potentiates therapeutic efficacy, *Cancer Res* 66 (2006) 10073-10082

Pedurthi, U.R., Ghosh, S., Mandal, S.K., Rao, L.V.M. Tissue factor activation: is disulfide bond switching a regulatory mechanism? *Blood* 110 (2007) 3900-3908

Peterson, G. A simplification of the protein assay method of Lowry et al. which is generally more applicable, *Anal Biochem* 83 (1977) 346-356

Philpott, M., Ching, L-M., Baguley, B.C. The antitumour agent 5,6 dimethylxanthenone-4-acetic acid acts in vitro on human mononuclear cells as a co-stimulator with other inducers of tumour necrosis factor, *Euro J Cancer* 37 (2001) 1930-1937

Philipp, J., Dienst, A., Unruh, M., Wagener, A., Grunow, A., Engert, A., Fries, J.W., Gottstein, C. Soluble tissue factor induces coagulation on tumor endothelial cells in vivo if coadministered with low-dose lipopolysaccharides, *Arterioscler Thromb Vasc Biol* 23 (2003) 905-910

Phillips, N.C., Gagne, L., Tsouka, C., Dahman, J. Immunoliposomes targeting to murine CD4⁺ leukocytes is dependent on immune status, *J Immunol* 152 (1994) 3168-3174

Phillips, N.C., Dahman, Immunogenicity of immunoliposomes: reactivity against species-specific IgG and liposomal phospholipids, *Immunol Letters* 45 (1995) 149-152

Plowman, J., Narayanan, V.L., Dykes, D., Szarvasi, E., Briet, P., Yoder, O.C., Paull, K. Flavone acetic acid: A novel agent with preclinical antitumor activity against colon adenocarcinoma 38 in mice, *Cancer Treat Rep* 70 (1986) 631-635

Polunovsky, V.A., Wendt, C.H., Ingbar, D.H., Peterson, M.S., Bitterman, P.B. Induction of endothelial cell apoptosis by TNF α : Modulation by inhibitors of protein synthesis, *Exp Cell Res* 214 (1994) 548-594

Proffitt, R.T., Williams, L.E., Presant, C.A., Tin, G.W., Uliana, J.A., Gamble, R.C., Baldeschwieler, J.D. Tumor-imaging potential of liposomes loaded with In-111-NTA: Biodistribution in mice, *J Nucl Med* 24 (1983) 45-51

Ramana, K.V., Bhatnagar, A., Srivastava, S.K. Aldose reductase regulates TNF- α -induced cell signalling and apoptosis in vascular endothelial cells, *FEBS Letters* 570 (2004) 189-194

Ramaswamy, B., Elias, A.D., Kelbick, N.T., Dodley, A., Morrow, M., Hauger, M., Allen, J., Rhoades, C., Kendra, K., Chen, H.X., Eckhardt, S.G., Shapiro, C.L. Phase II trial of bevacizumab in combination with weekly docetaxel in metastatic breast cancer patients, *Clin Cancer Res* 12 (2006) 3124-3129

Ran, S., Gao, B., Duffy, S., Watkins, L., Rote, N., Thorpe, P.E. Infarction of solid hodgkin's tumors in mice by antibody-directed targeting of tissue factor to tumor vasculature, *Cancer Res* 58 (1998) 4646-4653

Rao, I.V.M., Rapaport, S.I. Activation of factor VII bound to tissue factor: A key early step in the tissue factor pathway of blood coagulation, *PNAS* 85 (1988) 6687-6691

Rehemtulla, A., Ruf, W., Edgington, T.S. The integrity of cysteine 186-cystein 209 bond of the second disulfide loop of tissue factor is required for binding of factor VII, *J Biol Chem* 266 (1991) 10294-10299

Rewcastle, G.W., Atwell, G.J., Zhuang, L., Baguley, B.C., Denny, W.A. Potential antitumor agents. 61. structure-activity relationships for in vivo colon 38 activity among disubstituted 9-oxo-9H-xanthene-4-acetic acids, *J Med Chem* 34 (1991) 217-222

Rice, G.E., Munro, J.M., Bevilacqua, M.P. Inducible cell adhesion molecule 110 (INCAM-110) is an endothelial receptor for lymphocytes. A CD11/CD18-independent adhesion mechanism, *J Exp Med* 171 (1990) 1369-1374

Ricard, I., Payet, M., Dupuis, G. VCAM-1 is internalized by a clathrin-related pathway in human endothelial cells but its alpha 4 beta 1 integrin counter-receptor remains associated with the plasma membrane in human T lymphocytes, *Eur J Immunol* 28 (1998) 1708-1718

Riethmuller, G., Schneider-Gadicke, E., Schlimok, G. Randomised trial of monoclonal antibody for adjuvant therapy of resected Dukes' C colorectal carcinoma, *Lancet* 343 (1994) 1177-1183

Riethmuller G., Holz, E., Schlimok, G. Monoclonal therapy for resected Dukes' C colorectal cancer: seven year outcome of a multicenter randomized trial, *J Clin Oncol* 16 (1998) 1788-1794

Robinson, J.P. Flow cytometry, *Encyclopedia of Biomaterials and Biomedical Engineering* (2004) 630-640

Rosenthal, M., Pili, R. Randomized phase II study of docetaxel with or without DMXAA (AS1404) in hormone-refractory metastatic prostate cancer (HRMPC), *2007 Prostate Cancer Symposium* (2007) 219

Ryan, D., Nuccie, B., Abboud, C., Winslow, J. Vascular cell adhesion molecule-1 and the integrin VLA-4 mediate adhesion of human B cell precursors to cultured bone marrow adherent cells, *J Clin Invest* 88 (1991) 995-1004

Schiffelers, R.M., Koning, G.A., ten Hagen, T.L.M., Fens, M.H.A.M., Schraa, A.J., Janssen, A.P.C.A., Kok, R.J. Molema, G. Storm, G. Anti-tumor efficacy of tumor vasculature-targeted liposomal doxorubicin, *J Control Release* 91 (2003) 115

Scott, R.C., Wang, B., Nallamotheu, R., Pattillo, C.B., Perez-Liz, G., Issekutz, A., Del Valle, L., Wood, G.C., Kiani, M.F. Targeted delivery of antibody conjugated liposomal drug carriers to rat myocardial infarction, *Biotechnol Bioeng* 96 (2007) 795-802

Seetharam, S., Murphy, K., Atkins, C., Feuerstein, G. Cloning and expression of rat coagulation factor VII, *Thromb Res* 109 (2003) 225-231

Semple, S.C., Chonn, A., Cullis, P.R. Interactions of liposomes and lipid-based carrier systems with blood proteins: Relation to clearance behavior in vivo, *Adv Drug Delivery Rev* 32 (1998) 3-17

Sedgwick, J.D., Czerkinsky, C., Detection of cell-surface molecules, secreted products of single cells and cellular proliferation by enzyme immunoassay, *J Immunol Methods* 150 (1992) 159-175

Seshadri, M., Mazurchuk, R., Spornyak, J.A., Bhattacharya, A., Rustum, Y.M., Bellnier, D.A. Activity of the vascular-disrupting agent 5,6 dimethylxanthenone-4-acetic acid against human head and neck carcinoma xenografts, *Neoplasia* 8 (2006) 534-542

Seshadri, M., Spornyak, J.A., Maier, P.G., Cheney, R.T., Mazurchuk, R., Bellnier, D.A. Visualizing the acute effects of vascular-targeted therapy *in vivo* using intravital microscopy and magnetic resonance imaging: Correlation with endothelial apoptosis, cytokine induction, and treatment outcome, *Neoplasia* 9 (2007) 128-135

Seron, D., Cameron, J., Haskard, D. Expression of VCAM-1 in the normal and diseased kidney, *Nephrol Dial Transplant* 6 (1991) 917-922

Seynhaeve, A.L., Hoving, S., Schipper, D., Vermeulen, C.E., de Wiel-Ambagtsheer, G., van Tiel, S.T., Eggermont, A.M., Ten Hagen, T.L. Tumor necrosis factor alpha mediates homogeneous distribution of liposomes in murine melanoma that contributes to a better tumor response, *Cancer Res* 67 (2007) 9455-9462

Seynhaeve, A.L., Eggermont, A.M., ten Hagen, T.L. TNF and manipulation of the tumor cell-stromal interface: “ways to make chemotherapy effective”, *Front Biosci* 13 (2008) 3044-3045

Shahinian, S. Silvius, J.R. A novel strategy affords high-yield coupling of antibody Fab' fragments to liposomes, *BBA* 1239 (1995) 157-167

Sharma, A., Sharma, U.S. (1997) Liposomes in drug delivery: Progress and limitations, *Int J Pharmaceut* 154 (1997) 123-140

Sharma, L., Melis, E., Hickey, M.J., Clyne, C.D., Erlich, J., Khachigian, L.M., Davenport, P., Morand, E., Carmelit, P., Tipping, P.G. The cytoplasmic domain of tissue factor contributes to leukocyte recruitment and death in endotoxemia, *Am J Pathol* 165 (2004) 331-340

Shen, B-Q., Lee, D.Y., Cortopassi, K.M., Damico, L.A., Zioncheck, T.F. Vascular endothelial growth factor KDR receptor signaling potentiate tumor necrosis factor-induced tissue factor expression in endothelial cells, *J Biol Chem* 276 (2001) 5281-5286

Shinkarku, S., Bayle, M., Laín.G., Déléris, G. Vascular endothelial cell growth factor (VEGF), and emerging target for cancer chemotherapy, *Curr Med Chem* 3 (2003) 95-117

Siemann, D.W., Mercer, E., Lepler, S., Rojiani, A.M. Vascular targeting agents enhance chemotherapeutic agent activities in solid tumor therapy, *Int J Cancer* 99 (2002) 1-6

Siemann, D.W., Chaplin, D.J., Morsman, M.R. Vascular-targeting therapies for treatment of malignant disease, *Cancer* 100 (2004) 2491-2499

Siemann, D.W., Bibby, M.C., Dark, G.G., Dicker, A.P., Eskens, F.A.L.M., Horsman, M.R., Marmé, D., LoRusso, P.L. Differentiation and definition of vascular-targeted therapies, *Clin Cancer Res* 11 (2005) 416-420

Simberg, D., Duza, T., Park, J.H., Essler, M., Pilch, J., Zhang, L., Derfus, A.M., Yang, M., Hoffman, R.M., Bhatia, S., Sailor, M.J., Ruoslahti, E. Biomimetic amplification of nanoparticle homing to tumors, *PNAS* 104 (2007) 932-936

Spragg, D.D., Alford, D.R., Greferath, R., Larsen, C.E., Lee, K.-D., Gurtner, G.C., Cybulsky, M.I., Tosi, P.F., Nicolau, C., Gimbrone, M.A. Jr., Immunotargeting of liposomes to activated vascular endothelial cells: A strategy for site-selective delivery in the cardiovascular system, *PNAS* 94 (1997) 8795-8800

Starns, C.O. Coley's toxins in perspective, *Nature* 357 (1992) 11-12

Stoelcker, B., Ruhland, B., Hehlgans T., Bluethmann, H., Luther, T., Mannel, D. Tumor necrosis factor induces tumor necrosis via tumor necrosis factor receptor type-1 expressing endothelial cells of the tumor vasculature, *American J Pathology* 156 (2000) 1171-1176

Sung, C., Dedrick, R.L., Hall, W.A., Johnson, P.A., Youle, R.J. The spatial distribution of immunotoxins in solid tumors: Assessment by quantitative autoradiography, *Cancer Res* 53 (1993) 2092-2099

Takai, T. Fc receptors and their role in immune regulation and autoimmunity, *J Clin Immunol* 25 (2005) 1-18

Tannock, I.F. Tumour physiology and drug resistance, *Cancer Metastasis Rev* 20 (2001) 123-32

Temming, K., Schiffelers, R.M., Molema, G., Kok, R.J. RGD-based strategies for selective delivery of therapeutics and imaging agents to the tumour vasculature, *Drug Resistance Updates* 8 (2005) 381-402

Ten Hagen, T.L., Seynhaeve, A.L., van Tiel, S.T., Ruiter, D.J., Eggermont, A.M. Pegylated liposomal tumor necrosis factor-alpha results in reduced toxicity and synergistic antitumor

activity after systemic administration in combination with liposomal doxorubicin (Doxil) in soft tissue sarcoma-bearing rats, *Int J Cancer* 97 (2002) 115-120

Ten Hagen, T.L.M, Eggermont, A.M.M. Tumor vascular therapy with TNF, critical review on animal models, *Methods Mol Med* 98 (2004) 227-245

Thorpe, P. Vascular targeting agents as cancer therapeutics, *Clin Cancer Res* 10 (2004) 415-427

Torchilin, V.P. Immunoliposomes and PEGylated immunoliposomes: possible use for targeted delivery of imaging agents, *Immunol Methods* 4 (1994) 244-258

Tsourkas, A., Shinde-Patil, V.R., Kelly, K.A., Patel, P., Wolley, A., Allport, J.R., Weissleder, R. In vivo imaging of activated endothelium using an anti-VCAM-1 magneto-optical probe, *Bioconj Chem* 16 (2005) 576-581

Utsumi, T., Hung, M-C., Klostergaard, J. Preparation and characterization of liposomal-lipophilic tumor necrosis factor, *Cancer Res* 51 (1991) 3362-3366

Van der Veen, A.H., Alexander M.M. Eggermont, A.M.M., Seynhaeve, A.L.B., van Tiel, S.T., ten Hagen, T.L.M. Biodistribution and tumor localisation of stealth liposomal tumor necrosis factor- α in soft tissue sarcoma bearing rats, *Int J Cancer* 77 (1998) 901-906

Van der Veen, A.H., ten Hagen, T.L.M., de Wilt, J.H.W., van Ijken, M.G.A., Eggermont, A.M.M. An overview on the use of TNF- α : our experience with regional administration and developments towards new opportunities for systemic application, *Anticancer Res* 20 (2000) 3467-3474

Van Horsen, R., ten Hagen, T.L.M., Eggermont, A.M.M. TNF- α in cancer treatment: Molecular insights, antitumor effects, and clinical utility, *The Oncologist* 11 (2006) 397-408

Vauple, P., Kallinowski, F., Okunieff, P. Blood flow, oxygen and nutrient supply, and metabolic microenvironment of human tumors: A review, *Cancer Res* 49 (1989) 6449-6465

Vauple, P. Tumor microenvironmental physiology and its implications for radiation oncology, *Seminars Radiation Oncol* 14 (2004) 198-206

Veenendaal, L.M., Jin, H., Ran, S., Cheung, L., Navone, N., Marks, J.W., Waltenberger, J., Thorpe, P., Rosenblume, M.G. *In vitro* and *in vivo* studies of a VEGF₁₂₁/rGelonin chimeric fusion toxin targeting the neovasculature of solid tumors, *PNAS* 99 (2002) 7866-7871

Verhoef C, de Wilt J.H., Grünhagen D.J., van Geel A.N., Ten Hagen T.L., Eggermont A.M. Isolated limb perfusion with melphalan and TNF-alpha in the treatment of extremity sarcoma, *Curr Treat Options Oncol* 8 (2007) pubmed ahead of print

Vermes, I., Haanen, C., Steffens-Nakken, H. Reutelings-Sperger, C. A novel assay for apoptosis Flow cytometric detection of phosphatidylserine expression on early apoptotic cells using fluorescein labelled Annexin V, *J Immunol Methods* 184 (1995) 39-51

Voinea, M., Manduteanu, I., Dragomir, E., Capraru, M., Simionescu, M. Immunoliposomes directed toward VCAM-1 interact specifically with activated endothelial cells—A potential tool for specific drug delivery, *Pharmaceutical Res* 22 (2005) 1906-1917

Volkel, T., Holig, P., Merdan, T., Muller, R., Kontermann, R.E. Targeting of immunoliposomes to endothelial cells using a single-chain Fv fragment directed against human endoglin (CD105), *BBA* 1663 (2004) 158-166

Wakabayashi, T., Yoshida, J., Ishiyama, J., Mizuno, M. Antitumor activity of recombinant human tumor necrosis factor- α (rH-TNF- α) liposome-entrapped rH-TNF- α , *Neurol Med Chir (Tokyo)* 37 (1997) 739-746

Walter-Yohrling, J., Morgenbesser, S., Rouleau, C., Bagley, R., Callahan, M., Weber, W., Teicher, B.A. Murine endothelial cell lines as models of tumor endothelial cells, *Clin Cancer Res* 10 (2004) 2179-2189

Watanabe, N., Niitsu, Y., Umeno, H., Kuriyama, H., Neda, H., Yamauchi, N., Maeda, M., Urushizaki, I. Toxic effect of tumor necrosis factor on tumor vasculature in mice, *Cancer Res* 48 (1988) 2179-2183

Westrick, R.J., Bodary, P.F., Xu, Z., Shen, Y-C., Broze, G.J., Eitzman, D.T. Deficiency of tissue factor pathway inhibitor promotes atherosclerosis and thrombosis in mice, *Circulation* 103 (2001) 3044-3046

Wewetzer, K., Heininger, C., Seilheimer, B. An improved cell-ELISA for the differential screening of antibodies against cell surface molecules of viable adherent Schwann cells, *J Immunol Methods* 191 (1996) 171-178

Wildgoose, P., Nemerson, Y., Hansen, L.L., Nielsen, F.E., Glazer, S., Hedner U. Measurement of basal levels of factor VIIa in hemophilia A and B patients, *Blood* 80 (1992) 25-28

Woon, S-T., Zwain, S., Schooltink, M.A., Newth, A.L., Baguley, B.C., Ching, L-M. NF-kappa B activation *in vivo* in host and tumor cells by the antivascular agent 5,6 dimethylxanthenone-4-acetic acid (DMXAA), *Euro J Cancer*, 39 (2003) 176-1183

Wrobel, K., Claudio, E., Segade, F., Ramos, S., Lazo, P.S., Measurement of cytotoxicity by propidium iodide staining of target cell DNA application to the quantification of murine TNF- α , *J Immunol Methods* 189 (1996) 243-249

Wu, T-C. The role of vascular cell adhesion molecule-1 in tumor immune evasion, *Cancer Res* 67 (2007) 6003-6006

Wurthrich, R.P. Cell adhesion molecules and inflammatory renal diseases, *Nephrol Dial Transplant* 9 (1994) 1063-1065

Xia, Z., Liu, M., Sharma, V., Luo, T., Ouyang, J., McNeill, J.H. N-Acetylcysteine attenuates TNF- α -induced human vascular endothelial cell apoptosis and restores eNOS expression, *Euro J Pharmacol* 350 (2006) 134-142

Xu, L., Huang, C-C., Huang, W., Tang, W-H., Rait, A., Yin, Y.Z., Crúz, I., Xiang, L-M., Pirollo, K.F., Chang, E.H. Systemic tumor-targeted gene delivery by anti-transferrin receptor scFv-immunoliposomes, *Mol Cancer Ther* 1 (2002) 337-346

Yang, X.Y., Chen, E., Jiang, H., Hartmann, W.K., Mitra, G., Hecht, T., Soman, G. Development of a quantitative cell-based ELISA, for a humanized anti-IL-2/IL-15 receptor β antibody (HuMik β_1), and correlation with functional activity using an antigen-transfected murine cell line, *J Immunol Methods* 311 (2006) 71-80

Yu, J.L., may, L., Klemen, P., Weitz, J.I., Rak, J. Oncogenes as regulators of tissue factor expression in cancer: Implications for tumor angiogenesis and anti-cancer therapy, *Seminars Thromb Hemosta* 30 (2004) 21-30

Yuyamaa, Y., Tsujimotob, M., Fujimotoa, Y., Okua, N. Potential usage of thermosensitive liposomes for site-specific delivery of cytokines, *Cancer Letters* 155 (2000) 71-77

Zhang, Y., Deng, Y., Luther, T., Muller, M., Ziegler, R., Waldherr, R., Stern, D.M., Nawroth, P.P. Tissue factor controls the balance of angiogenic and antiangiogenic properties of tumor cells in mice, *J Clin Invest* 94 (1994) 1320-1327

Zhao, L., Ching, L-M., Kestell, P., Baguley, B.C. The antitumour activity of 5,6 dimethylxanthenone-4-acetic acid (DMXAA) in TNF receptor-1 knockout mice, *British J Cancer* 87 (2002) 465-470

Zhou, S., Paxtona, J.W., Tinglea, M.D., Kestell, P. Determination of unbound concentration of the novel anti-tumour agent 5,6-dimethylxanthenone-4-acetic acid in human plasma by ultrafiltration followed by high-performance liquid chromatography with fluorimetric detection, *J Chromat B* 757 (2001) 359-363

Zhou, S., Feng, X., Kestell, P., Paxton, J.W., Baguley, B.C., Chan, E. Transport of the investigational anti-cancer drug 5,6-dimethylxanthenone-4-acetic acid and its acyl glucuronide by human intestinal Caco-2 cells, *Euro J Pharmaceut Sci* 24 (2005) 513-524

Zwaal R.F.A., Comfurius, P., Bevers, E.M. Lipid-protein interactions in blood coagulation, *BBA* 1376 (1998) 433-453

Øgendahl, L. Lysspredning. Noter til Ph.D kursus i molecular Biophysics, 2001, KVL,

Erklärung

Hiermit versichere ich, dass ich die vorliegende Arbeit selbständig und ohne fremde Hilfe verfasst, keine anderen als die von mir angegebenen Quellen und Hilfsmittel benutzt und die den verwendeten Werken wörtlich oder inhaltlich entnommenen Stellen als solche kenntlich gemacht habe.

Bonn

Publications

1. Gosk, S., Moos, T., Gottstein, C. and Bendas, G. VCAM-1 directed immunoliposomes selectively target tumour vasculature *in vivo*. Accepted 2007
2. Moos, T., Gosk, S. and Morgan, E.H., Transferrin fails to mediate transcytotic transport through brain capillary endothelial cells, *J. Neurochem.*, 2006, 98(6), 1946-58
3. Gosk, S., Gottstein, C., and Bendas, G., Targeting of immunoliposomes to endothelial cells expressing VCAM: a future strategy in cancer therapy. *Int. J. Clin. Pharmacol. Ther.* 2005, 43(12), 581-2.
4. Gosk S., Vermehren C., Storm G. and Moos T., Targeting anti-transferrin receptor antibody (OX26) and OX26-conjugated liposomes to brain capillary endothelial cells using in situ perfusion. *J. Cereb. Blood Flow Metab.* 2004, 24 (11), 1193-1204.